DOTTORATO DI RICERCA IN

TERAPIE AVANZATE E FARMACOLOGIA SPERIMENTALE

CICLO XXXVI

COORDINATRICE Prof.ssa VARANI KATIA

PHARMACOLOGICAL CHARACTERIZATION OF NEW MODULATORS OF THE ENDOCANNABINOID SYSTEM: FROM SINGLE TARGET TO MULTI-TARGET COMPOUNDS

Settore Scientifico Disciplinare BIO/14

Dottoranda

Dott.ssa CONTRI CHIARA

Tutore

Prof.ssa VARANI KATIA

_____   _____

Anni 2020/2023

TABLE OF CONTENTS

ABBREVIATIONS LIST

2-AG	2-arachidonoylglycerol	Ih	hyperpolarization-activated cation channels
5-HT	5-hydroxytryptamine receptor	IL-10	Interleukin 10
AA	Arachidonic Acid	IL-6	Interleukin 6
ABDH	serine hydrolase/hydrolase	INF-ɣ	interferon-gamma
ACh	Acetylcholine	IOP	intraocular pressure
AD	Alzheimer's Disease	K_i	inhibitory binding constant values
AEA	N-arachidonoylethanolamine	LPS	Lipopolysaccharide
ALS	Amyotrophic lateral sclerosis	LPS	lipopolysaccharide
ATP	adenosine triphosphate	LTD	long-term depression
Aβ	β-amyloid	MAG	monoacylglycerols
BM	bone marrow	MAGL	monoacylglycerol lipase
BMD	bone mineral density	MAPK	mitogen-activated protein kinase
BP	blood pressure	MLT	Melatonin
cAMP	cyclic adenosine monophosphate	MMP-3	matrix metalloproteinase-3
CBD	Cannabidiol	MS	multiple sclerosis
CBR	CB receptor	MSE	Metabotropic-induced variations involve suppression of excitation
CCL2	chemokine ligand 2	MSI	Metabotropic-induced variations involve suppression of inhibition
cGMP	guanylyl cyclase	MTR	melatonin receptor
ChEIs	cholinesterase inhibitors	MTT	3-(4,5-dimethyl-2-thiazolyl)-2,5-diphenyl-2H-tetrazolium bromide
CHO	Chinese Hamster Ovary	NAC	N-acetylcysteine
CNR1	cannabinoid receptor 1 gene	NAPE	N-arachidonoyl phosphatidyl ethanolamine
CNS	central nervous system	NAPE-PLD	N-acyl phosphatidylethanolamine phospholipase D
COX	cyclooxygenase	NAT	N-acyltransferase
CVDs	cardiovascular diseases	Nrf2	nuclear erythroid 2-related factor 2
DAG	diacylglycerol	NSAIDs	Nonsteroidal anti-inflammatory drugs
DR	Dopamine Receptor	NTG	nitroglycerin
DSE	depolarization-induced suppression of excitation	OCD	obsessive-compulsive disorder
DSI	depolarization-induced suppression of inhibition	PD	Parkinson's disease
eCBs	Endocannabinoids	PEA	palmitoylethanolamide
ECS	Endocannabinoid System	PET	positron emission tomography
EM	episodic migraine	PI	propidium iodide

EpFAs	epoxidized fatty acids	PIP2	phosphatidylinositol bisphosphate
FAA	Fatty acid amide	PPARs	peroxisome proliferator-activated receptors
FAAH	Fatty acid amide hydrolase	PTSD	posttraumatic stress disorder
FBS	fetal bovine serum	RGCs	retinal ganglion cells
Forskolin	7β-acetossi-8,13-epossi-1α,6β,9α-triidrossilabd-14-en-11-one	Ro 20-1724	4-(3-butoxy-4-methoxybenzyl)-2-imidazolidinone
GABA	Gamma-aminobutyric acid	ROS	reactive oxygen species
GAD	generalized anxiety disorder	SAD	social anxiety disorder
G_i	inhibitory G proteins	sEH	Soluble Epoxide Hydrolase
GIRK	G-protein-gated inwardly rectifying potassium	T2DM	Type 2 diabetes
GPCRs	G protein-coupled receptors	TBHP	tert-Butyl hydroperoxide
G_s	Stimulatory G proteins	TGF-β1	growth factor β1
HCN	hyperpolarization-activated cyclic nucleotide-gated	TNFα	Tumor necrosis factor
HD	Huntington's disease	TRP	Transient receptor potential
HT	hypertension	TRPV	transient receptor potential vanilloid
IBD	Inflammatory Bowel Disease	α-SMA	α-smooth muscle actin
IC_{50}	Half-maximal inhibitory concentration	Δ^9-THC	Delta-9-tetrahydrocannabinol

INTRODUCTION

1. Endocannabinoid System

The endocannabinoid system (ECS) is composed of endocannabinoids (eCBs), cannabinoid type 1 and type 2 receptors (CB_1R and CB_2R), and proteins involved in the transport, synthesis, and catabolism of eCBs. Most ECS components are multifunctional; therefore, the ECS influences and is influenced by many other signaling pathways. This is particularly important to consider when evaluating the effects of drugs targeting the ECS (Papa et al., 2022).

1.1. Endocannabinoids

The most extensively researched eCBs are derivatives of arachidonic acid (AA), namely N-arachidonoylethanolamine (AEA) and 2-arachidonoylglycerol (2-AG) (Figure 1 A-B). ECBs have been identified in all tissues, organs, and bodily fluids examined to date. Both AEA and 2-AG function as natural agonists for CB_1R and CB_2R (Hillard, 2018). In addition to 2-AG and AEA, there exist other structurally related lipids that interact with cannabinoid receptors, such as 2-arachidonoyl-glyceryl ether, O-arachidonoyl-ethanolamine, N-arachidonoyl-dopamine, and oleamide. Although N-oleoylethanolamine and N-palmitoylethanolamine do not exhibit a strong affinity for CB receptors (CBR), they are still considered eCBs (Grabiec & Dehghani, 2017; Iannotti et al., 2016). On the flip side, 2-AG and AEA possess the capacity to stimulate a diverse array of G protein-coupled receptors (GPCRs), nuclear receptors, and ion channels. Additionally, 2-AG assumes a critical role in lipid metabolism, notably serving as a precursor of AA for the synthesis of prostaglandins (Nomura, Morrison, et al., 2011). In nature, there are over 60 exogenous ligands, including those found in cannabis sativa. These ligands have similar structures and physical properties, posing challenges in their separation. The initial isolation of the active component, delta-9-tetrahydrocannabinol (Δ^9-THC) (Figure 1C), occurred in 1964 (Crocq, 2020). Interestingly, while the chemical structures of most phytocannabinoids are now well-documented and exhibit close relationships, the primary mood-altering compound remains Δ^9-THC. Another significant phytocannabinoid is cannabidiol (CBD) (Figure 1D), which has gained prominence over the past two decades as a potent anti-inflammatory agent. It has been

demonstrated to alleviate the memory-related impairments induced by Δ^9-THC and elicit a range of other effects, as detailed in reference (Mechoulam & Parker 2013). While 2-AG and AEA exhibit structural similarities, they undergo distinct synthesis and degradation processes, each with unique physiological functions. Intriguingly, among these two eCBs, AEA seems to have a greater association with schizophrenia. The ECS is a versatile signaling network with involvement in diverse aspects of mammalian physiology and well-being, offering a promising avenue for the advancement of novel therapeutic medications (Lu & Mackie, 2021). However, it's important to note that eCBs and some of their counterparts also interact with a broader spectrum of receptors, including members of the transient receptor potential (TRP) channels, peroxisome proliferator-activated receptors (PPARs), and other GPCRs. After the discovery of eCBs, lipid signaling molecules related to them have been either newly identified or revisited, often sharing common metabolic pathways, as described in reference (Iannotti et al., 2016).
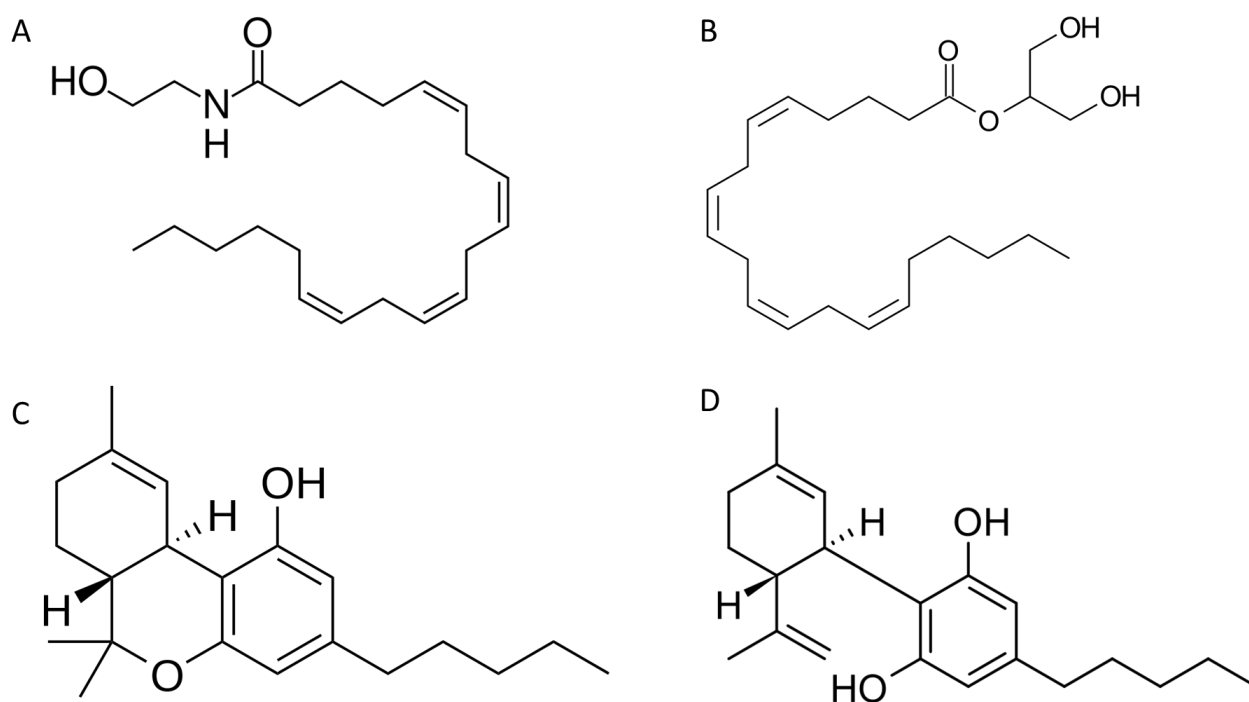
Figure 1: Chemical Structures of the most significant eCBs: (A) N-arachidonoylethanolamine or Anandamide (AEA), (B) 2-arachidonoylglycerol (2-AG), (C) delta-9-tetrahydrocannabinol (Δ^9-THC) and (D) cannabidiol (CBD).

1.2. *Cannabinoid receptors*

CB_1R and CB_2 receptors are GPCRs, which couple primarily to inhibitory G proteins (G_i) (Papa et al., 2022). Three main chemical classes of ligands activate CB_1R and CB_2R: cannabinoids (Δ^9-THC and, to a lesser extent, cannabinol) and their synthetic analogs, eicosanoids, such as AEA and 2-AG, and aminoalkylindoles. It is important to underline that Δ^9-THC is a low-efficacy CB_1R agonist, while for example 2-AG and most synthetic CB_1R agonists are high-efficacy agonists. CB_1R is expressed in all areas of the brain it is known as the most abundant GPCR in the mammalian brain (Pertwee, 2010). In most brain areas, CB_1R is expressed in the presynaptic terminals of both glutamatergic acid and gamma-aminobutyric acid (GABA) neurons which have been observed to exhibit both homodimeric and heterodimeric structures (Baggelaar et al., 2018). Furthermore, CB_1R is also found in non-neuronal cells of the brain, particularly in astrocytes, where its activation promotes the release of neurotransmitters (Stella, 2010). Following the synthesis of eCBs at postsynaptic sites, they move in a reverse direction to activate CB_1R located on presynaptic terminals. Subsequently, hydrolytic enzymes deactivate them. Consequently, the production of eCBs, serving as retrograde signals, in conjunction with the CB_1R-mediated K+ activation and the inhibition of Ca2+ channels, play a role in regulating the duration of synaptic activities and, consequently, various forms of long-term synaptic plasticity (Di Marzo & De Petrocellis, 2012). Nevertheless, the existence of ionic CB_1R and transient receptor potential vanilloid 1 ($TRPV_1$) within postsynaptic neurons implies that eCB signaling can also occur through non-retrograde or autocrine mechanisms (Castillo et al., 2012). Furthermore, CB_1R are found throughout the peripheral nervous system and are widely distributed in nearly all mammalian tissues and organs, encompassing the gastrointestinal tract, heart, liver, adipose tissue, lungs, adrenal glands, smooth and skeletal muscles, the male and female reproductive systems, bones, and skin. The role of CB_2R is often interconnected with that of CB_1R. Similarly, the CB_2R subtype is categorized as a GPCR and is linked to G_i/G_0 proteins. Consequently, its activation suppresses the activity of adenylate cyclase (AC) and triggers the activation of mitogen-activated protein kinase (MAPK) (Iannotti et al., 2016). In contrast to CB_1R, CB_2R levels in the brain are notably low. Emerging research has revealed that their expression is confined to specific neuronal cells and becomes more prevalent in microglia and activated astrocytes (Valant et al., 2009). However, the role of CB_2R in the brain is still controversial and whether or not this receptor participates in affective behavior remains to be

definitively established (Iannotti et al., 2016). Conversely, it is well-established that CB_2R is extensively expressed in immune system cells such as monocytes, macrophages, as well as B and T cells. Within these cell populations, the activation of CB_2R has several notable effects, including the reduction of proinflammatory cytokine and lymphangiogenic factor release (Staiano et al., 2016). Additionally, CB_2R is also found in various peripheral organs and cell types implicated in immune responses, encompassing the spleen, tonsils, thymus gland, mast cells, keratinocytes, and the gastrointestinal system (Iannotti et al., 2016). $TRPV_1$ and G protein-coupled receptor 55 (GPR_{55}) have been identified as other suspected cannabinoid receptors. $TRPV_1$ belongs to a subclass of ion channels characterized by weak voltage sensitivity and non-selective permeability to monovalent and divalent cations including Mg^{2+}, $Ca^{2+,}$ and Na^+ (Morphy, 2010). $TRPV_1$ activation contributes to pain transmission, neurogenic inflammation, and, as suggested by more recent studies, also to synaptic plasticity, neuronal overexcitability, and neurotoxicity (Julius, 2013; Nagy et al., 2014). $TRPV_1$ channels are widely expressed in dorsal root ganglia and sensory nerve fibers, but also non-neuronal cells and tissues such as keratinocytes and skeletal muscle. GPR_{55} belongs to the large GPCR family and is currently considered a potential CBR. The endogenous ligand of this receptor is lysophosphatidylinositol, but GPR_{55} appears to be activated by Δ^9-THC and some synthetic CB_1R agonists and antagonized by the non-psychotropic phytocannabinoid CBD (Pertwee, 2010). The exact function of GPR_{55} is not yet fully understood, but recent findings have suggested that activation of GPR_{55} may play an opposite role to that of CB_1R by increasing neurotransmitter release (Iannotti et al., 2016).
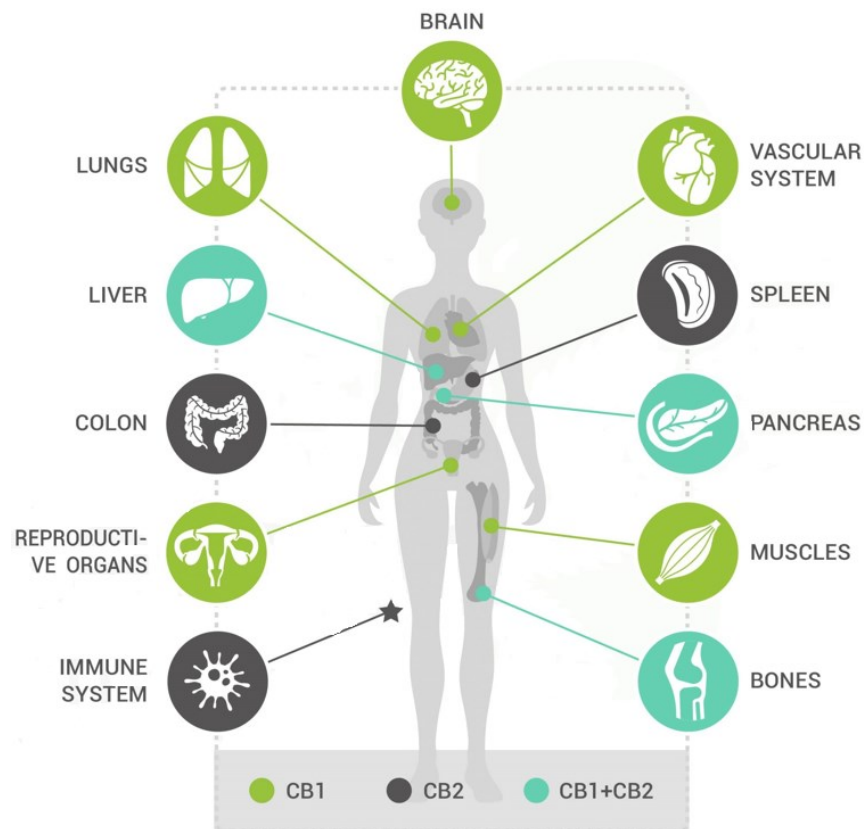
Figure 2: Localization of CBR in human body. CB$_1$Rs are expressed in all areas of the brain it is known as the most abundant GPCR in the mammalian brain, furthermore they are expressed in the vascular system, lung, muscles, and reproductive organs. CB$_2$Rs are found in various peripheral organs and cell types implicated in immune responses, encompassing the spleen, tonsils, thymus gland, mast cells, keratinocytes, and the gastrointestinal system. Both CBRs are expressed in bones, liver and pancreas.

1.3. Synthesis and transport of endocannabinoids

Numerous studies have contributed to the idea that the prevailing mode of eCB synthesis is referred to as "on-demand". The essence of on-demand synthesis entails the presence of eCBs as precursors within membrane lipids, with their release triggered by the activation of enzymes, typically lipases, prompted by specific signals such as G proteins or elevated intracellular calcium levels. This differs from classical neurotransmitters, which are manufactured and stored in vesicles. The "produced as needed" nature of eCBs results in their release with exceptional precision in terms of timing and location. Consequently, it is understandable that the outcomes of cannabinoids administered systemically may diverge from those of naturally released eCBs. This provides a rationale for driving research into medications that specifically target ongoing endocannabinoid signaling, such as inhibitors of eCB transport or degradation, or allosteric

modulators of CBRs [8]. Numerous synthetic and degradative enzymes have been identified that dynamically regulate the levels of eCBs in both typical and pathological conditions, making them potential focal points for therapeutic interventions. Both AEA and 2-AG originate from the breakdown of plasma membrane phospholipids. The synthesis of AEA involves a two-step process in which its precursors, AA, and phosphatidylethanolamine, are sequentially acted upon by two intracellular enzymes: N-acyltransferase (NAT) and N-acyl phosphatidylethanolamine phospholipase D (NAPE-PLD) (Scotter et al., 2010). Various synthetic routes contribute to eCB production, and the significance of each pathway can vary across different tissues, developmental stages, and potentially in specific medical conditions. The conventional mechanism for producing 2-AG involves a two-step process: first, the removal of inositol triphosphate from arachidonoyl-containing phosphatidylinositol bisphosphate (PIP2), followed by the removal of the acyl group at position 1 by an enzyme called diacylglycerol lipase (DAG lipase) (Kohnz & Nomura, 2014). There are two isoforms of diacylglycerol lipase: DAG lipase alpha and DAG lipase beta. Both are abundant in the brain, with DAG lipase α typically playing a more significant role in the synaptic production of 2-AG and DAG lipase β being more crucial for microglial generation of 2-AG (Lu & Mackie 2021). The specific synaptic positioning of DAG lipase α seems to be influenced by homer proteins, and neurological disorders have been linked to the disturbance of DAG lipase α's synaptic localization. When the misplacement of DAG lipase α leads to behavioral and physiological impairments, these issues frequently ameliorate upon inhibiting 2-AG degradation, underscoring a therapeutic strategy worthy of deeper exploration (Jung, Sepers, et al., 2012). The canonical pathway for AEA production involves the hydrolysis of N-arachidonoyl phosphatidyl ethanolamine (NAPE) by an enzyme called NAPE-PLD, although other well-documented pathways may operate in a tissue-specific manner (J. Liu et al., 2008). Regarding the location of AEA synthesis, NAPE-PLD is primarily found in presynaptic regions, suggesting that AEA synthesized by NAPE-PLD is unlikely to play a significant role as a retrograde neuromodulator. The mechanism by which these highly lipophilic eCBs are released from the membrane into both synaptic and extrasynaptic spaces remains a topic of uncertainty (Scotter et al., 2010). The movement of eCBs across the cell membrane is crucial following their synthesis and in anticipation of their degradation. Since eCBs are produced from phospholipids located on the inner side of the membrane, a mechanism for their release from the cell is essential for them to exert their effects on neighboring cells (Adermark & Lovinger, 2007). In a similar vein, the enzymes responsible for breaking down

eCBs are predominantly found within cells, necessitating a mechanism for their entry into cells to terminate the action of eCBs. Due to the polar nature of eCBs, they cannot easily traverse cell membranes through simple diffusion. There is limited evidence suggesting that adenosine triphosphate (ATP) or Na^{2+} is required for eCB transporters, implying that transporter-mediated facilitated diffusion is the probable mechanism for facilitating the transmembrane transport of eCBs (Nicolussi & Gertsch, 2015). Significant evidence supports the notion that both AEA and 2-AG utilize a common endocannabinoid membrane transporter (EMT) for their transport. The concept that blocking eCB uptake serves as a strategy to extend the duration of eCB activity for therapeutic benefits has driven the creation of EMT inhibitors. As the movement of eCBs is guided by concentration gradients, a medication that hinders the breakdown of eCBs will likewise impede their uptake. This effect is notably pronounced for AEA, while it is less pronounced for 2-AG, possibly due to differing immediate destinies of transported AEA and 2-AG, such as distinct mechanisms for intracellular sequestration. Hence, meticulous experimentation is essential (e.g., assessing the initial uptake rates, inhibiting enzymes responsible for endocannabinoid degradation, performing experiments in cells devoid of eCB-degrading enzymes, and measuring the inhibition of endocannabinoid efflux) to pinpoint genuine EMT inhibitors (Chicca et al., 2012). Considering these factors, multiple sets of EMT inhibitors have been formulated and examined across a range of physiological and behavioral setups. Broadly, EMT inhibitors elevate eCB levels, enhance eCB effects, and induce cannabimimetic responses. Advancements in this domain will be significantly advanced through the discovery of specific EMTs (Lu & Mackie, 2021).

1.4. Endocannabinoids as messengers

One key role of the ECS in the mature nervous system involves its function as a retrograde messenger, facilitating various types of synaptic plasticity through eCB signaling (Ohno-Shosaku & Kano, 2014). In this process, eCBs synthesized by the post-synaptic neuron travel in a retrograde manner across the synapse, activating presynaptic cannabinoid receptors and subsequently dampening neurotransmission from terminals expressing CB_1R. Synaptic plasticity, governed by eCBs, manifests in transient and enduring forms initiated by post-synaptic neuron stimulation either via depolarization and calcium influx or activation of a $G_{q/11}$-linked GPCR. Transient variations include depolarization-induced suppression of excitation

(DSE) and depolarization-induced suppression of inhibition (DSI). Metabotropic-induced variations involve suppression of excitation (MSE) or suppression of inhibition (MSI), operating over seconds. Repetitive low-frequency stimulation at excitatory synapses induces persistent eCB-mediated long-term depression (LTD), dependent on continuous eCB production. Once established, LTD becomes unresponsive to eCBs or CB1R. Effects of eCB-mediated plasticity hinge on CB_1R-expressing synapse activity and the connection between signals triggering eCB synthesis and CB_1R-containing presynaptic terminals. Beyond retrograde messaging, eCBs impact neuronal excitability through direct ion channel modulation, GIRK channel activation, and enhancement of hyperpolarization-activated cation channels (Ih). Furthermore, eCBs regulate various ion channels, including serotonin receptor type 3, TRPV1, $GABA_A$, and glycine, among others (Lu & Mackie, 2021). It is crucial to determine the specific conditions under which such modulation holds significance in vivo, as certain effects necessitate elevated concentrations of eCBs. The activation of G-protein-gated inwardly rectifying potassium (GIRK) channels by CB_1R represents a well-documented signaling pathway. Therefore, it's not surprising that when neuronal activity reaches high levels, eCBs are produced, leading to the activation of somatic CB_1R and the subsequent opening of GIRK channels. This process may operate either autonomously within a cell (i.e., as a form of self-inhibition) or in a non-cell autonomous manner (Bacci et al., 2004). Ih is a cation channel primarily found in dendrites, where it regulates dendritic excitability and plays a pivotal role in synaptic plasticity and learning (Shah, 2014). The enhancement of Ih activity can have a detrimental impact on learning. The activation of Ih by CB_1R has been proposed as a potential mechanism underlying THC-induced learning impairment. The coupling of Ih to dendritic CB_1R involves a signaling cascade that includes c-Jun-N-terminal kinase 1 (JNK1), guanylyl cyclase (cGMP), and hyperpolarization-activated cyclic nucleotide-gated (HCN) channels, ultimately leading to the augmentation of Ih (Maroso et al., 2016).

1.5. Degradation of endocannabinoids

Inactivation of eCBs occurs rapidly in vivo via cellular uptake and enzymatic hydrolysis. Fatty acid amide hydrolase (FAAH) is primarily responsible for the degradation of the AEA. Inactivation of 2-AG occurs preferentially through hydrolysis by the presynaptically localized monoacylglycerol lipase (MAGL) enzyme (Tripathi, 2020). To a lesser extent, 2-AG is also

metabolized by FAAH, serine hydrolase/hydrolase (ABDH) 6 and 12, and cyclooxygenase (COX) 2 (Bedse et al., 2014).

1.5.1. *Fatty Acid Amide Hydrolase (FAAH)*

FAAH is a member of the serine hydrolase family, residing within the cell membrane. This particular enzyme plays a pivotal role in breaking down bioactive lipids known as fatty acid amides (FAAs), both in the central nervous system and peripheral tissues (Tripathi, 2020). FAAH exhibits widespread distribution throughout the body. In rats, it is notably abundant in the liver, followed by the small intestine, testes, uterus, kidneys, ocular tissues, spleen, and potentially the lungs, whereas it is absent in skeletal muscle and the heart. However, any observed activity in the heart is likely attributed to FAAH found in the endothelial cells that line blood vessels (Maccarrone et al., 2000). Immunohistochemical investigations have revealed extensive FAAH distribution in principal neurons, including Purkinje cells in the cerebral cortex, pyramidal cells in both the cerebral cortex and hippocampus, and mitral cells in the olfactory bulb. The enzyme is also prominently expressed within intracellular membranes, such as the outer mitochondrial membrane and the smooth endoplasmic reticulum within the neuronal somatodendritic compartment (Papa et al., 2022). Its integration was detected in microsomal, mitochondrial, myelinated, and synaptosomal fractions, signifying regional variability in FAAH enzyme expression. The most notable enzyme activity was observed in the hippocampus and globus pallidus, while the brainstem exhibited the lowest activity. Additionally, FAAH predominantly localizes in large neurons that are postsynaptic to CB_1R (Tripathi, 2020). Neurochemical investigations conducted in FAAH knockout mice revealed a remarkable 10–15-fold increase in endogenous levels of AEA and other N-acetyl ethanolamines across various brain regions, including the cerebellum, hippocampus, and cortex (Crocq, 2020). Intriguingly, these heightened FAA levels within the central nervous system (CNS) exhibited a strong correlation with CB1R-mediated anxiolytic and analgesic effects. These collective findings underscore the pivotal role of FAAH as a central enzyme governing FAA catabolism in vivo and underscore its influence on pain pathways regulated by FAAH-controlled eCB tone (Tripathi, 2020). Moreover, the chemical inhibition of FAAH results in heightened neuronal signaling and serves as a countermeasure against neuroinflammatory responses and pain, including conditions associated with depression and anxiety (Huang et al., 2016). Consequently,

FAAH has emerged as a promising therapeutic target for various disorders affecting both the peripheral and CNS. In addition to their role in mitigating neuropathic pain and neuroinflammation, FAAH inhibitors have shown promise in addressing nicotine addiction and its associated effects (Justinova et al., 2015; Sloan et al., 2018). These effects manifest without any alterations in weight gain, mobility, sleep patterns, or other side effects commonly associated with direct CB_1R agonists (Tripathi, 2020). The primary function of FAAH inhibitors is to elevate the natural levels of AEA, thereby prolonging its physiological impact, and offering a potential therapeutic approach for various medical conditions (Greco et al., 2018).

1.5.2. *Monoacylglycerol Lipase (MAGL)*

MAGL is a soluble enzyme associated with cellular membranes, categorized within the serine hydrolase superfamily. MAGL exhibits a preference for hydrolyzing monoacylglycerols into glycerol and fatty acids, with no specific preference for sn-1(3) or 2-monoacylglycerols (MAG) (Staiano et al., 2016). MAGs are always short-lived lipid molecules that can originate from both intra- and extracellular sources. Among the significant MAGs, the eCB 2-AG stands out, as it can be metabolized into AA and glycerol (Maccarrone et al., 2000). In most tissues, including the brain, it has been observed that over 80% of 2-AG's hydrolytic activity is impeded by inhibiting MAGL, underscoring the predominant role of MAGL in the breakdown of 2-AG (Blankman et al., 2007). Additional research has suggested that MAGL may also play a role in the hydrolysis of glycerol esters of prostaglandins, which are inflammatory mediators (Savinainen et al., 2014). More recent studies have identified MAGL as an enzyme capable of breaking down fatty acid ethyl esters that form in response to alcohol consumption (Heier et al., 2016). MAGL exhibits high expression levels in various tissues, including the brain, liver, adipose tissue, and intestine, with its influence demonstrated through genetic and pharmacological inhibition studies in mice. Within the brain, MAGL is found in neurons, astrocytes, and oligodendrocytes, and to a lesser extent, in microglia (Maccarrone et al., 2000). AA, derived from 2-AG and AEA metabolism, serves as the primary precursor for the synthesis of proinflammatory prostaglandins. Given that physiological levels of 2-AG surpass those of AEA significantly, there has been a resurgence of interest in identifying inhibitors for the enzyme responsible for this process (Baggelaar et al., 2018). Nomura and colleagues established that MAGL plays a pivotal role as the primary enzyme providing AA for eicosanoid production

in specific tissues (Nomura, Lombardi, et al., 2011). Moreover, a multitude of studies, encompassing both genetic and pharmacological approaches, have firmly established the significant role of MAGL in the regulation of eCB and eicosanoid signaling pathways (Papa et al., 2022). The pharmacological inhibition of MAGL leads to an impressive 80% reduction in the hydrolytic activity of 2-AG in most tissues, including the brain. Consequently, MAGL emerges as a highly promising target for potential therapeutic interventions aimed at treating a range of disorders, such as neurodegenerative conditions, inflammation, metabolic disorders, and even cancer (Maccarrone et al., 2000). Traditionally, cannabinoids have been employed as pain relievers, and it's only in recent times that researchers have established a connection between ECS and inflammation (Mechoulam & Parker, 2013). Inflammatory mechanisms are consistently intertwined with various neurodegenerative conditions. Additionally, pain and inflammatory responses are recognized as common features of neurological diseases, including Alzheimer's Disease (AD), Parkinson's disease (PD), multiple sclerosis (MS), and stroke (Glass et al., 2010). Agonists for CB_1R and CB_2R, along with inhibitors of COX enzymes, have demonstrated their positive impact on various inflammatory conditions. Nevertheless, the application of COX-1 and 2 inhibitors has been restricted due to their potential to induce gastrointestinal and cardiovascular harm. Interestingly, MAGL has been identified as a factor that decreases AA and prostaglandin levels in certain tissues, indicating its promise as a therapeutic target for combating inflammation. In mice treated with lipopolysaccharide (LPS), the administration of a MAGL inhibitor led to a reduction in the production of prostaglandins and proinflammatory cytokines (Nomura, Lombardi, et al., 2011). Inhibition of MAGL exhibited neuroprotective effects in animal models of both PD and MS. The accumulation of 2-AG resulting from MAGL inhibition triggers the activation of CBR. Notably, these neuroprotective responses seem to be mediated not via the CBR-dependent pathway but by the reduction of proinflammatory eicosanoids. In animal models, the diminished neuroinflammatory responses were not reversed when CBR antagonists were administered. This suggests that the observed protective effects were predominantly a result of reduced levels of prostaglandins and cytokines within the brain. Nevertheless, it's worth noting that the long-term inhibition of MAGL, which leads to functional desensitization of the ECS, might also play a role in the neuroprotective response (Papa et al., 2022).
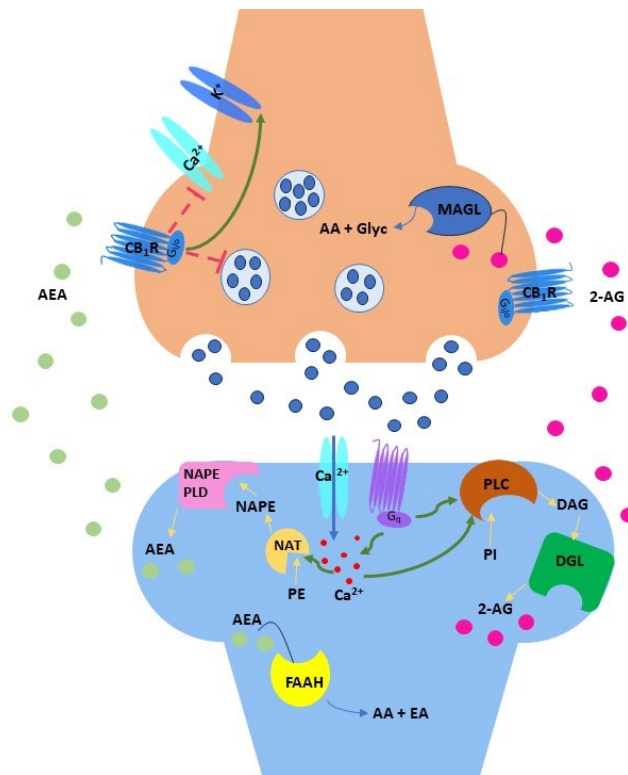
Figure 3: General model illustrating the endocannabinoid signaling from the biosynthetic pathways to degrading enzymes. Upon release of neurotransmitter (eg, glutamate), postsynaptic depolarization causes increased intracellular Ca^{2+} levels through activation of AMPA, NMDA receptors and/or Gq-coupled receptors (eg, mGluR1/5) and voltage-gated Ca^{2+} channels. Intracellular Ca^{2+} elevation increases endocannabinoid biosynthesis, although there is evidence for Ca^{2+}-independent forms of endocannabinoid synthesis as well. This model illustrates the two primary biosynthetic pathways for anandamide (AEA) and 2-arachidonoyl glycerol (2-AG), respectively. AEA is synthesized from phospholipid precursors (eg phosphatidylethanolamine, PE) by a Ca^{2+}-dependent transacylase, N-acyltransferase (NAT), yielding N-arachidonoyl PE (NAPE). NAPE is then hydrolyzed by a phospholipase D (NAPE-PLD) to yield AEA. Ca^{2+} influx and/or the activation of Gq-coupled receptors stimulate phospholipase C (PLC), which hydrolyses phosphatidylinositol (PI) into diacylglycerol (DAG). DAG is converted to 2-AG by diacylglycerol lipase (DGL). AEA and 2-AG then migrate from postsynaptic neurons to bind presynaptic-located cannabinoid type 1 receptors (CB_1Rs). Once activated, CB_1Rs couple through Gi/o proteins to inhibit adenylyl cyclase and regulate ion channels and ultimately suppress neurotransmitter release. Endocannabinoid signaling is then terminated by degrading enzymes. AEA is mainly hydrolyzed to arachidonic acid (AA) and ethanolamine (EA) by fatty acid amide hydrolase (FAAH), located postsynaptically. 2-AG is hydrolyzed presynaptically to AA and glycerol (Glyc) by monoacylglycerol lipase (MAGL).

2. *Therapeutic Potential of the Endocannabinoid System*

In recent years, there has been a growing interest in the potential of the ECS in influencing various aspects of health and disease. Its components are increasingly recognized as potential targets for pharmacotherapy across a broad spectrum of conditions, including but not limited to general pain, headaches, migraines, glaucoma, inflammation, mood and anxiety disorders, obesity/metabolic syndrome, osteoporosis, neuromotor and neuropsychological disorders, as well as neurodegenerative diseases. The ECS, due to its involvement in multiple physiological processes, presents promising avenues for the development of novel therapeutic drugs based on cannabinoids. These drugs can be designed to target various components and cell-signaling pathways within the ECS, with the ultimate goal of delivering therapeutic benefits (Lowe et al., 2021).

2.1. Neurological/neurodegenerative diseases

Neurodegenerative disorders are distinguished by inflammation and disruptions in normal neuronal function, often leading to the ongoing and progressive decline of neurons, as outlined in reference (Kubajewska & Constantinescu, 2010). This group of conditions encompasses AD, Huntington's disease (HD), PD, Amyotrophic lateral sclerosis (ALS), Batten disease, fatal familial insomnia, and, in certain hypotheses, schizophrenia (Basavarajappa et al., 2017). While these diseases lack a cure, cannabinoids have demonstrated the potential to alleviate some of the associated symptoms. In particular, cognitive impairments in AD patients are closely associated with disruptions in specific brain regions, particularly the frontal cortex, and the hippocampus, both of which are rich in CB_1R (Biegon & Kerman, 2001). Research has revealed that senile plaques present in AD patients exhibit the presence of CB_1R and CB_2R, and these are associated with markers indicating the activation of microglial cells. CB_2R levels were found to be elevated in AD patients and showed strong correlations with two key molecular markers of AD ($A\beta$-42 levels and senile plaque score), although not with cognitive function (Solas et al., 2013). An interesting observation was that the administration of WIN-55,212-2 (a CB_1R agonist) rescued AD-like pathology and mitigated learning and memory deficits induced by $A\beta$ in rats. In addition, cannabinoids like HU-210, WIN-55,212-2, and JWH-133 were found to prevent the activation of microglial cells induced by $A\beta$ in cultured glial cells (Basavarajappa et al., 2017).

Many studies suggest that eCBs are dysregulated in several brain regions of animal models of HD. There is a decline in cannabinoid signaling within the basal ganglia in HD. Furthermore, it has been established that the impairment of CB_1R function contributes to the progression of HD, exacerbating both the symptoms and neuropathological aspects in a mouse model expressing mutant Huntingtin exon 1 and lacking CB_1R (Blázquez et al., 2011). These findings suggest that CB_1R agonists or agents targeting the inactivation of eCBs could hold therapeutic promise for treating various manifestations of HD. The administration of CB_2R-specific agonists alleviated striatal neurodegeneration by activating microglia (Palazuelos et al., 2009). Elevated eCB activity in the globus pallidus has been linked to the manifestation of Parkinsonian symptoms. Although CB_1R is not highly prevalent in dopamine neurons of the substantia nigra, the presumed involvement of ECs in the degeneration of these neurons is apparent from various studies. URB597, an inhibitor of FAAH, demonstrated a protective effect by inhibiting the death of dopaminergic neurons, reducing microglial activity, and ameliorating motor impairments in mice lesioned with MPTP (Celorrio et al., 2016). Numerous research studies suggest that inflammation plays a significant role in the process of neurodegeneration. Given that cannabinoids exhibit both anti-inflammatory and neuroprotective properties, recent preclinical investigations provide compelling evidence indicating that CB_2Rs play a pivotal role in curbing the inflammatory responses triggered by microglial activation. The use of CB_2R selective agonists without the psychoactive effects may provide neuroprotection against the neurodegenerative processes of PD (Basavarajappa et al., 2017). Cannabinoids are recognized for their involvement in regulating inflammation, including neuroinflammation, and for their contributions to neuroprotection (Fernández-Ruiz et al., 2015). Furthermore, cannabinoids like CBD have exhibited analgesic, anxiolytic, and immunosuppressive qualities that could be beneficial in addressing certain neurological conditions (Choi et al., 2019). Additionally, cannabinoids have been associated with the modulation of adult neurogenesis in regions such as the hippocampus and lateral ventricles. Long-term administration of the synthetic cannabinoid HU-210, which targets both CB_1R and CB_2R, has been observed to enhance cell survival and proliferation in mouse models of hippocampal neurogenesis. This effect is attributed to its anxiolytic and antidepressant properties. Furthermore, several other synthetic cannabinoids, including JWH-133, AM1241, JWH-056, AM251, WIN55,212-2, and URB597, have also demonstrated the ability to promote neurogenesis (Prenderville et al., 2015). Several

studies highlight that the use of CB$_2$R agonists and CB$_1$R antagonists is an interesting, unique, and potential therapeutic advance for neurodegenerative disorders (Basavarajappa et al., 2017).

2.2. Mood and Anxiety Disorders

Anxiety represents the body's innate survival reaction to potentially harmful or threatening circumstances, marked by heightened reactivity, defensive instincts, and heightened vigilance. Neuropsychiatric conditions related to anxiety encompass panic disorder, social anxiety disorder (SAD), generalized anxiety disorder (GAD), posttraumatic stress disorder (PTSD), and obsessive-compulsive disorder (OCD) (Blessing et al., 2015). On a global scale, anxiety-related disorders stand as the most prevalent among all mental health conditions, presenting a substantial social and economic burden. The presently available anxiolytic and antidepressant drugs exhibit restricted response rates, limited tolerance, and undesirable side effects. Hence, cannabinoids hold promise as potential novel therapeutic agents, offering an alternative to conventional anxiolytics and antidepressants. The activation of the CB$_1$R plays a role in natural rewards, such as social interaction, sexual activity, enjoyable food, and the rewarding effects of pharmacological substances (Parsons & Hurd, 2015). Hence, CB$_1$R holds the potential to serve as a compelling novel target for the pharmacological management of mood and anxiety disorders (Lowe et al., 2021). Additionally, the ECS can influence the synaptic transmission of various neurotransmitters, including mesocorticolimbic dopamine, acetylcholine, glutamate, opioid peptides, and GABA. These neurotransmitters play a pivotal role in regulating our emotions and behaviors (Stampanoni Bassi et al., 2018). The CB$_1$R is notably abundant in the brain, particularly in regions associated with reward processing, including the amygdala, hippocampus, and orbitofrontal cortex (Koob & Volkow, 2010). Consequently, the ECS also plays a role in what can be termed as emotional cascades (Stampanoni Bassi et al., 2018). Moreover, genetic variations, such as single nucleotide polymorphisms (mutations), in the cannabinoid receptor 1 (CNR1) gene that encodes the CB$_1$R have been linked to conditions like depression, nicotine addiction, alcohol dependence, and potentially other substance use disorders that often stem from mood and anxiety disorders (Lowe et al., 2021).

2.3. General Pain

Pain is a symptom of many diseases. Both anecdotal accounts and scientific data substantiate the utilization of Cannabis Sativa L. and its secondary compounds for the alleviation of general pain. Furthermore, they exhibit efficacy in treating chronic pain, both as a standalone remedy and in combination with other drugs. Historical records even trace the use of Cannabis Sativa L. for pain management back to approximately 5000 years ago, as documented in the Chinese Pharmacopoeia. More recently, the ECS has emerged as a player in pain management, as cannabinoids have been found to interact with ECS components (Vučković et al., 2018). These components include non-CB_1R/ CB_2R cannabinoid receptors like GPR_{55}, G protein-coupled receptor 18 (GPR_{18}), also known as N-arachidonoyl glycine receptor (NAGly), as well as the opioid receptor, 5-hydroxytryptamine (5-HT) receptor, $TRPV_1$, and PPARα and γ (Lowe et al., 2021). Additionally, it's worth noting that in a mouse model, the GPR_{55} receptor regulates proinflammatory cytokines like IL-4, IL-10, IFN-γ, and GM-CSF, resulting in the alleviation of hyperalgesia (Staton et al., 2008). Inflammatory and nociceptive pain models have also shown antinociceptive effects with CB_2R antagonists. This action likely occurs through inhibition of AEA metabolism and could involve modulation of peroxisome proliferator-activated receptor α agonists, $TRPV_1$ antagonists, and α2-adrenergic receptor modulators (Anand et al., 2009).

2.4. Inflammation

Inflammation can be a common feature in various diseases, encompassing cancer, asthma, and autoimmune disorders like rheumatoid arthritis, hepatitis, colitis, MS, and various skin conditions. Cannabinoids, as a whole, exhibit potent anti-inflammatory characteristics. Both eCBs like AEA and 2-AG and phytocannabinoids such as Δ^9-THC and CBD have demonstrated their anti-inflammatory and immunosuppressive effects through CB_1R and CB_2R. These cannabinoids have been shown to effectively reduce the production of cytokines and chemokines, thereby exerting a suppressive influence on inflammatory responses (Nagarkatti et al., 2009). Inflammation is a complex process and the roles of eCBs and their biosynthetic and catabolic enzymes are not fully understood (Szafran et al., 2018). However, promising results are demonstrating that eCBs regulate the immune response at both an innate and adaptive level. Immune cells not only can be influenced but are also capable of generating and secreting eCBs

leading to the modulation of the production of factors involved in inflammation (Katchan et al., 2016). Preclinical studies demonstrate that the anti-inflammatory effects of eCBs are due to their direct action on immune cells. An example is in rheumatoid arthritis where one study, demonstrated that eCBs can block the progression of joint inflammation. The anti-inflammatory potential is attributable to the CB_2R which, with its protective action, includes the suppression of pro-inflammatory cytokines and the secretion of harmful proteinases as well as regulating the adhesion and migration of immune cells towards the inflamed joint (Barrie & Manolios, 2017). The ECS has been implicated in gastrointestinal physiology and homeostasis and the pathogenesis of inflammatory bowel disease, as confirmed by anecdotal data, human studies, epidemiological data, mouse models of colitis, and other pathophysiological conditions (Lowe et al., 2021). CB_2Rs are mainly expressed in cells of the immune system and may play a role in mucosal immunity. This notion gains support from the immunosuppressive characteristics exhibited by certain cannabinoids and their ability to hinder the generation of proinflammatory cytokines, likely mediated by CB_2R (Katchan et al., 2016). This implies a potential involvement of CB_2R in the regulation of gastrointestinal inflammation, including cases related to colitis. It is proposed that the ECS may contribute to immunomodulation in gastrointestinal inflammatory conditions. The presence of CB_2R in the gastrointestinal tract implies its potential involvement in controlling visceral sensitivity, managing pain, and overseeing gastrointestinal motility (Wright et al., 2008). Additionally, Methanandamide, an AEA analog resistant to hydrolysis, has been documented for its impact on mucosal proinflammatory reactions, specifically in the downregulation of proinflammatory cytokines like interferon-γ and tumor necrosis factor-α. The inflamed mucosal tissue in individuals with Inflammatory Bowel Disease (IBD) exhibited notably reduced levels of the eCB AEA (Di Sabatino et al., 2011). In research conducted by Storr and collaborators, it was suggested that medications aimed at inhibiting the breakdown of the ECS, which includes the regulation of FAAH expression, might hold potential as therapeutic candidates for managing IBD (Muller et al., 2019). In a distinct investigation conducted by Storr and associates, mouse models deficient in CB_2R and induced with trinitrobenzene sulfonic acid (TNBS)-related colitis were subjected to intraperitoneal injections of either CB_2R agonists (JWH133, AM1241) or the CB_2R antagonist AM630. Following a 3-day treatment, AM630 exacerbated colitis entirely, whereas JWH133 or AM1241 significantly ameliorated colitis (Storr et al., 2009).

2.5. Autoimmune diseases

Immune system disorders are the result of dysregulation (hypo- or hyperactivity) of the immune system. Autoimmune diseases, in particular, are characterized by an overactive immune system that leads to the production of antibodies attacking the body's tissues instead of foreign invaders. The ECS has been implicated in immune regulation, as both eCBs and synthetic cannabinoids (such as ajulemic acid, JWH-015, SR144528, and WIN55,212-12), along with phytocannabinoids (like Δ^9-THC and CBD), have demonstrated immunosuppressive properties, primarily through the apoptosis pathway (Nagarkatti et al., 2009). The ECS is proposed to hold therapeutic potential for various autoimmune and neurological disorders, CB_1R and CB_2R have been detected in microglial cells and are widely distributed throughout the CNS, which includes the brain and spinal cord (Katz et al., 2017). In particular, CB_2Rs are primarily found in immune system cells (Cabral et al., 2008). This is corroborated by the immunosuppressive characteristics exhibited by certain cannabinoids and their capacity to hinder the generation of proinflammatory cytokines, likely through interaction with CB_2R. By interacting with CB_1R and CB_2R, cannabinoids have been shown to trigger apoptosis in T cells and macrophages (Katchan et al., 2016). CB_1R and CB_2R are present in microglial cells, with CB_2R being more abundant, and their distribution and expression levels are believed to influence microglial function. Microglial cells share morphological, phenotypical, and functional characteristics with macrophages. In 'resting' macrophages, CB_2R is not typically observed (Lowe et al., 2021). Notably, among macrophages, inflammatory macrophages express the highest levels of CB_2R. This implies that cannabinoids may have a limited timeframe during which they can exert their therapeutic effects (Cabral et al., 2008). CB_1R is expressed in microglia at notably low levels. In both in vivo and in vitro contexts, the 2-AG engages with CB_2R, eliciting a chemotactic response. Conversely, exogenous cannabinoids like Δ^9-THC and CP55940 interact with CB_2R to hinder microglial chemotaxis induced by Acanthamoeba Culbertson, an opportunistic pathogen linked to Granulomatous Amoebic Encephalitis (Lowe et al., 2021). The anti-inflammatory properties of cannabinoids have positioned them as potential therapies for managing inflammation associated with autoimmune conditions such as type 1 diabetes mellitus, MS, and neuropathic pain (Katchan et al., 2016). In animal models of experimental autoimmune encephalomyelitis and MS, cannabinoids have exhibited the ability to suppress experimental autoimmune encephalomyelitis through the activation of CB_1R expressed in neurons. Experimental

autoimmune encephalomyelitis-related inflammation has also been demonstrated to be regulated by CB$_2$R expressed in encephalitogenic T cells (Maresz et al., 2007). The absence of CB$_2$R in these T cells aggravated the progression of experimental autoimmune encephalomyelitis, leading to elevated production and propagation of inflammatory cytokines, and additionally rendering these T cells resistant to apoptosis (Lowe et al., 2021). This CB$_2$R function was substantiated in research conducted by Stipe and fellow researchers, who examined the impact of a dinucleotide polymorphism within a human gene on the suppression of eCB-induced T-cell proliferation. The CB$_2$R cDNA polymorphism at positions 188–189 (AA to GG) arises from the substitution of glutamate with arginine at amino acid position 63. It is believed that the frequency of this polymorphism is elevated in autoimmune diseases. In summary, genetic variations in the CB$_2$R gene are proposed to increase an individual's susceptibility to autoimmune conditions (Sipe et al., 2005). Given their immunomodulatory, immunosuppressive, and analgesic properties, cannabinoids hold promise as therapeutic agents for managing rheumatoid arthritis (Lowe et al., 2021). CB$_2$R is considered a potential therapeutic target for addressing rheumatoid arthritis, as indicated by its heightened expression in synovial tissues within rheumatoid joints. A selective CB$_2$R agonist, JWH133, was found to suppress the production of inflammatory mediators like IL-6, matrix metalloproteinase-3 (MMP-3), and chemokine ligand 2 (CCL2) in fibroblast-like synoviocytes stimulated by CB$_2$R in rheumatoid joint-derived synovial tissues (Moreno et al., 2018). Additionally, JWH133 inhibited osteoclast formation in peripheral blood monocytes, a process also involved in rheumatoid arthritis (M. Zhu et al., 2019). In a rheumatoid arthritis mouse model, another CB$_2$R agonist, JWH-015, exhibited anti-inflammatory effects against interleukin-1β-induced inflammation in rheumatoid arthritis synovial fibroblasts, partially through glucocorticoid receptor activation (Fechtner et al., 2019).

2.6. Cancer

Cannabinoids have demonstrated well-established analgesic, antinausea, antidepressant, antiemetic, antinociceptive, and orexigenic properties and, consequently, have been studied and used in the treatment of cancer patients undergoing chemotherapy or radiotherapy and in AIDS/HIV patients. Beyond the widely recognized symptom-relief effects of Δ^9-THC and CBD in cancer-related conditions, numerous natural, endogenous, and synthetic cannabinoids exhibit

their potential anticancer attributes through various suggested mechanisms. These mechanisms encompass, but are not confined to, the initiation of apoptosis, autophagy, and cell cycle halt, along with the inhibition of processes such as tumor cell migration, metastasis, angiogenesis, neovascularization, adhesion, and invasion (Lowe et al., 2021). These characteristics are most likely linked to their involvement in the endocannabinoid signaling pathways associated with tumor-related processes. These pathways encompass the MEK extracellular signal-regulated kinase signaling cascade and the adenylate cyclase cyclic AMP-protein kinase-A pathway (Rosengren & Cridge, 2013). In conclusion, harnessing cannabinoids to modulate ECS signaling associated with the development of these tumors is an extremely promising avenue that is gaining growing recognition in the medical field. Multiple studies additionally affirm the clear relationship between the heightened expression of the mentioned CBR, eCBs metabolic enzymes, and endogenous ligands within cancerous tissues (Lowe et al., 2021). Interactions among tumor cells have been found to involve cannabinoid signaling (Chakravarti et al., 2014). There is a study proposing that the ECS might contribute to tumor suppression (Velasco et al., 2016). Multiple research investigations have further established the apoptotic, anti-metastatic, anti-angiogenic, and anti-inflammatory qualities of both cannabinoid and non-cannabinoid secondary compounds found in Cannabis Sativa L. This implies that therapies based on cannabinoids hold promise for treating various cancer types, in addition to the previously mentioned disorders. Cannabinoids like AEA, Met-F-AEA, 2-AG, Δ^9-THC, CBD, CBDA, HU120, WIN-552122, JWH-133, AME121, and R-(+)-MET have all exhibited anti-cancer properties in diverse cancer models, including breast, lung, prostate, testicular, stomach, skin, colon, bone cancer, glioblastomas, lymphomas, leukemias, and neuroblastomas. These cannabinoids operate through various mechanisms in these tumors, spanning from triggering apoptosis and halting the cell cycle to suppressing DNA synthesis, hindering multiple signaling pathways like PI3K/AKT/mTOR/AMPK or EGF/EGFR, restraining angiogenesis, impeding tumor growth, inducing tumor regression, and curtailing metastasis (Lowe et al., 2021).

2.7. Cardiovascular Diseases

The ECS exhibits minimal expression in a healthy individual's heart; however, this dynamic undergoes significant changes during the progression of various cardiovascular diseases (CVDs). As a response to prolonged deviations from homeostasis, the ECS loses its regulation

and transitions into a pathological signaling mechanism. This dual nature of the ECS is notably characterized by alterations in CBR expression and changes in the concentration of eCBs. Specifically, eCBs, when binding to CB_2R on immune cells, induce anti-inflammatory effects. Conversely, when the same eCBs bind to upregulated CB_1R on stressed cardiomyocytes, they activate pro-apoptotic signals, such as increased levels of reactive oxygen species (ROS) and intracellular Ca^{2+} (Rabino et al., 2021). The ECS has the potential to influence both acute and chronic cardiac disorders, particularly those associated with ischemia/reperfusion (I/R) injury. Bouchard and colleagues conducted a study where they showed that after brief ischemic pre-/post-conditioning (IPC), the cardioprotective effects were inhibited when both CB_1R and CB_2R were antagonized, indicating the involvement of both receptors in IPC-induced cardioprotection. Notably, in a rat model of I/R injury caused by coronary occlusion and re-occlusion, AEA reduced both the infarct size and ventricular arrhythmias by activating CB_2R, rather than ATP-dependent K^+ channels (Rabino et al., 2021). Consistent findings were reported in another in vivo study using a mouse model of myocardial I/R injury, where a potent agonist for both CB_1R and CB_2R (WIN 55,212-2) was found to reduce leukocyte-mediated myocardial damage. This effect was likely mediated through CB_2, as the administration of a CB_2 antagonist (AM630) negated the cardioprotective effects (Di Filippo et al., 2004). Immune cells constitute the primary source of eCBs within the cardiovascular system. Consequently, it is not surprising that the ECS can exert influence over immune functions, potentially offering therapeutic benefits in managing CVDs, notably atherosclerosis, which prominently involves inflammation. Among the CBR, CB_2R, primarily associated with immune system regulation, is notably abundant in bone marrow (BM), lymphoid tissues, and various immune cells (Fulmer & Thewke, 2018). Consequently, it has been proposed that the protective immunomodulatory effects of eCBs may be mediated by CB_2R, while pro-atherosclerotic effects could be linked to CB_1R. The selective activation of CB_2R has demonstrated the ability to diminish the CD36-dependent buildup of oxidized low-density lipoprotein, a significant contributor to atherosclerosis. Additionally, it has influenced the secretion of inflammatory cytokines by foam cells, further emphasizing its potential in modulating atherosclerosis-related inflammation (Chiurchiù et al., 2014). The ECS might be involved in regulating blood pressure through mechanisms operating in both the central and peripheral systems. When cannabinoids are administered centrally, their effects can vary from sympathoinhibition to sympathoexcitation, depending on the specific injection site. In terms of peripheral mechanisms, the activation of

cardiac CB_1R receptors leads to negative chronotropic and ionotropic effects, which potentially occur independently of the central nervous system (Haspula & Clark, 2020). During hypertension (HT), the ECS becomes overactive as a compensatory mechanism aimed at limiting elevated blood pressure (BP) and reducing myocardial workload. This overactivity is characterized by continuous ECS stimulation, primarily due to increased CB_1R expression in cardiac and vascular endothelial cells. This connection was corroborated by Gorelick and colleagues, who found that symptomatic hypotension in cannabis smokers could be reversed by administering a CB_1R antagonist called rimonabant. Drugs that increase basal levels of eCBs are frequently investigated as HT treatments (Rabino et al., 2021). Numerous cardiac rhythm abnormalities associated with cannabis use have been documented, including atrial fibrillation/flutter, atrioventricular block/asystole, sick sinus syndrome, ventricular tachycardia, and Brugada-like patterns (Singh et al., 2018). Specifically, smoking cannabis can lead to arrhythmias linked to atrial fibrillation. Regarding the potential therapeutic applications of targeting the ECS, research has explored the impact of CBD on the occurrence and progression of cardiac arrhythmias during and after ischemia. Walsh et al. found that CBD effectively reduced the total number of ischemia-induced arrhythmias and the size of infarctions in a dose-dependent manner when administered just before the onset of ischemia (Walsh et al., 2010).

2.8. Diabetes

Diabetes, a metabolic disorder characterized by elevated blood sugar levels, poses a substantial risk for CVD, including conditions like stroke, vascular disease, and coronary heart disease. It exerts its damaging effects on the nerves and blood vessels within the cardiovascular system, potentially impacting other organs such as the eyes and kidneys (Lowe et al., 2021). CB_1R seems to emerge as a promising therapeutic target for managing Type 2 diabetes (T2DM), given the demonstrated involvement of the ECS in the insulin resistance commonly associated with T2DM (Jourdan et al., 2013). The ECS has also been implicated in regulating normal appetite, determining the desirability of food, maintaining weight, and addressing issues related to obesity. This is supported by evidence showing that cannabimimetic drugs, which interact with the ECS, can influence obesity. For instance, SR141716A, a potent and selective antagonist of the CB_1R found throughout the brain, has demonstrated its ability to impact eating behaviors and reduce the consumption of a highly appealing cane sugar mixture in marmosets.

SR141716A has exhibited the capability to regulate the desire, motivation, and physical activity associated with the consumption of alcoholic beverages, with its effects varying based on dosage. This suggests that SR141716A could have potential applications in the treatment of alcoholism (Scopinho et al., 2011). Additionally, the cannabinoid CB_1R agonist CP55940, known as (-)-cis-3-[2-hydroxy-4-(1,1-dimethylheptyl)phenyl]-trans-4-(3-hydroxypropyl) cyclohexanol, has been demonstrated to stimulate a preference for flavorful drinks. Disruptions in eCB signaling may contribute to the development of eating disorders. This is evident from the increased expression of CB_1R mRNA in the blood of individuals with anorexia nervosa and bulimia nervosa, as well as the notable reduction in body weight loss and physical activity on running wheels observed in an activity-based anorexia animal model when treated with the CB_1R/ CB_2R agonist Δ^9-THC and the synthetic CB_1R/ CB_2R agonist CP55940 (Scherma et al., 2017).

2.9. Respiratory Diseases

Studies examining cannabinoid receptor expression and function in the respiratory system are limited and unclear. Both CB_1R and CB_2R are expressed in human lung tissue and bronchi, however, CB_1R receptor expression is higher (Turcotte et al., 2016). Respiratory epithelial cells display both CB_1R and CB_2R (Fantauzzi et al., 2020). The pulmonary arteries also express CB_1R and CB_2R but with a predominance of CB_1R (Karpińska et al., 2017). The expression of CB_2R on fibroblasts and CB_1R receptors on alveolar type II cells has been confirmed in cultures of rodent cells. While various antifibrotic treatments exist for pulmonary fibrosis, the current available options have proven to be insufficient. Activation of CB_2R has been shown to exert an anti-fibrotic effect, as demonstrated in studies utilizing both agonists and antagonists of these receptors (Kicman et al., 2021). In an in vitro study, the CB_2R agonist, JWH-133, effectively inhibited the proliferation and migration of fibroblasts induced by transforming growth factor β1 (TGF-β1). This treatment also resulted in reduced levels of α-smooth muscle actin (α-SMA) and collagen I, along with decreased mRNA levels for these proteins (Fu et al., 2017). These beneficial effects were attributed to the direct activation of CB_2Rs. Conversely, the administration of a CB_2R antagonist, AM630, had the opposite effect, increasing pulmonary fibrosis and promoting the deposition of α-SMA and connective tissue growth factor. This observation further underscores the role of CB_2Rs in mediating an anti-fibrotic response

(Wawryk-Gawda et al., 2018). The CBRs are also implicated in asthma symptoms. Giannini et al. reported a beneficial impact of CP55940 in the ovalbumin-induced asthma model. CP55940 alleviated asthma symptoms such as breathlessness and coughing. Examination of lung tissues indicated a reduction in pathological changes and DNA damage caused by free radicals, subsequently leading to a decrease in the levels of a DNA damage marker, 8-hydroxy-2′-deoxyguanosine. In bronchoalveolar lavage fluid, CP55940 treatment resulted in lowered concentrations of TNF-α and prostaglandin PGD2. CP55940's effects were contingent on the activation of both CBRs, but its anti-inflammatory properties were primarily mediated by CB_2R situated on mast cells and eosinophils. The reduction in breathing abnormalities was attributed to the activation of CB_1R receptors located on the axon terminals of postganglionic vagal nerves (Giannini et al., 2008). CBRs are found on pulmonary macrophages and dendritic cells in the respiratory system and other immune system cells recruited in respiratory diseases (Fu et al., 2017). Remarkably, lung cancer cells have also been found to express CBR. The presence of both CB_1R and CB_2R has been verified in cancerous tissue sourced from individuals afflicted with non-small-cell lung carcinoma through immunohistochemical staining. Additionally, these receptors have been identified in human lung cancer cell lines like A549 and SW-1573, confirmed through reverse transcription polymerase chain reaction or Western blot analysis (Kicman et al., 2021). Interestingly, an upregulation of CBRs has been linked to extended survival in patients (Milian et al., 2020). Nevertheless, according to Xu et al., increased CB_2R expression was indicative of a less favorable prognosis. The assessment of CBR expression holds promise as a potential tumor marker, yet further investigation is required to elucidate the relationship between CBR and the severity, stage, and specific types of lung cancer (Xu et al., 2019). Aside from their potential in cancer treatment, FAAH and MAGL inhibitors have demonstrated significant therapeutic promise in models of acute lung injury and pulmonary ischemia-reperfusion injury. According to another study, JZL184 effectively reduced lung damage and pathological alterations observed in bronchoalveolar lavage fluid. Similarly, as reported by Yin et al., URB937 enhanced oxygenation rates, reduced the lung's wet/dry ratio (W/D ratio), and mitigated histopathological lung changes. Comparable outcomes were achieved in a pulmonary ischemia-reperfusion injury model using URB602, as indicated by Xiong et al. The favorable effects of FAAH and MAGL inhibitors are likely attributed to their ability to inhibit the hydrolysis of 2-AG and AEA, leading to CBR activation and a decrease in

the production of AEA and 2-AG metabolites, particularly AA metabolites, which are known mediators of inflammation (Xiong et al., 2018; Yin et al., 2019).

2.10.   *Migraine*

Migraine is a complex and highly debilitating neurological disorder, and its treatment remains a significant challenge for many patients, even with the recent introduction of the first specific preventive drugs, namely monoclonal antibodies targeting calcitonin gene-related peptide (Goadsby et al., 2017). Consequently, researchers in the field of headache medicine are actively exploring new therapeutic avenues. Preclinical and clinical evidence indicates a potential role for eCBs and related lipids, including palmitoylethanolamide (PEA), in the management of migraine-related pain. Notably, research has been particularly focused on modulating eCB tone through the inhibition of enzymes responsible for eCB breakdown in animal models of migraine-related pain. Pini et al. conducted a study in which they examined the effects of a synthetic cannabinoid called Nabilone in individuals suffering from medication-overuse headaches. They observed reductions in both the duration and intensity of pain, as well as a decrease in the daily consumption of analgesic medications among the participants. The concept of eCB deficiency in migraine pathophysiology was initially proposed in the early 2000s. This theory gained support from subsequent research, which revealed elevated activity of both FAAH and the AEA transporter in female migraine patients compared to control subjects (Greco et al., 2022). Additionally, a positron emission tomography (PET) study demonstrated increased CB_1R binding in specific brain regions involved in pain processing among individuals with episodic migraine (EM) (Van Der Schueren et al., 2012). This heightened CB_1R activity, linked to changes in the gene expression of metabolic enzymes, was also observed in peripheral blood mononuclear cells, suggesting that these cells may serve as a reflection of cerebral alterations (Greco, Demartini, Zanaboni, Tumelero, et al., 2021). Plasma levels of AEA and PEA were not found to differ between patients with EM and healthy individuals. However, it's worth noting that PEA plasma levels were observed to increase during the ictal phase of experimentally induced migraine-like attacks triggered by nitroglycerin (NTG) administration (De Icco et al., 2021). This suggests that the release of PEA could be a compensatory mechanism aimed at counteracting the neurovascular changes that occur during the early phase of NTG-induced attacks. There is preliminary evidence indicating the potential utility of PEA in preventing

migraine attacks in both adult and pediatric populations, offering a novel therapeutic approach for managing this condition. PEA may exert indirect effects on CBRs, FAAH expression, and TRPV$_1$ channels. By inhibiting FAAH, PEA could modulate anandamide levels, which, in turn, may stimulate CB$_2$R or CB$_1$R receptors or desensitize TRPV$_1$ channels, thereby mediating analgesic and anti-inflammatory effects (Greco et al., 2022). Experimental models of migraine have also shown alterations in the ECS, suggesting that targeting this system or related compounds could offer potential avenues for future therapeutic approaches. For instance, in an animal model of migraine induced by NTG, increased activity of FAAH and MAGL enzymes was observed, along with a heightened number of CBR binding sites in the mesencephalon four hours after NTG administration (Greco et al., 2018). Additionally, heightened FAAH activity was noted in the hypothalamus and medulla. These findings indicate that ECS dysregulation could be a part of migraine's pathophysiology, or it may represent an adaptive response to the migraine condition. In the same migraine model, the administration of AEA led to a reduction in NTG-induced hyperalgesia, as observed in the plantar formalin test, and a decrease in neuronal activation within the trigeminal nucleus caudalis (Greco et al., 2011). This effect is likely attributed to the activation of CB$_1$R and CB$_2$ receptors. AEA has demonstrated a significant reduction in neurogenic inflammation in various animal models of migraine (Greco et al., 2022). The systemic administration of the peripherally restricted FAAH inhibitor URB937 demonstrated a reduction in NTG-induced trigeminal and spinal hyperalgesia in rats. This effect coincided with elevated levels of anandamide and PEA and reduced mRNA expression of CGRP, substance P, TNF-α, and IL-6 in the trigeminal ganglion. Similar outcomes were observed in the acute NTG model when rats were pre-treated with URB597, a global FAAH inhibitor. Specifically, we found that URB597 had a regulatory effect on NTG-induced neuronal activation in structures associated with migraine-related pain, including the trigeminal nucleus caudalis (Greco, Demartini, Zanaboni, Casini, et al., 2021). Correspondingly, research by Nozaki et al. also indicated that URB597, when administered 2 hours before NTG, abolished NTG-induced mechanical allodynia and c-Fos expression in the trigeminal nucleus caudalis in mice. Of interest, using the dual FAAH/MAGL inhibitor JZL195 in the NTG model, recently suggested a synergistic role for AEA and 2-AG in trigeminal pain modulation (Greco, Demartini, Francavilla, et al., 2021).

2.11. *Glaucoma*

Glaucoma is an incurable eye condition leading to the gradual loss of retinal ganglion cells (RGCs). Currently, the only alterable risk factor is intraocular pressure (IOP) and reducing IOP can decrease the risk of glaucoma progression. The ECS has garnered significant interest as a potential therapeutic avenue for glaucoma treatment, primarily due to the observed IOP-reducing effects following the administration of external cannabinoids. Nevertheless, recent findings indicate that ECS modulation might also have neuroprotective properties (Cairns et al., 2016). The ECS is distributed throughout various ocular tissues, including those involved in regulating IOP and the retina. Both eCBs, 2-AG and AEA, are present in the eye, except for the lens (Chen et al., 2005). CB_1R can be found in the ciliary body, trabecular meshwork, Schlemm's canal, and retina. Regarding CB_2R, there has been some debate over their localization. Some studies have indicated CB_2R expression in the retina, while others have struggled to confirm this due to the lack of reliable immunohistochemical markers (Cairns et al., 2016). All current pharmacotherapies for glaucoma primarily focus on reducing IOP (Carta et al., 2012). Cannabinoids have shown the ability to modulate IOP, which has been consistently demonstrated in various studies using both endogenous and exogenous cannabinoids in rodents, rabbits, and nonhuman primates. Several small-scale human studies have reported the effectiveness of the natural phytocannabinoid Δ^9-THC and the synthetic CB_1R agonist WIN 55,212-2 in lowering IOP. While the hypotensive effects of cannabinoids on IOP are primarily attributed to their action at CB_1R, it is important to note that these effects on IOP may also involve CB1R-independent mechanisms (Cairns et al., 2016). Numerous studies investigating the modulation of the ECS in glaucoma models have unveiled that, beyond their ability to lower IOP, ECS modulation exhibits neuroprotective effects. This neuroprotection extends to the use of compounds that directly target CBR, as well as substances that influence cannabinoid metabolism. Furthermore, these compounds have displayed their neuroprotective attributes in models of RGC loss that are not reliant on elevated pressure, such as scenarios involving neural excitotoxicity and axotomy (Pinar-Sueiro et al., 2013; Slusar et al., 2013). This suggests that ECS modulation may confer neuroprotection to the retina independently of any alterations in IOP. Strategies that reestablish or increase eCB levels may provide retinal neuroprotection. FAAH inhibition has proven effective in mitigating RGC damage induced by transient high IOP-induced ischemia, resulting in reduced RGC loss with URB597 administration. The

neuroprotective effects of FAAH inhibition were attributed to actions on both CB_1R and $TRPV_1$. Notably, URB597 also exhibited neuroprotection in a pressure-independent RGC loss model (axotomy), suggesting partial independence from IOP modulation (Nucci et al., 2007).

2.12.   Osteoporosis

Bone remodeling is an ongoing cycle involving osteoclast-driven resorption and osteoblast-driven formation. This crucial process maintains ideal bone density, structure, and strength, and any imbalance can result in conditions such as osteoporosis (Florencio-Silva et al., 2015). In 2001, osteoporosis was defined as a "skeletal disorder characterized by weakened bone strength, predisposing individuals to an elevated risk of fractures. This bone strength primarily results from the combination of bone density and bone quality (Miller, 2016). Numerous components of the ECS are present in bone tissue. This includes the presence of CBR and the enzymes responsible for eCB synthesis, in osteoclasts, osteoblasts, and bone marrow cells (Idris et al., 2005). Furthermore, the primary eCBs, 2-AG and AEA, are locally produced within bone tissue by osteoblasts and osteoclasts. AEA, which selectively activates CB_2R, has been shown to promote osteoblast proliferation in vitro. Additionally, research has identified the presence of the biosynthetic and degrading enzymes responsible for 2-AG and AEA, NAPE-PLD, and FAAH, in bone cells eCBs also impact the process of bone remodeling (Bab et al., 2009). For instance, the deactivation of CB_1R results in higher bone mineral density (BMD) due to a reduction in osteoclast activity. Additionally, research findings suggest that CB_1R is expressed in sympathetic neurons that innervate bone, indicating its potential involvement in a neural mechanism that helps regulate bone turnover (Clouse et al., 2022). CB_1R-deficient ($CB_1 (-/-)$) mice exhibit higher BMD compared to control mice, as well as impaired osteoclast differentiation, protecting against osteoporosis (Idris et al., 2005). These findings demonstrate that CB_1R plays pivotal roles in both osteoblasts and osteoclasts, thereby influencing the equilibrium of bone remodeling (Idris & Ralston, 2010). CB_2R plays a significant role in regulating osteoclast activity and bone resorption. It is highly expressed in osteoblasts, osteocytes, and osteoclasts. When CB_2R is stimulated in osteoblast precursor cells, it increases the number of pre-osteoblastic cells and enhances alkaline phosphatase activity, which promotes matrix mineralization. Additionally, CB_2R activation reduces the count and activity of human multinucleated osteoclasts, potentially decreasing bone resorption. CB_2R signaling also

mediates the differentiation of monocytes into mature osteoclasts. Furthermore, CB_2R-selective agonists in breast cancer cells enhance PI3K/AKT activity, leading to increased levels of osteolytic and osteogenic factors. Mice lacking either CB_1R or CB_2R showed abnormal bone phenotypes, such as an increase in BMD as well as protection against ovariectomy-induced bone loss, confirming that the ECS has a role in regulating bone mass (Clouse et al., 2022). Recent research has shown that CB_1R hurts the release of norepinephrine from synaptic nerve terminals, which subsequently hinders bone formation by interacting with the osteoblastic adrenergic β_2 receptor. When 2-AG activates CB_1R, it inhibits norepinephrine release, thus promoting the formation of new bone. Additionally, heightened CB_1R expression enhances the survival of mesenchymal stem cells during the process of osteogenesis in vitro (Gowran et al., 2013). The formation of osteoclasts was reduced when selective antagonists for CB_1R and CB_2R, namely AM251 and SR144528, were used, and it was enhanced when CBR agonists were applied (Clouse et al., 2022). The deficiency of CB_2R has been shown to negatively impact both bone loss and formation, as indicated by several studies. Additionally, AEA has been associated with stimulating the proliferation of osteoblasts in vitro and increasing the number of osteoclasts (Idris et al., 2005). The activation of CB_2R by HU308 promotes the generation of new bone, thereby offering protection against bone loss resulting from estrogen deficiency. Additionally, CB_2R agonists exhibit anti-inflammatory properties, reducing the expression of cytokines that promote bone resorption, while increasing the expression of TNF and IL-1 receptors, along with their antagonist. These effects contribute to the inhibition of osteoclast formation (Ofek et al., 2006).

3. *Multi-Target Approach on Endocannabinoid System*

Traditional research has generally focused on creating extremely precise molecules with minimal or no unintended interactions with other targets, aiming to reduce the molecule's potential side effects. This strategy has proven effective, particularly in the case of straightforward illnesses with well-understood mechanisms. Nevertheless, in the case of intricate and multifaceted diseases like cancer, CNS disorders, and infections, a single-target strategy proves less efficacious (Tan et al., 2016). For these conditions, a multi-target approach can be significantly more beneficial as it addresses a multitude of proteins and pathways implicated in the initiation and progression of the disease (Proschak et al., 2019). In the

traditional approach to molecule design, the objective was to identify a primary structure capable of selectively binding to a specific target, such as an enzyme or a receptor. This approach can be succinctly described as a medication that focuses on a molecular target, the modification of which initiates an observable pharmacodynamic response (Papa et al., 2022). The primary advantage attributed to the drug was its limited binding to targets other than the principal one, as it was believed to provide a reduced risk of adverse effects (Proschak et al., 2019). Nevertheless, recent advancements in biochemical and molecular sciences indicate that this approach appears overly straightforward for developing contemporary drugs to treat complex, multifactorial diseases (Ryszkiewicz et al., 2023). Paradoxically, what was once seen as a factor greatly compromising the safety of prospective therapeutic molecules – namely, off-target effects arising from their affinity with unintended targets – has evolved into a driving force for a wholly new paradigm. The happenstance and accidental discovery of new targets after drug approval have now transformed into a meticulously orchestrated process long before the registration phase commences (Lamens & Bajorath, 2023). It is for this reason that many research groups are now opting for multi-targeted drug design, considering the many advantages it has over conventional single-target drug design. Several studies have shown that, although a drug is highly specific for its target, it may fail to achieve the necessary therapeutic effect, thus demonstrating the need for a multi-target approach (Peters, 2013). Notably, the ECS is closely related to other systems and cooperates to regulate many cognitive and physiological processes, mainly through the control of GABAergic and glutamatergic neurons in the synaptic terminals of many brain areas involved in emotional behaviors, including social and cognitive activity (Lu & Mackie, 2021). Thanks to interconnections with other systems, the ECS is attracting new interest in many neurological and neuropsychiatric diseases (Vitale et al., 2021). Several studies have provided evidence that GPCRs, including CBR, can form dimers or higher-order complexes, influencing receptor signaling, trafficking, and ligand binding (Farran, 2017; Franco et al., 2016). Although the physiological significance of this dimerization in CBR has not been entirely elucidated, recent years have witnessed extensive reports of the presence of both homo- and heterodimeric CBR in specific tissues (Morales & Reggio, 2017). A significant interplay has been discovered between the ECS and the dopaminergic system. Dopamine, a crucial neurotransmitter in the brain, holds a key role in functions such as learning, motivation, reward processing, emotions, executive functions, and motor control (Klein et al., 2019). The ECS serves as a localized input filter in the midbrain and terminal regions, influencing the processing

of incoming information to modulate its transmission to dopamine neurons and their target destinations (Covey et al., 2017). Several research studies strongly indicate that eCBs influence dopamine levels through different neuronal subgroups, including GABAergic and glutamatergic neurons (Papa et al., 2022). The dopamine system also holds a pivotal role in the development of dependence and withdrawal from various substances. Commonly abused substances like cocaine, amphetamines, morphine, nicotine, and alcohol elevate extracellular dopamine levels in the striatum. Consequently, modulating the ECS could present a promising avenue for novel therapeutic strategies in addressing withdrawal and substance abuse across various scenarios (Sagheddu et al., 2015). The interaction between the ECS and the dopaminergic system is highly intricate and intricate, influencing all neurobehavioral aspects controlled by dopamine. These aspects encompass motivation and reward, which are fundamental for the pursuit of needs ranging from basic survival instincts to higher aspirations like self-realization (Laksmidewi & Soejitno, 2021). Furthermore, eCBs also engage with the serotonergic system, with extensive reports on their joint behavioral effects. This interaction extends to the regulation of emotional states, stress management, cognitive functions, appetite control, and sleep regulation. Remarkably, there is a notable overlap in the distribution patterns of the serotonergic system and the ECS in the brain, leading to numerous studies highlighting their functional interaction and even close interdependence in modulating endocannabinoid and serotonin signaling (Colangeli et al., 2021). Additionally, the ECS exhibits a significant interaction with the cholinergic system. Studies have indicated that the activation of M_1 muscarinic receptors leads to tonic inhibition of endocannabinoid release at glutamatergic synapses by suppressing channel-mediated calcium currents (Wang et al., 2006). Within the striatum, acetylcholine (ACh), acting on M_1 muscarinic receptors, continuously enhances depolarization-induced eCB release from medium-spiny neurons. These released eCBs transiently suppress inhibitory synaptic inputs to medium spiny neurons by retrogradely activating presynaptic CB_1Rs. Hence, the regulation of the muscarinic system over the production and release of eCBs in the striatum may play a role in motor control (Narushima et al., 2007).

3.1. Cannabinoid Receptor Heteromers

CBRs can form heteromers with various GPCRs. Increasing evidence indicates an important role of heteromer formation among various GPCRs in modulating receptor function. However,

determining the functional characteristics of heteromers and, especially, identifying heteromers in tissue often presents a challenge. It has been demonstrated that CB_1R and CB_2R can form heteromers and the specific characteristic of CB_1R - CB_2R heteromers is bidirectional cross-antagonism (meaning the ability of CB_1R antagonists to block the effects of CB_2R agonists and, conversely, the ability of CB_2R antagonists to block the effects of CB_1R agonists) (Callén et al., 2012). Therefore, both CB_1R and CB_2R may negatively modulate each other in signaling pathways involving eCBs, such as brain development and neural cell differentiation (López-Carballo et al., 2002). Specifically, CB_1R - CB_2R heteromers can have a profound impact on the function of the CNS in a variety of neurological and immunological systems, and data suggest that these heteromers should be considered when designing therapeutic approaches for disorders involving the endocannabinoid system (Callén et al., 2012). Furthermore, CB_1R is believed to form heteromers under specific conditions with various receptors, including serotonin, angiotensin, opioid, GPR_{55}, somatostatin, dopamine, and adenosine receptors, among others. While there is less research on CB_2R, recent studies have revealed its ability to create heterodimers with the GPR_{55}, $5-HT_{1A}R$, or chemokine receptor $CXCR_4$ (Papa et al., 2022). The presence of these heterodimers has been linked to various medical conditions. CBRs interact with GPR_{55} and these heteromers seem to be implicated in PD (Martínez-Pinilla et al., 2020). $CB_1R-A_{2A}R$ and CB_1R-D_2R heteromers have been suggested to have physiological implications in neurodegenerative disorders such as AD, PD, epilepsy, and autism, as well as in neuropsychiatric disorders like anxiety, depression, and psychotic conditions. The CB_1R -OX_1R interaction can occur in neuronal membranes at nerve terminals in many brain regions. This is particularly true in the hippocampus, where co-expression of CB_1R and OX_1R is evident. In light of this, changes in CB_1R /OX_1R expression could be a biomarker for CNS disease in some brain regions (F. Zhu et al., 2015). Regarding CB_2R, different results show that $CB_2R-CXCR_4$ and CB_2R-GPR_{55} dimers have been associated with cancer progression (Morales & Reggio, 2017; Vitale et al., 2021). The functionality of the CB_2R-GPR_{18} heteromer has been studied in HEK-293T cells at the level of various signaling pathways. A negative cross-talk has been observed, meaning that when both receptors are activated, the signal does not become additive but instead decreases. Different studies suggest that CB_2R-GPR_{18} complexes deserve attention as potential targets for the treatment of neuroinflammation occurring in neurodegenerative diseases, for example, AD treatment (Reyes-Resina et al., 2018). Different studies show that $5-HT_{1A}R$- CB_2R heteromers are important in CNS development. Both the distribution and activity

of 5-HT$_{1A}$R- CB$_2$R heteroreceptor complexes increase after a hypoxic-ischemic insult (Franco et al., 2019). Both 5-HT$_{1A}$R agonists and CB$_2$R agonists provide neuroprotection in cells subjected to OGD and in models of hypoxia and/or stroke in adult animals. Complementary research has shown that targeting both CB$_2$Rs and 5-HT$_{1A}$Rs results in neuroprotection in a stroke model where agents targeting CB$_1$R did not (Zhang et al., 2012). In addition to all the heteromers that CBRs can form, identifying new multitarget agents capable of addressing diseases characterized by early and significant inflammatory cascades could be based on dual ligands targeting CB2Rs and FAAH. Simultaneous activation of the CB2R and inhibition of FAAH may represent a synergistic anti-inflammatory strategy. The study conducted by Intranuovo F. et al. identified several compounds with excellent affinity for the CB2R and moderate FAAH inhibitory activity. Functional studies revealed that some selected compounds were full agonists of the CB2R. It is important to emphasize that these compounds significantly reduced the production of proinflammatory cytokines and, at the same time, induced anti-inflammatory cytokines in macrophages and monocytes, primarily in the inflammatory activation state. This effect was not completely abolished by the CB2R inverse agonist JTE907, suggesting a contribution likely due to FAAH inhibition, although off-target effects should also be considered (Intranuovo et al., 2023).

3.2. Dual FAAH and MAGL inhibitors

Over the past few years, both academic and industrial endeavors have placed significant emphasis on crafting specific inhibitors targeting FAAH or MAGL, envisioning their potential therapeutic utility in numerous conditions like MS, epilepsy, neuropathic pain, and chronic pain disorders (Papa et al., 2022). The concurrent inhibition of the two primary ECS-degrading enzymes presents itself as a promising therapeutic approach. Elevated levels of 2-AG and AEA resulting from the dual blockade of FAAH and MAGL have demonstrated effectiveness in alleviating inflammatory pain without triggering cannabinoid-like effects (Anderson et al., 2014). The involvement of the ECS in pain regulation appears to be potent when employing dual FAAH/MAGL inhibitors, which have been shown to induce antinociceptive effects in a visceral pain model. Two notable examples of hybrid FAAH/MAGL inhibitors, JZL195 and SA-57, have been documented in the literature and extensively studied in various disease models. Long et al. introduced the first dual FAAH/MAGL inhibitor, JZL195, which

demonstrated Half-maximal inhibitory concentration (IC$_{50}$) values of 13 nM and 19 nM against FAAH and MAGL, respectively, functioning as a covalent inhibitor. When administered at varying doses (3–20 mg/kg i.p., 4 h), JZL195 exhibited dose-dependent inactivation of FAAH and MAGL, leading to elevated levels of AEA and 2-AG in vivo. These findings were comparable to those observed with selective FAAH and MAGL inhibitors, specifically PF-3845 and JZL184 (Papa et al., 2022). In vivo pharmacological studies were conducted to explore the roles of AEA and 2-AG in specific processes. Treatment with JZL195 and JZL184 resulted in hypomotility and hyperreflexia, whereas PF-3845 did not induce these effects, indicating that the AEA-FAAH pathway is not involved in these behaviors. JZL195 exhibited a dose-dependent reduction in motor activity across all tested doses, whereas JZL184 only increased 2-AG levels. Interestingly, pretreatment with a CB1R antagonist reversed the effects of JZL195, suggesting a CB1R-mediated mechanism, while the reduced locomotor activity from JZL184 seems unrelated to increased 2-AG levels, pointing to a CB1R-independent pathway. Conversely, the antinociceptive effects were more pronounced in mice treated with the dual inhibitor JZL195, underscoring the regulatory role of both 2-AG and AEA in pain perception (Seillier et al., 2014). Adamson et al. examined the effectiveness of JZL195 in murine models of inflammatory pain. Their study involved treating C57BL/6 mice with JZL195, a selective FAAH inhibitor (URB597), a selective MAGL inhibitor (JZL184), and a non-selective CB1R /2 agonist (WIN55,212-2). The dual inhibitor, JZL195, notably displayed a significant reduction in inflammation and induced allodynia at lower doses without the cannabinoid-related side effects seen with higher doses. Additionally, JZL195 outperformed the mono-target inhibitors (JZL184 and URB597) in reducing allodynia, suggesting the potential of dual FAAH/MAGL inhibitors in pain management. In catalepsy tests, monotherapy with WIN55,212 or PF-3845 did not yield significant effects, while JZL195 and the coadministration of JZL184 and PF-3845 induced milder cataleptic conditions compared to those induced by CB1R agonists (Adamson Barnes et al., 2016). Due to various clinical concerns associated with opioid prescriptions for pain management, Wilkerson et al. demonstrated the inherent antinociceptive properties of another dual FAAH/MAGL inhibitor, SA-57, and its capacity to enhance morphine-induced antinociception, as well as reduce heroin-seeking behavior in male C57BL/6J mice. This compound significantly decreased heroin self-administration across all tested doses. In summary, these findings underscore the potential of dual FAAH and MAGL inhibition as a viable therapeutic approach to reduce opioid doses in clinical pain management and address

opioid dependence (Wilkerson et al., 2017). Dong and colleagues investigated the impact of JZL195 on depressive behavior in WKY female rats, a model for depression. JZL195 administration led to increased BDNF, 2-AG, and AEA levels in ventral striatal tissue, correlating with improved results in the forced swim test, suggesting potential antidepressant effects. Simultaneous inhibition of FAAH and MAGL enhanced reward sensitivity in WKY rats. In a separate study by Wise and colleagues, JZL195 induced alterations in short-term memory, producing effects similar to Δ^9-THC in mice (Dong et al., 2020). Yesilyurt and colleagues investigated the potential of FAAH, MAGL, and dual FAAH/MAGL inhibitors as antipruritic agents. They examined the dose-dependent antipruritic effects of PF-3845, JZL184, and JZL195 administered systemically or intrathecally (i.t.) in a serotonin-induced scratching model in Balb-C mice. Both systemic and i.t. administration of these compounds displayed dose-dependent antipruritic effects, suggesting their potential as therapeutic options for pruritic diseases involving the spinal cord in itch modulation (Yesilyurt et al., 2016). Except for derivatives JZL195 and SA-57, which have undergone comprehensive pharmacological investigations, there is a noticeable scarcity of substantial pharmacological studies on dual FAAH/MAGL inhibitors. This scarcity may be attributed to the challenges associated with striking an optimal balance between potency and achieving a suitable therapeutic window for this category of compounds. Nevertheless, recent literature does contain a few instances of dual FAAH/MAGL inhibitors (Butini et al., 2013).

In light of the significant influence of AEA on neuromodulation, the FAAH enzyme was chosen in recent years as a promising target for various polypharmacological applications. Given the role of CB_1R and COX enzymes in pain regulation, there has been a growing interest in the development of dual inhibitors that target both FAAH and COXs, offering potential therapeutic solutions for pain management (Cipriano et al., 2013). The activation of CB_2 receptors through epoxidized fatty acids (EpFAs), in conjunction with the effects of AEA on CB receptors, provided a logical foundation for the development of multi-target inhibitors that simultaneously target FAAH and Soluble Epoxide Hydrolase (sEH). These compounds were envisioned as antinociceptive agents (Sasso, Wagner, et al., 2015). Additionally, the neuroprotective qualities of FAAH inhibitors were merged with the therapeutic effectiveness of anti-cholinesterase agents to create hybrid inhibitors that simultaneously target FAAH and COXs, showing potential utility in the treatment of AD (Rampa et al., 2012). Adopting a dual approach that targets both the ECS and the dopaminergic system could offer a novel strategy to combat drug abuse and mitigate

withdrawal responses (Parsons & Hurd, 2015). Furthermore, in the context of glaucoma treatment, the utilization of dual antagonists targeting FAAH, and melatonin receptors has emerged as a promising and innovative strategy (Spadoni et al., 2018). An interesting new study demonstrated that the ABHD6/MAGL dual inhibitor compound AM11920 offered neuroprotection against AMPA-induced retinal cell death and reduced the activation of micro- and macroglia via activation of CB_1Rs and CB_2Rs. In the same study, the selective ABHD6 inhibitor AM12100 was less effective in this model, suggesting that dual inhibition may lead to higher 2-AG levels and a better pharmacological profile. Therefore, agents such as AM11920 are promising therapeutic targets for retinal disease characterized by neurodegeneration and neuroinflammation (Kokona et al., 2021). Beyond the existence of hybrid dual inhibitors targeting FAAH/MAGL and MAGL/ABHD6, there are no documented instances in the literature that demonstrate the participation of MAGL enzymes in multi-target approaches. This scarcity of examples may be attributed to the intricate nature of the MAGL pharmacophore, which complicates the amalgamation of essential structural elements required for the creation of potential multitarget compounds. Furthermore, the complexity involved in this rational design may pose challenges in chemical synthesis, potentially discouraging the development of multi-target derivatives centered around MAGL (Papa et al., 2022).

3.3. Dual FAAH/COX Inhibitors

Nonsteroidal anti-inflammatory drugs (NSAIDs), which exert their action by inhibiting COX-1 or -2, are widely used treatments for acute and chronic pain. Both CB_1R and COX are involved in pain perception by monitoring endogenous levels of arachidonoyl-based mediators (Aiello et al., 2016). In particular, NSAIDs exert their therapeutic effects by inhibiting COX-1 and COX-2, two intracellular enzymes that initiate the conversion of membrane-derived compounds AA into inflammatory prostanoids such as prostaglandin PGE_2 and prostacyclin PGI_2. In addition to these agents, cells within inflamed tissues can produce lipid mediators that counteract the inflammatory response (Morisseau & Hammock, 2013). One such mediator is AEA which is released from macrophages and T lymphocytes upon activation of pattern recognition receptors (J. Liu et al., 2006). AEA employs a combination of CB_1R and CB2R-dependent mechanisms to inhibit neutrophil migration and deter the recruitment of dendritic cells and T cells (Chiurchiù et al., 2013). In alignment with AEA's regulatory role in inflammation, genetic or

pharmacological interventions that inhibit the enzymatic hydrolysis of AEA to AA and ethanolamine, catalyzed by FAAH, mitigate inflammatory responses in animal models. Despite their contrasting effects on inflammation, both AEAs and prostanoids share similar protective effects on the gastrointestinal mucosa. It is believed that inhibiting the formation of PGE_2 is the primary, though not the sole, factor responsible for the gastrointestinal damage induced by NSAIDs, which is a common and serious side effect of this drug class. The upregulation of COX-2 expression contributes to pathology in chronic inflammation. In certain inflammatory conditions, there is also an elevated degradation of AEA mediated by FAAH (Sasso, Migliore, et al., 2015). In this regard, clinical research has shown that the pain-relieving effects of NSAIDs can be enhanced by simultaneously administering FAAH inhibitors, underscoring the value of dual FAAH/COX inhibition as an effective approach for pain management. This multi-target strategy harnesses the synergistic benefits of FAAH and COX blockade, mitigates the potential side effects associated with COX inhibition, and reduces the clinical risks stemming from drug-drug interactions (Papa et al., 2022). Beyond their ability to alleviate pain and inflammation, these FAAH substrates also offer protection to the gastrointestinal mucosa. Indeed, experiments conducted on animal pain models have shown that co-administering FAAH and COX inhibitors results in a synergistic enhancement of pain relief while simultaneously reducing gastric damage. In numerous chronic inflammatory disorders, such as IBD, both FAAH and COX-2 are notably overexpressed (Patrono & Baigent, 2009). In cases of IBD, heightened expression of both COX-2 and FAAH is observed, leading to an imbalance in endocannabinoid regulation. FAAH's increased activity weakens AEA's anti-inflammatory potential, allowing more AA for prostanoid synthesis, while COX-2's enhanced activity strengthens prostanoid signaling and generates inflammatory mediators through COX-2-dependent AEA oxidation. This concurrent upregulation of FAAH and COX-2 may initiate a cycle intensifying inflammation by amplifying COX-dependent signals, potentially compromising AEA-mediated protective responses. Medications targeting both FAAH and COX are hypothesized to offer significant anti-inflammatory effectiveness while minimizing gastrointestinal side effects. The compound ARN2508, acting as a potent dual inhibitor of FAAH and COX intracellular activities, demonstrates profound anti-inflammatory effects in IBD mouse models without inducing COX-related gastric toxicity (Sasso, Migliore, et al., 2015). By orally administering ARN2508, a highly potent and selective inhibitor of FAAH, COX-1, and COX-2, it has been demonstrated that this compound reduces systemic levels of inflammatory prostanoids derived from COX

while increasing levels of anti-inflammatory lipid amides, such as AEA, PEA, and OEA, typically degraded by FAAH. These dual effects likely contribute to the significant effectiveness of ARN2508 in models of intestinal inflammation. Additionally, the substantial target exposure resulting from enterohepatic cycling may also enhance its efficacy. Furthermore, ARN2508 appears to protect both the upper and lower gastrointestinal tract against NSAID-induced damage, primarily through FAAH blockade. Studies indicate that FAAH inhibitors synergistically enhance the analgesic effects of NSAIDs, preventing AEA degradation and superadditively potentiating NSAID-induced pain relief. These findings suggest that dual FAAH/COX inhibitors, exemplified by ARN2508, could potentially surpass current non-narcotic analgesics in pain management (Fowler et al., 2009).

3.4. Hybrid FAAH/CBR/TRPV$_1$ inhibitors

The TRPV$_1$ receptor, a non-selective cation channel mainly found in the peripheral and central terminals of sensory neurons, plays a role in both afferent (pain sensation) and efferent (release of neurotransmitters and neuropeptides) functions. In peripheral nerve terminals, TRPV$_1$ can initiate nociceptive signaling by triggering action potentials and increasing membrane permeability to certain cations, including Ca^{2+} ions. Inflammatory conditions lower the activation threshold of TRPV$_1$, leading to receptor sensitization. Within the endovanilloid system, numerous endogenous substances, including the endocannabinoid AEA, directly activate or modulate TRPV$_1$ activity. AEA acts as a partial agonist of TRPV$_1$ and, through its activation of both nociceptive TRPV$_1$ and anti-hyperalgesic CB$_1$R, appears to have a dual regulatory influence on the excitability of neurons co-expressing these receptors (Aiello et al., 2016). In recent years, a multi-target approach has been explored, focusing on fine-tuning the activity of both the ECS and the vanilloid system in complex conditions involving both systems. The ECS plays a significant neuromodulatory role in managing anxiety states. For instance, the FAAH inhibitor URB597, when directly injected into the rat prefrontal cortex at low doses, reduces anxiety-like behaviors. Interestingly, at high doses of URB597 under the same conditions, opposite effects are observed, which can be reversed by using a TRPV$_1$ antagonist (Rubino et al., 2008). This outcome suggests that TRPV$_1$, as a secondary target of AEA, is implicated in anxiety modulation. In rats, blocking TRPV$_1$ promotes anxiolytic-like effects, whereas administration of TRPV$_1$ agonists leads to anxiogenic behavior. In 2007, Maione and

colleagues demonstrated that the FAAH inhibitor N-arachidinoyl-5-hydroxytryptamine (AA-5-HT) exhibited $TRPV_1$ antagonist properties, marking it as the prototype of a dual FAAH-$TRPV_1$ antagonist with potential applications as an analgesic agent (Maione et al., 2007). As reported by Micale and his team, this dual inhibitor, AA-5-HT, also proved effective in mitigating anxiety states in mice, reaffirming the contrasting roles of the ECS and the vanilloid system in the regulation of anxiety-related behaviors in mice (Micale et al., 2009). Furthermore, the administration of AA-5-HT in mice led to improvements in the forced swim test, which can be correlated with its impact on the hypothalamus-pituitary-adrenal axis—a system that plays a pivotal role in the development and progression of anxiety and depression states (Navarria et al., 2014). AEA decreases neuropathic pain with a mechanism that involves both CB_1R and $TRPV_1$. Treatment of neuropathic pain with intrathecal administration of URB597, an inhibitor of FAAH, may increase AEA levels (Aiello et al., 2016). In rats, the administration of a 200 μg dose of URB597 leads to an increase in the levels of PEA, OEA, and 2-AG, while also completely inhibiting thermal and tactile nociception. Interestingly, this effect is uniquely reversed by a $TRPV_1$ antagonist. The comprehensive blockade of FAAH serves as a valuable tool to uncover various metabolic pathways involving AEA. The production of 15-hydroxy-AEA, in conjunction with OEA and PEA, may contribute to the induction of $TRPV_1$-mediated analgesia in rats subjected to chronic constrictor nerve injury. Just like acetaminophen, the inhibition of FAAH and the interference with $TRPV_1$/ CB_1R and spinal serotonergic receptors are effective in preventing the antinociceptive action of 4-aminophenol. The functional versatility of the ECS and endovanilloid system is partly due to certain chemical resemblances among the various ligands that interact with their receptors and enzymes (Marzo & Petrocellis, 2010). The scientific literature highlights instances where newly designed molecules, initially targeted for one system, demonstrate the capability to interact with the other. However, many $TRPV_1$ antagonists described have undesirable properties, including body temperature elevation, hindering further development. Designing dual inhibitors for FAAH and $TRPV_1$ has emerged as a potential solution to mitigate the typical side effects of selective $TRPV_1$ inhibitors. Notably, the endogenous lipid amide AA-5-HT inhibits FAAH, elevating cannabinergic activity without enhancing TRPV1 effects. Maione and colleagues found that AA-5-HT also acts as a $TRPV_1$ antagonist, reversible by capsazepine or 5′-iodo-resiniferatoxin. Yet, like other FAAH inhibitors, AA-5-HT's efficacy against TRPV1 receptors diminishes at lower tissue pH, suggesting reduced effectiveness in chronic inflammatory conditions. In the same study, AA-5-

HT produced anti-hyperalgesic effects in vivo, dependent on the administration method and test animal species (Maione et al., 2007). The compound AA-5-HT demonstrates superior potency compared to selective FAAH inhibitors or $TRPV_1$ antagonists, suggesting its potential as a prototype for a dual FAAH- $TRPV_1$ inhibitor. Rose and colleagues designed serotonin amide derivatives, with fenoprofen-5-HT and naproxen-5-HT emerging as serotonin blockers among the synthesized compounds. Interestingly, these displayed comparable potency as $TRPV_1$ and COX-2 inhibitors to AA-5-HT but lacked FAAH inhibition. On the other hand, derivatives of 2-aryl propionic acid, namely ibuprofen-5-HT, and flurbiprofen-5-HT, exhibited inhibitory activity against all three enzymes, presenting a promising avenue for developing molecules with inhibitory effects on FAAH, COX, and $TRPV_1$. Additionally, the role of eCBs has been explored in a rheumatoid arthritis model, where AEA-related acylamides like OEA and PEA mitigate inflammation through TRPV1 desensitization. While PEA and OEA alone may not moderate hyperalgesia and inflammation induced by cytokines and MMP-3, they effectively enhance Nimesulide, a COX-2 inhibitor, leading to reduced production of proinflammatory mediators. Notably, both direct-acting CBR agonists like eCBs and FAAH inhibitors show measurable analgesic effects in acute and inflammatory pain models (Rose et al., 2014).

3.5. FAAH and Soluble Epoxide Hydrolase Inhibitors

sEH is a multifunctional enzyme with distinct activities in its N-terminal and C-terminal domains. The N-terminal domain contains a phosphatase activity, the specifics of which are not fully understood, while the C-terminal domain exhibits hydrolase activity. The C-terminal domain of sEH processes lipid mediators like EpFAs, converting their epoxide reactive moiety into the corresponding dihydroxy fatty acid. Notably, EpFAs mildly selectively activate CB2Rs. This partial activation, combined with the effects of AEA, suggests a potential complementary and synergistic role of EpFAs and fatty acid ethanolamides in pain modulation. Inhibiting sEH increases cellular concentrations of EpFA, showing promise in therapeutic applications for pain, inflammation, and neurodegenerative diseases (Morisseau & Hammock, 2013). sEH also synergistically interacts with FAAH, enhancing their combined potency in inflammatory and neuropathic pain models. sEH regulates the bioactivity of epoxy fatty acids by converting them into less active diols. The synergy between sEH and FAAH may be mediated through the formation of EpFEA, acting as CB_2R agonists and likely metabolized by both enzymes. The

analgesic effect of sEH inhibitors alone is partially attenuated by CB2R antagonists, supporting the hypothesis of CB$_2$R involvement in their enhanced efficacy (Kodani et al., 2018). Complementarity between these two systems was demonstrated through the co-administration of the sEP inhibitor 1-trifluoromethoxyphenyl-3-(1-propionylpiperidin-4-yl) urea TPPU at various doses (0.03, 0.1, 0.3, 1, 3 mg/kg) with the peripherally restricted FAAH inhibitor URB937 also at different doses (0.03, 0.1, 0.3, 1, 3 mg/kg). This combination was tested in a mouse model of acute inflammation and a rat model of neuropathy, revealing significant synergistic effects in reducing pain in both animal models (Basavarajappa et al., 2017). Additionally, the sEH inhibitor trans-4-[4-(3-trifluoromethoxyphenyl-l-ureido)-cyclohexyloxy]-benzoic acid t-TUCB exhibited a weaker inhibitory potency against FAAH. Building upon these findings, one study devised an innovative series of dual FAAH/sEH inhibitors by integrating the essential structural elements required to engage both enzymatic systems (Papa et al., 2022). Sasso et al. demonstrated that combinations of the sEH inhibitor TPPU and the FAAH inhibitor URB937 produced robust synergistic antinociception against carrageenan-induced acute inflammatory pain (Sasso, Wagner, et al., 2015). Nevertheless, the co-administration of a selective sEH inhibitor and a selective FAAH inhibitor presents potential challenges. Not only could it lead to undesirable effects due to possible drug interactions, but it may also result in an imbalanced dual treatment owing to the differing pharmacological profiles of both compounds. Furthermore, the introduction of multiple drugs can have adverse impacts on normal behavior, a facet seldom assessed in animal pain studies. The concept of multi-target direct ligands, known as polypharmacology, represents a contemporary approach in medicinal chemistry, aiming to design a single bioactive molecule that interacts with multiple targets (Proschak et al., 2019). In a separate study, a dual inhibitor was identified, demonstrating efficacy in relieving acute inflammatory pain in rats. Doses of this dual inhibitor were as effective as the conventional nonsteroidal anti-inflammatory drug ketoprofen (Wilt et al., 2021). However, a crucial aspect of drug discovery for pain management is ensuring that therapeutic doses of the drug do not elicit unwanted adverse effects on regular behavior. The pharmaceutical objective of pain relief extends beyond mere discomfort alleviation to ensuring that normal activities remain unaffected (Angelia et al., 2023).

3.6. FAAH and Cholinesterase Inhibitors

Since AEA exhibits neuroprotective effects, and inhibition of its degradative enzyme, FAAH has been considered a promising avenue for the treatment of neurodegenerative diseases, such as AD. Memory loss, cognitive impairment, and a decline in cholinergic function are frequently observed in patients with AD. These symptoms arise from the loss of cholinergic neurons in the basal forebrain. To address these issues, cholinesterase inhibitors (ChEIs) are employed. They work by decreasing the degradation of ACh, resulting in enhanced cholinergic neurotransmission in the affected brain region. Ultimately, this approach aims to ameliorate the clinical condition of individuals suffering from AD (Maleki et al., 2021). In particular, reduction of the cholinergic tone, associated with memory and cognitive dysfunction, represents the main feature of AD (Rampa et al., 2012). Since the relevant role played by cholinergic neurons in this multifactorial disease, ChEIs temporarily improve clinical conditions by selective or dual inhibition of AChE and butyrylcholinesterase. Furthermore, elevated levels of IL-1, IL-6, TNF-α, and ROS have been identified in the brains of individuals with AD, indicating the involvement of neuroinflammatory processes in AD pathogenesis. As a result, targeting the ECS holds promise as a potential treatment approach for addressing the neuroinflammation associated with AD. This therapeutic potential stems from the observed reduction in brain levels of AEA in AD patients (Jung, Astarita, et al., 2012). In line with this, Rampa and colleagues have explored the use of multitargeted ligands that modulate both the endocannabinoid and cholinergic systems as an innovative therapeutic strategy for addressing this intricate disease (Rampa et al., 2012).

3.7. FAAH and Dopaminergic System Modulators

In mesocorticolimbic areas, which play a key role in drug abstinence responses, ECS and the dopaminergic system are strongly connected. Indeed, AEA activates dopaminergic conduction and the use of FAAH inhibitors increases dopaminergic tone. Several pieces of evidence indicated that in smokers, D_2R/D_3R availability resulted noticeable decrease. These data suggested that nicotine abuse can be treated with modulators of D_2R/D_3R or using multitarget FAAH/ D_2R/D_3R ligands (Papa et al., 2022). Based on the hypothesis that a multitarget approach aiming to inhibit FAAH and down-regulate D_3R transmission could reduce the primary reinforcing effects of nicotine, a study examined the effect of ARN15381, a FAAH inhibitor,

and partial D_3R agonist, on rats' tendency to self-administer nicotine (De Simone et al., 2017). ARN15381 demonstrated selective capacity in reducing nicotine self-administration at a dose of 15 µg per infusion. It's worth noting that neither targeted FAAH inhibition with URB597 nor D_3R modulation through the partial agonist CJB090 caused a significant reduction in nicotine self-administration when administered separately. However, it was observed that the combination of CJB090 and URB597 was effective, demonstrating the concept that concurrent inhibition of FAAH and partial activation of D_3R is essential to reduce nicotine self-administration. In conclusion, these results indicate that the simultaneous inhibition of FAAH activity and modulation of D_3R transmission through the partial agonism exerted by ARN15381 was effective, whereas each mechanism alone did not achieve the same outcome. It's important to highlight that while URB597 caused only a minor reduction in self-administration, ARN15381 was highly effective. This underscores the significance of ARN15381's dual action on both FAAH and D_3R. As previously suggested, ARN15381 might have succeeded where URB597 fell short because its partial agonist effect on D_3R could have dampened any remaining dopamine transmission following the inactivation of the adrenergic β_2 receptor by FAAH inhibition (Lunerti et al., 2022).

3.8. FAAH and Melatonin Receptors Ligands

Melatonin, the primary neurohormone produced by the pineal gland, plays a crucial role in regulating the sleep-wake cycle and various physiological functions. Its influence is mediated through both receptor-dependent and non-receptor signaling pathways (L. Liu et al., 2019). Within the mammalian brain, melatonin's receptor-dependent effects occur through the activation of two GPCRs, known as the melatonin receptor type 1 (MT_1R) and melatonin receptor type 2 (MT_2R). These receptors can form homodimers or heterodimers with each other or other GPCRs, such as GPR_{50} (Jockers et al., 2016). While melatonin's cytoprotective properties have often been attributed to its ability to scavenge free radicals, thanks to its indole ring, mounting evidence suggests that its receptor activity also plays a significant role in functions such as antioxidation, immunomodulation, and neuroprotection. This occurs through the activation of the nuclear erythroid 2-related factor 2 (Nrf2) pathway and the suppression of pro-inflammatory NF-κB signaling (Nikolaev et al., 2021). WIN55,212-2-mediated CBR stimulation and activation of MT_1 and MT_2 were shown to reduce IOP leading to benefits in the

glaucoma treatment. Lately, a research team has formulated dual-function compounds that possess strong and well-balanced properties, acting as potent inhibitors of FAAH while also acting as agonists on melatonin receptors. Hybrid compounds able to activate both ECS and melatonergic systems seem to represent an innovative pharmacological tool for the treatment of glaucoma, as reported, furthermore, they could be excellent candidates for promoting neuroprotection and resolution of inflammation (Papa et al., 2022). Numerous pieces of evidence have highlighted the involvement of the melatonergic system in various neurodegenerative disorders. AD, for instance, adversely affects the melatonergic system, with melatonin showing effectiveness in inhibiting the synthesis and fibril formation of β-amyloid ($A\beta$). Importantly, these effects can be reversed by pharmacological blockade of melatonin receptors. In PD patients, there have been reports of reduced expression of MT_1R and MT_2R in the amygdala and substantia nigra pars compacta. Additionally, melatonin plays a protective role against ischemic damage through its receptors, and its capacity to enhance neurogenesis has been observed in cerebral ischemic/reperfusion mice, primarily through MT_2R activation. Furthermore, melatonin's neurogenic effects on mesenchymal stem cells are particularly mediated by MT_2Rs (Cammarota et al., 2023; Wongprayoon & Govitrapong, 2020).
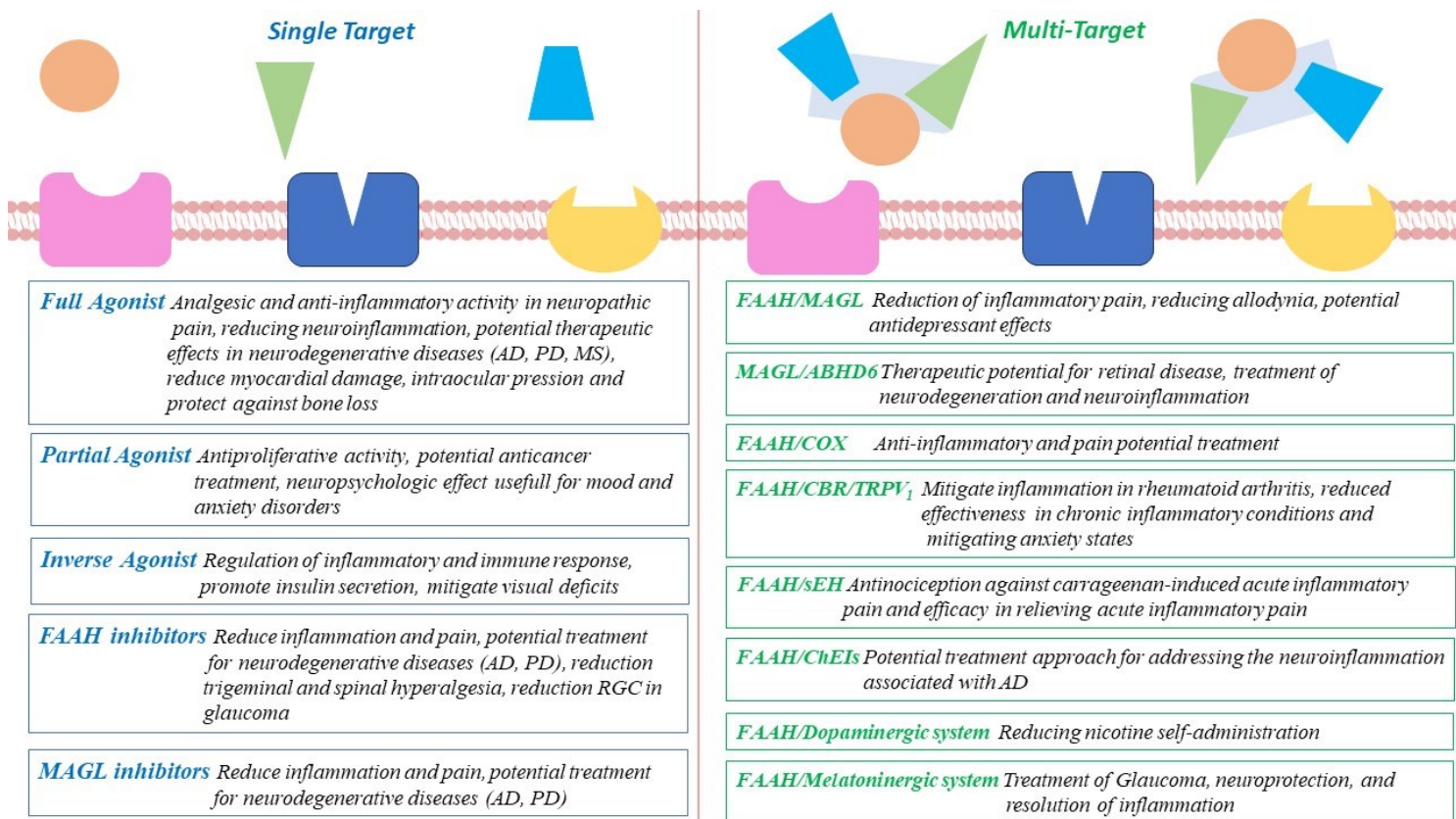
Figure 4 Summary diagram of the differences between single-target and multi-target molecules that modulate the ECS. Single-target molecules (left side) and multi-target molecules (right side) and their main therapeutic implications. In particular, for the single-target approach, full agonists for CBRs showed analgesic and anti-inflammatory activity in neuropathic pain, reducing neuroinflammation, potential therapeutic effects in neurodegenerative diseases like Alzheimer's Disease (AD), Parkinson's Disease (PD), and multiple sclerosis (MS). They also reduce myocardial damage, intraocular pressure, and protect against bone loss. Partial agonists, instead, showed antiproliferative activity, potential anticancer treatment, and neuropsychological effects useful for mood and anxiety disorders. Inverse agonists could regulate inflammatory and immune responses, promote insulin secretion, and mitigate visual deficits. Selective inhibitors of FAAH or MAGL reduce inflammation and pain and could be useful for the treatment of neurodegenerative diseases like AD and PD. Furthermore, FAAH inhibitors have shown to reduce trigeminal and spinal hyperalgesia and retinal ganglion cells (RGC) in glaucoma. For the multi-target approach, dual inhibition of FAAH and MAGL demonstrates a reduction in inflammatory pain, allodynia, and antidepressant effects. The dual inhibition of MAGL and ABHD6 showed therapeutic potential for retinal disease, the treatment of neurodegeneration, and neuroinflammation. The dual inhibition of FAAH and COX could be useful for anti-inflammatory and pain treatment potential. On the other hand, the inhibition of FAAH, CBR, and TRPV1 mitigates inflammation in rheumatoid arthritis, with reduced effectiveness in chronic inflammatory conditions and mitigating anxiety states. Moreover, the dual inhibition of FAAH with soluble epoxide hydrolase (sHE) demonstrates an antinociceptive effect against carrageenan-induced acute inflammatory pain and efficacy in relieving acute inflammatory pain. Conversely, the dual inhibition of FAAH with cholinesterase inhibitors (ChEIs) could be a potential treatment approach for addressing the neuroinflammation associated with AD. The inhibition of FAAH and the dopaminergic system proved useful for reducing nicotine self-administration, and the inhibition of FAAH and the melatoninergic system could be used for the treatment of glaucoma, neuroprotection, and the resolution of inflammation.

AIM OF THE THESIS

The ECS is a widespread neuromodulatory network involved both in the developing CNS as well as playing a major role in tuning many cognitive and physiological processes. It holds a central position during nervous system development, while in its mature state, it regulates neuronal activity and network function. This system is composed of eCBs, CB_1R, and CB_2R, and proteins involved in the transport, synthesis, and catabolism of eCBs, rather than existing as an isolated entity, the ECS significantly impacts and is impacted by multiple signaling pathways. ECS is closely intertwined with other systems and collaborates in the regulation of numerous cognitive and physiological processes, primarily through the modulation of GABAergic and glutamatergic neurons at the synaptic terminals of various brain regions associated with emotional behaviors, including social and cognitive functions (Lu & Mackie, 2021). Renewed attention is being drawn to the ECS due to its intricate connections with other systems, making it a subject of interest in neurological and neuropsychiatric disorders. It appears to be a key regulator not only within the CNS but throughout the entire body (Vitale et al., 2021). Evidence strongly suggests that manipulating the ECS can offer therapeutic advantages across a wide spectrum of conditions, ranging from neurodegenerative diseases such as AD, PD, MS, HD, mood disorders, pain management, inflammation, autoimmune diseases, cancer, cardiovascular and respiratory ailments, metabolic disorders, migraines, glaucoma, and even osteoporosis (Papa et al., 2022). Recent studies indicate that modulating ECS using multi-target molecules could represent a new therapeutic strategy for numerous diseases. The strategy of employing multiple targets presents an innovative approach to tackle complex conditions such as tumors, neurodegenerative diseases, epilepsy, infections, cardiovascular diseases, and beyond. Currently, various research teams are committed to crafting new compounds that can engage with two or more targets. Unlike conventional therapeutic molecules that rely on a single compound targeting a single point, these multi-target therapeutic compounds contain functional groups within one compound, enabling interaction with two or more targets simultaneously (Ryszkiewicz et al., 2023).

On this background, the aim of this study is to evaluate new compounds that act on the ECS by utilizing its therapeutic potential and characterizing them from a pharmacological standpoint. The study in **Chapter 1** focuses on examining the binding affinity and functional effects of

newly synthesized ligands for CBRs. This involved conducting competition binding experiments and cyclic adenosine monophosphate (cAMP) assays for CB_1Rs and CB_2Rs. Specifically, the cAMP assay was instrumental in determining the behavior of the new compounds upon binding to the receptor under investigation, identifying whether they function as agonists, antagonists, partial agonists, or inverse agonists.

In **Chapter 2** a new series of compounds were tested to evaluate the inhibition potency for the enzyme involved in eCBs catabolism. The inhibition of enzymes crucial to eCB catabolism is significant as it amplifies their natural signaling without relying on synthetic agonists, which often accompany side effects. To achieve this, competition binding experiments and inhibitor screening assays were performed. Additionally, considering the promising role of selective inhibitors for the enzymes involved in the catabolism of eCBs as anti-inflammatories and neuroprotectants, investigations were carried out to assess how these new compounds might impact inflammatory conditions. Specifically, viability and ROS production assays were conducted. Cell damage in hippocampal explants was evaluated by incorporating a marker of compromised membrane integrity, propidium iodide, to gauge potential injury. The study delved into investigating new compounds that exhibit multitarget capabilities, interacting with multiple ECS targets and other systems. This exploration extended beyond the analysis of conventional molecules, which typically focus on a single target.

In **Chapter 3** the binding affinity values of melatoninergic receptor and FAAH inhibitor potency were evaluated for novel ligands. The study sought to explore the potential role of the melatoninergic system, which, like the ECS, may be implicated in various neurodegenerative diseases. Furthermore, melatonin plays a protective role against ischemic damage through its receptors, and its capacity to enhance neurogenesis. To comprehend the anti-inflammatory capacity of the new synthetic compounds, alphaLISA and ELISA assays were conducted to assess the release of inflammatory factors such as IL-6 and TNF-α, as well as anti-inflammatory factors like IL-10.

In **Chapter 4** the evaluation of the inhibitor potency of FAAH and HDAC6 were performed for a new series of compounds. In particular, HDACs are a group of enzymes responsible for removing acetyl groups from N-acetyl lysine amino acids on various proteins, both histone and non-histone. Moreover, the overexpression of HDACs is associated with numerous pathological conditions, including various cancers and neurodegenerative diseases. The research explores the potential development of multitarget drugs aimed at the endocannabinoid system and epigenetic

enzymes, such as HDACs. This innovative approach could potentially offer pharmacological assistance in treating CNS diseases associated with oxidative stress and inflammation. To achieve this, screening assays for inhibitors targeting FAAH, MAGL, HADC6, HDAC1, HDAC8, and HDAC10 were conducted. Furthermore, these compounds were assessed to determine their antioxidant capacity and their ability to mitigate damage induced by TBHP or glutamate performing ROS production and cell viability assays.

In conclusion, the aim of this thesis was to characterize new modulators for the ECS by examining both single-target and multitarget molecules. In particular, the widespread presence of CBRs signifies the ECS's involvement in diverse physiological processes and in maintaining homeostasis. This study aims to identify novel single target ligands (e.g., agonist, partial agonist, and inverse agonist) for ECS modulation, indicating therapeutic potential for various conditions including neurodegenerative diseases, inflammation, and CNS disorders. Selective FAAH inhibitors may treat inflammatory CNS disorders by raising eCB levels without employing CBR agonists and their potential side effects. Furthermore, the development of multi-target molecules that act by modulating the ECS and other signaling systems could be an innovative pharmacological approach for treating of neurodegenerative diseases, inflammations, and as potential anticancer agents.

CHAPTER 1
PHARMACOLOGICAL CHARACTERIZATION OF NEW
ENDOCANNABINOID RECEPTOR LIGANDS

1.1.   *MATERIALS AND METHODS*

Materials

Competition binding experiments were performed by using [^{3}H]-CP-55,940 (specific activity, 180 Ci/mmol) that was obtained from Perkin Elmer Life and Analytical Sciences (USA).

(R)-(+)-WIN 55,212-2 mesylate salt obtained from Sigma Aldrich (USA).

7β-acetossi-8,13-epossi-1α,6β,9α-triidrossilabd-14-en-11-one or Forskolin that was obtained from Sigma Aldrich (USA).

4-(3-butoxy-4-methoxybenzyl)-2-imidazolidinone (Ro 20-1724) that was obtained from Sigma Aldrich (USA).

Cell Culture

Chinese Hamster Ovary (CHO) cells transfected with human CB$_1$R or CB$_2$R (PerkinElmer) were grown adherently and maintained in Ham's F12 containing 10% fetal bovine serum (FBS), penicillin (100 U/ml), streptomycin (100 μg/ml) brains Geneticin (G418, 0.4 mg/ml) at 37 ∘C in 5% CO$_2$/95% air.

Competition Binding Experiments on CB$_1$Rs and CB$_2$Rs

To study CB$_1$R, rat brains (male Sprague-Dawley rats, Charles River) were removed, frozen in liquid nitrogen, and stored at -80°C. The rat brain tissue was suspended in 50 mM Tris HCl buffer, pH 7.4 at 4°C. The suspension was homogenized with a Polytron, centrifuged for 10 min at 2000 xg and the supernatant was centrifuged again for 20 min at 40,000 xg. The pellet was resuspended in a buffer containing 50 mM Tris HCl, 1 mM EDTA, 3 mM MgCl2, 0.5% fatty acid-free BSA, pH 7.4 at 30°C. Competition binding experiments to rat CB$_1$R were carried out using [^{3}H]-CP-55,940 (1.0 nM), a membrane suspension containing 40 μg of protein/100 μl, and different concentrations (1 nM-10 μM) of the examined compounds. To investigate CB$_2$R, a [^{3}H]-CP-55,940 binding assay was performed by using rat spleen (male Sprague-Dawley rats, Charles River) that was homogenized in 50 mM Tris HCl buffer, pH 7.4 at 4°C with a Polytron, centrifuged for 10 min at 2000 xg and the supernatant was centrifuged for 20 min at 40,000 xg. The pellet was resuspended in a buffer containing 50 mM Tris HCl, 1 mM EDTA, 3 mM MgCl2, 0.5% fatty acid-free BSA, pH 7.4 at 30°C. Competition binding experiments to rat CB$_2$Rs were performed using [^{3}H]-CP-55,940 (0.5 nM), a membrane suspension containing 80 μg of

protein/100 µl, and different concentrations (1 nM-10 µM) of the examined compounds. To obtain membranes, hCB₁R and hCB₂R CHO cells were washed with PBS and scraped off with ice-cold hypotonic buffer (5 mM Tris HCl, 2 mM EDTA, pH 7.4). The cell suspension was homogenized with a Polytron and then centrifuged for 30 min at 40,000×g. The membrane pellet was suspended in 50 mM Tris HCl buffer (pH 7.4) containing 2.5 mM EDTA, 5 mM MgCl2, 0.5 mg/mL BSA for CB₁R or in 50 mM Tris HCl (pH 7.4), 1 mM EDTA, 5 mM MgCl2, 0.5% BSA for CB₂R. Competition binding experiments were performed using 0.5 nM [³H]-CP-55,940 and different concentrations (1 nM-10 µM) of the examined compounds or the reference agonist WIN 55,212-2 for an incubation time of 90 or 60 min at 30°C for CB₁Rs or CB₂Rs, respectively. Bound and free radioactivity was separated by filtering the assay mixture through Whatman GF/C glass fiber filters using a Brandel cell harvester (Brandel Instruments, Unterföhring, Germany). The filter-bound radioactivity was counted using a Packard Tri-Carb 2810 TR scintillation counter from Perkin Elmer Life and Analytical Sciences (USA).

Cyclic AMP Assay

hCB₁R CHO or hCB₂R CHO cells were washed with phosphate-buffered saline, detached with trypsin, and centrifuged for 10 min at 200×g. Cells were seeded in a 96-well white half-area microplate in stimulation buffer composed of Hank Balanced Salt Solution, 5 mM HEPES, 0.5 mM Ro 20–1724, and 0.1% BSA. To assess potency, agonists were used in the presence of 1 µM forskolin to stimulate cAMP production. The antagonist's effect was evaluated based on its ability to counteract the WIN 55,212-2-induced reduction of forskolin-stimulated cAMP production. WIN 55,212-2 concentrations used in this experiment were 20 nM for the CB₁Rs or CB₂Rs. The cAMP levels were quantified by using the AlphaScreen cAMP Detection Kit (Perkin Elmer), following the manufacturer's instructions. The Alpha signal was read with a Perkin Elmer EnSight Multimode Plate Reader.

Data Analysis

The protein concentration was determined according to a Bio-Rad method (Bradford, 1976) with bovine albumin as standard reference. The inhibitory binding constant values (K_i) were calculated from the IC_{50} according to the Cheng & Prusoff equation $K_i = IC_{50}/(1+[C^*]/KD^*)$, where $[C^*]$ is the concentration of the radioligand and KD^* its dissociation constant. A weighted non-linear least-squares curve fitting program LIGAND was used for computer analysis of

inhibition experiments. All the data are expressed as the mean ± SEM of n=4 independent experiments for the assays. Statistical analysis of the data was performed using an unpaired two-sided Student's t-test.

1.2. *RESULTS AND DISCUSSION*

1.2.1 Full Agonists

Each of the newly synthesized compounds was examined in [^{3}H]-CP-55,940 competition binding experiments for their affinity and selectivity toward the rat and human recombinant CB_1Rs and CB_2Rs (Tables 1, 2, and 3). An initial set of twelve compounds (**CF01-CF12**, Table 1) were tested for the binding affinities for CB_1Rs and CB_2Rs. The compounds **CF02**, **CF03**, **CF04,** and **CF05** displayed high affinity at the CB_2Rs and low affinity at CB_1Rs. In particular, the compounds **CF03** and **CF05** were the most potent and selective in this group (**CF03**: hK$_i$ = 0.81 nM, selectivity index (SI) = 383, **CF05**: hK$_i$ = 3.45, SI = 133). The compound **CF01** showed lower affinity and poor selectivity at the CBRs.

The structural modifications of compounds **CF06** and **CF07** resulted in a 24-27-fold decrease of affinity (K$_i$ = 536 and 332 nM, respectively) compared to the compounds **CF02** and **CF04**. Compound **CF08** was inactive at both CBRs, confirming that the affinity of this class of molecules is quite sensitive to modifications at C-2 of the oxazinoquinoline nucleus. Interestingly, the structural modifications (introduction of a methyl group at the para-position of the aryl-moiety at C-3) of compounds **CF09** and **CF10** resulted in a significant loss of affinity and selectivity for the CB_2Rs and CB_1Rs in comparison with the corresponding compounds **CF02** and **CF04**. The introduction of a methyl group at C-9 of the heterocyclic nucleus (**CF11**, K$_i$ of 18.4 nM) resulted in a modest decrease in affinity and selectivity when compared to the analog compound **CF02**. The **CF12** wasn't tested due to its poor solubility in DMSO/water. Successively second set of compounds was tested for the binding affinities for CB_1Rs and CB_2Rs (Table 2, compounds **CF13-CF39**). Derivatives **CF13-CF15** each displayed a lower affinity for both CB_2Rs and CB_1Rs, relative to the compounds **CF02**, **CF03,** and **CF04,** bearing a phenyl moiety, although the selectivity for the CB_2R was improved with the cycloheptyl and adamant-1-yl amides (**CF14** and **CF15**, respectively). Optimal activity with this group of compounds was obtained for the compound **CF14** (K$_i$ = 38, SI > 263). The compounds **CF16-CF18** enhanced affinity for both the CB_1Rs and CB_2Rs, although there was an apparent loss in

selectivity. The structural modifications for compounds **CF16-CF23** demonstrate that the affinity and selectivity for CB_2R are quite sensitive to modifications of the 6-carboxamide group. Optimal activity and selectivity in this series of compounds were achieved with the 5-methylhexan-2-yl carboxamide chain (**CF20**, Ki = 15.8 nM, SI > 633).

Further structural modification of the compounds **CF24**, **CF25**, **CF26,** and **CF27** provided further improvements in receptor affinity without significantly affecting selectivity. In particular, compound **CF24** proved to have the greatest affinity for the CB_2R affinity in this series, with a K_i value of 0.32 nM. Replacing the n-propyl moiety at C-3 with a cyclopropyl (**CF30-CF32**) or 2-propyl group (compound **CF33**) led to a loss in affinity when compared to the analogous compound **CF24**. Structural modifications of the compound **CF35** did not significantly alter affinity at the CB_2R relative to compound **CF18**, although the selectivity decreased about 1.5-fold. The **CF36** was found to be less active than the compound **CF35** (K_i = 33 vs 7.34 nM), without impacting selectivity. Similarly, the compounds **CF28** and **CF29** have demonstrated a significant reduction in affinity, particularly at the CB_2R, leading also to reduced selectivity. Together, these compounds indicate that the two receptor subtypes are quite sensitive to modifications in this portion of the molecular scaffold. Additional substitutions at C-9 allowed us to explore this sensitivity further. Compounds **CF37** and **CF39**, in which the fluorine atom of compound **CF35** is displaced by a methoxy or N-methylpiperazine moiety retain high receptor binding affinity, especially for compound **CF37** at the CB_2R, suggesting a difference between the two receptor subtypes in steric tolerance at this position. Better results were obtained with compound **CF38** showing high affinity and remarkable selectivity at the CB_2Rs (K_i = 16.3, SI > 613). The modifications of compound **CF34** don't significantly alter affinity for the CB_2R relative to compound **CF15** but have a profound effect on selectivity (K_i = 56 nM, SI = 4). This suggested the possibility of a difference between the two receptor subtypes in the stereofacial preference for substituents at this position. To evaluate this possibility were tested a number of the compounds **CF13**, **CF15**, **CF17**, **CF18,** and **CF33** as single enantiomers rather than racemic mixtures (Table 3). With the two compounds **CF13** and **CF15** a stereochemical preference for the (R)-enantiomers over the corresponding (S)-enantiomers is observed. Interestingly, the (R)-**CF13** enantiomer (K_i = 24 nM, SI = 119), displays a greater affinity for the CB_2R than the racemic mixture (K_i = 60 nM, SI = 36), but poorer affinity for the CB_1R. As a consequence, (R)-**CF13** also shows greater selectivity than the racemic mixture. Similarly, the (R)-enantiomer of **CF15** binds with greater affinity than the

(S)-enantiomer, although the (R)-enantiomer does not appear to offer any improvement in affinity or selectivity over the racemic compound. Extending this analysis to other compounds was found that the (R)-enantiomers of **CF17** and **CF18** both show approximately a two-fold enhancement in affinity over the racemic compounds. However, there is also an approximately two-fold loss in selectivity of the (R)-enantiomers for the CB_2R. This reflects a nearly four-fold improvement in the affinity of the (R)-enantiomers for the CB_1R. In contrast, the (S)-enantiomers of **CF17** and **CF18** displayed an 11- to 20-fold loss in affinity for the CB_2R with almost complete loss of selectivity. Similarly, **CF33** the (R)-enantiomer bound with greater affinity to both the CB_1R and CB_2R than the (S)-enantiomer or the racemic mixture (R-**CF33**: h CB_1R $K_i = 88$ nM, h CB_2R $K_i = 1.24$ nM; S-51: h CB_1R $K_i = 858$ nM, h CB_2R $K_i = 16.2$ nM; 51: h CB_1R $K_i = 323$ nM, h CB_2R $K_i = 3.74$ nM). However, the affinity enhancement was slightly greater for the CB_1R, resulting in an apparent loss in selectivity relative to the racemic mixture. Finally, the last two compounds were tested. The compound (R)-**CF40**, binds to the CB_2R with high affinity and exceptional selectivity ($K_i = 9.24$ nM, SI > 1082), and the compound (R)-**CF41** shows an improved affinity at the CB_2R, with a K_i of 3.72 nM, and a modest improvement in selectivity (SI = 28). The potency of the novel compounds was measured in a functional assay, evaluating the capability of the compounds to inhibit forskolin-induced cAMP production in hCB_2R CHO cells (Table 4). The competition binding curves obtained from receptor binding experiments (Figure 1A) and the dose-response curves (Figure 1B) from cAMP assays are shown for select compounds (**CF24**, **CF02**, **CF03**, (R)-**CF18** and **CF37**). High-affinity values, expressed as K_i values, are seen to be closely associated with high potency, represented by IC_{50} values (Tables 1-3 and Figure 1). The affinity and potency of the novel compounds were also compared with the reference compound WIN 55,212-2 which is characterized by high affinity and potency but very low selectivity (Tables 1-3). Interestingly, the affinity values of the examined compounds at the respective rat and human receptors were not significantly different, suggesting a high degree of similarity between the two receptor subtypes across the two species.

This novel series of compounds offers an attractive starting point for further optimization and represents novel pharmacological tools to evaluate the therapeutic potential of CB_2R agonists in various disease settings, especially inflammatory pain.

Table 1 Affinity (K_i, nM) and selectivity index (SI) of novel CB compounds on rat and human CB_1Rs and CB_2Rs.

Cmpd No	R¹	R²	R⁴	R⁵	R⁷	rat CB₁[a]	rat CB₂[b]	hCB₁[c]	hCB₂[d]	SI
						K_i (nM)				
	WIN 55,212-2					15.6 ± 1.4	7.58 ± 0.72	12.4 ± 1.3	4.53 ± 0.42	2.74
CF01	H	H	H	Phenyl	Cyclopentyl	150 ± 16	110 ± 12	132 ± 12	98 ± 10	1.35
CF02	H	H	H	Phenyl	Cyclohexyl	1150 ± 110	19.3 ± 2.3	420 ± 38	2.52 ± 0.21	166
CF03	H	H	H	Phenyl	Cycloheptyl	372 ± 36	14.7 ± 1.5	310 ± 29	0.81 ± 0.07	383
CF04	H	H	H	Phenyl	Adamant-1-yl	670 ± 65	18.3 ± 2.4	265 ± 24	14.2 ± 1.5	19
CF05	H	H	H	Phenyl	3,5-Dimethyl-adamant-1-yl	545 ± 53	46 ± 3	460 ± 48	3.45 ± 0.42	133
CF06	H	H	CH₃	Phenyl	Cyclohexyl	3520 ± 320	710 ± 44	3126 ± 288	536 ± 58	5.83
CF07	H	H	CH₃	Phenyl	Adamant-1-yl	2640 ± 225	443 ± 26	2435 ± 231	332 ± 28	7.33
CF08	H	H	Phenyl	Phenyl	Adamant-1-yl	>10000	>10000	>10000	>10000	ND
CF09	H	H	H	4-Tolyl	Cyclohexyl	4566 ± 425	547 ± 32	4108 ± 380	468 ± 42	8.78
CF10	H	H	H	4-Tolyl	Adamant-1-yl	4154 ± 410	482 ± 43	3877 ± 362	412 ± 40	9.41
CF11	H	CH₃	H	Phenyl	Cyclohexyl	1568 ± 164	25 ± 3	1346 ± 125	18.4 ± 1.9	73
CF12	H	CH₃	H	Phenyl	Adamant-1-yl	ND	ND	ND	ND	ND

The data are expressed as the mean ± SEM of n=4 independent experiments. The affinity values were calculated by using [³H]-CP-55,940 as radioligand on a) rat brain for CB_1Rs, b) rat spleen for CB_2Rs, c) human CB_1R CHO membranes, d) human CB_2R CHO membranes.

Table 2 Affinity (K_i, nM) and selectivity index (SI) of the novel CB compounds on rat and human CB_1Rs and CB_2Rs.
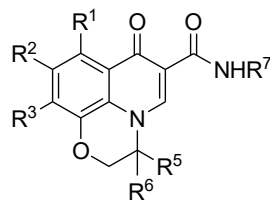
Cmpd No	R^1	R^2	R^3	R^5	R^6	R^7	Rat $CB_1{}^a$	Rat $CB_2{}^b$	$hCB_1{}^c$	$hCB_2{}^d$	SI
								K_i (nM)			
WIN 55,212-2							15.6 ± 1.4	7.58 ± 0.72	12.4 ± 1.3	4.53 ± 0.42	2.74
CF13	H	H	H	CH_3	H	Cyclohexyl	2630 ± 254	65.2 ± 6.1	2150 ± 207	60.3 ± 3.4	36
(R)-CF13	H	H	H	H	CH_3	Cyclohexyl	3560 ± 355	30 ± 4	2866 ± 245	24 ± 3	119
(S)-CF13	H	H	H	CH_3	H	Cyclohexyl	5242 ± 534	250 ± 27	4652 ± 425	188 ± 16	25
CF14	H	H	H	CH_3	H	Cycloheptyl	>10000	52.4 ± 3	>10000	38.3 ± 2.4	>263
CF15	H	H	H	CH_3	H	Adamant-1-yl	>10000	55.8 ± 4.4	>10000	47.2 ± 4.1	>212
(R)-CF15	H	H	H	H	CH_3	Adamant-1-yl	>10000	52 ± 5	>10000	47 ± 3	>212
(S)-CF15	H	H	H	CH_3	H	Adamant-1-yl	>10000	86 ± 8	>10000	78 ± 7	>128
CF16	H	H	H	Ethyl	H	Cyclohexyl	972 ± 83	24.1 ± 1.2	821 ± 78	22.8 ± 2.3	37
CF17	H	H	H	Ethyl	H	Cycloheptyl	498 ± 52	11.4 ± 1.3	433 ± 42	9.24 ± 0.92	47
(R)-CF17	H	H	H	H	Ethyl	Cycloheptyl	126 ± 11	6.03 ± 0.52	105 ± 9	4.12 ± 0.38	25
(S)-CF17	H	H	H	Ethyl	H	Cycloheptyl	913 ± 87	203 ± 19	843 ± 77	187 ± 16	4.5
CF18	H	H	H	Ethyl	H	Adamant-1-yl	725 ± 73	13.5 ± 1.5	689 ± 64	7.83 ± 0.82	88
(R)-CF18	H	H	H	H	Ethyl	Adamant-1-yl	242 ± 21	6.17 ± 0.53	197 ± 15	4.93 ± 0.45	40
(S)-CF18	H	H	H	Ethyl	H	Adamant-1-yl	653 ± 58	97 ± 8	578 ± 44	88 ± 7	7
CF19	H	H	H	Ethyl	H	Adamant-2-yl	425 ± 39	16.1 ± 1.5	389 ± 35	13.2 ± 1.2	30

CF20	H	H	H	Ethyl	H	5-Methyl-hexan-2-yl	>10000	196 ± 17	>10000	15.8 ± 1.4	>633
CF21	H	H	H	Ethyl	H	Pyridin-4-yl	1375 ± 112	183 ± 16	1150 ± 104	152 ± 14	8
CF22	H	H	H	Ethyl	H	Thiazol-2-yl	1622 ± 157	324 ± 28	1365 ± 115	265 ± 21	5
CF23	H	H	H	Ethyl	H	N,N-Diisopropyl	>10000	104 ± 10	>10000	85.2 ± 7.9	>118
CF24	H	H	H	Propyl	H	Cyclohexyl	13.4 ± 1.5	1.84 ± 0.16	10.2 ± 0.9	0.32 ± 0.03	32
CF25	H	H	H	Propyl	H	Cycloheptyl	ND	ND	ND	ND	ND
CF26	H	H	H	Propyl	H	Adamant-1-yl	240 ± 25	2.73 ± 0.25	215 ± 20	2.34 ± 0.21	92
CF27	H	H	H	Propyl	H	3,5-Dimethyl-adamant-1-yl	476 ± 44	10.7 ± 1.1	200 ± 23	3.62 ± 0.41	55
CF28	CH₃	H	H	Propyl	H	Cyclohexyl	874 ± 78	43.1 ± 2.4	756 ± 72	38.7 ± 3.4	20
CF29	CH₃	H	H	Propyl	H	Adamant-1-yl	476 ± 45	13.2 ± 1.1	450 ± 43	10.4 ± 1.1	43
CF30	H	H	H	Cyclo-propyl	H	Cyclohexyl	123 ± 12	18.2 ± 1.7	102 ± 9	15.3 ± 1.4	7
CF31	H	H	H	Cyclo-propyl	H	Cycloheptyl	101 ± 10	3.52 ± 0.36	91.2 ± 7.9	3.12 ± 0.27	29
CF32	H	H	H	Cyclo-propyl	H	Adamant-1-yl	482 ± 46	10.3 ± 1.2	389 ± 37	8.92 ± 0.91	44
CF33	H	H	H	Iso-propyl	H	Adamant-1-yl	366 ± 31	4.22 ± 0.38	323 ± 28	3.74 ± 0.32	86
(R)-CF33	H	H	H	H	Isopropyl	Adamant-1-yl	95 ± 9	1.75 ± 0.14	88 ± 7	1.24 ± 0.11	71
(S)-CF33	H	H	H	Isopropyl	H	Adamant-1-yl	864 ± 82	19.3 ± 1.9	858 ± 79	16.2 ± 1.8	53
CF34	H	H	H	CH₃	CH₃	Adamant-1-yl	276 ± 22	68.1 ± 4.1	221 ± 18	56.2 ± 3.5	4
CF35	H	H	F	Ethyl	H	Adamant-1-yl	452 ± 44	9.51 ± 0.88	389 ± 34	7.34 ± 0.68	53

61

							a	b	c	d	
CF36	H	F	F	Ethyl	H	Adamant-1-yl	1824 ± 176	37.5 ± 2.1	1752 ± 165	33.1 ± 1.3	53
CF37	H	H	OCH₃	Ethyl	H	Adamant-1-yl	589 ± 51	9.12 ± 0.86	521 ± 48	6.78 ± 0.62	77
CF38	H	H	Pyrrolidin-1-yl	Ethyl	H	Adamant-1-yl	>10000	21.8 ± 1.2	>10000	16.3 ± 1.7	>613
CF39	H	H	4-Methyl-piperazin-1-yl	Ethyl	H	Adamant-1-yl	>10000	61.2 ± 3.5	>10000	42.7 ± 2.3	>238
CF40	H	H	H	H	Isobutyl	Adamant-1-yl	>10000	10.2 ± 1.1	>10000	9.24 ± 0.84	>1082
CF41	H	H	H	H	Benzyl	Adamant-1-yl	121 ± 10	4.65 ± 0.43	105 ± 9	3.72 ± 0.32	28

The data are expressed as the mean ± SEM of n=4 independent experiments. The affinity values were calculated by using [³H]-CP 55,940 as radioligand on a) rat brain for CB_1Rs, b) rat spleen for CB_2Rs, c) human CB_1R CHO membranes, d) human CB_2R CHO membranes.

Table 3 Potency (*IC$_{50}$*, nM) of the novel CB compounds in hCB$_2$CHO cells on cAMP assays.

Compound	*h*CB$_2$ IC$_{50}$ (nM)	Compound	*h*CB$_2$ IC$_{50}$ (nM)	Compound	*h*CB$_2$ IC$_{50}$ (nM)
WIN 55,212-2	13.7 ± 0.1	(*R*)-CF15	153 ± 14	CF28	122 ± 11
CF01	472 ± 43	(*S*)-CF15	250 ± 23	CF29	42 ± 5
CF02	15.2 ± 1.7	CF16	62 ± 7	CF30	67 ± 6
CF03	5.23 ± 0.42	CF17	42 ± 3	CF31	12.4 ± 1.3
CF04	26 ± 3	(*R*)-CF17	17.2 ± 1.6	CF32	32 ± 3
CF05	18.3 ± 1.9	(*S*)-CF17	682 ± 67	CF33	12.4 ± 1.7
CF06	2749 ± 245	CF18	38 ± 4	(*R*)-CF33	9.84 ± 0.91
CF07	1684 ± 152	(*R*)-CF18	18.1 ± 1.7	(*S*)-CF33	55 ± 6
CF08	ND	(*S*)-CF18	413 ± 38	CF34	242 ± 23
CF09	2457 ± 213	CF19	57 ± 6	CF35	27 ± 2
CF10	2215 ± 211	CF20	62 ± 6	CF36	145 ± 12
CF11	110 ± 9	CF21	683 ± 66	CF37	24 ± 3
CF12	ND	CF22	1127 ± 104	CF38	58 ± 5
CF13	245 ± 28	CF23	423 ± 37	CF39	196 ± 17
(*R*)-CF13	90 ± 8	CF24	1.53 ± 0.16	(*R*)-CF40	36 ± 3
(*S*)-CF13	724 ± 75	CF25	ND	(*R*)-CF41	17.5 ± 1.8
CF14	210 ± 23	CF26	15.3 ± 1.4		
CF15	230 ± 22	CF27	20 ± 3		

The data are expressed as the mean $\pm$ SEM of n=4 independent experiments. IC$_{50}$ values were calculated on cAMP experiments performed on human CB$_2$R CHO cells.

Figure 1
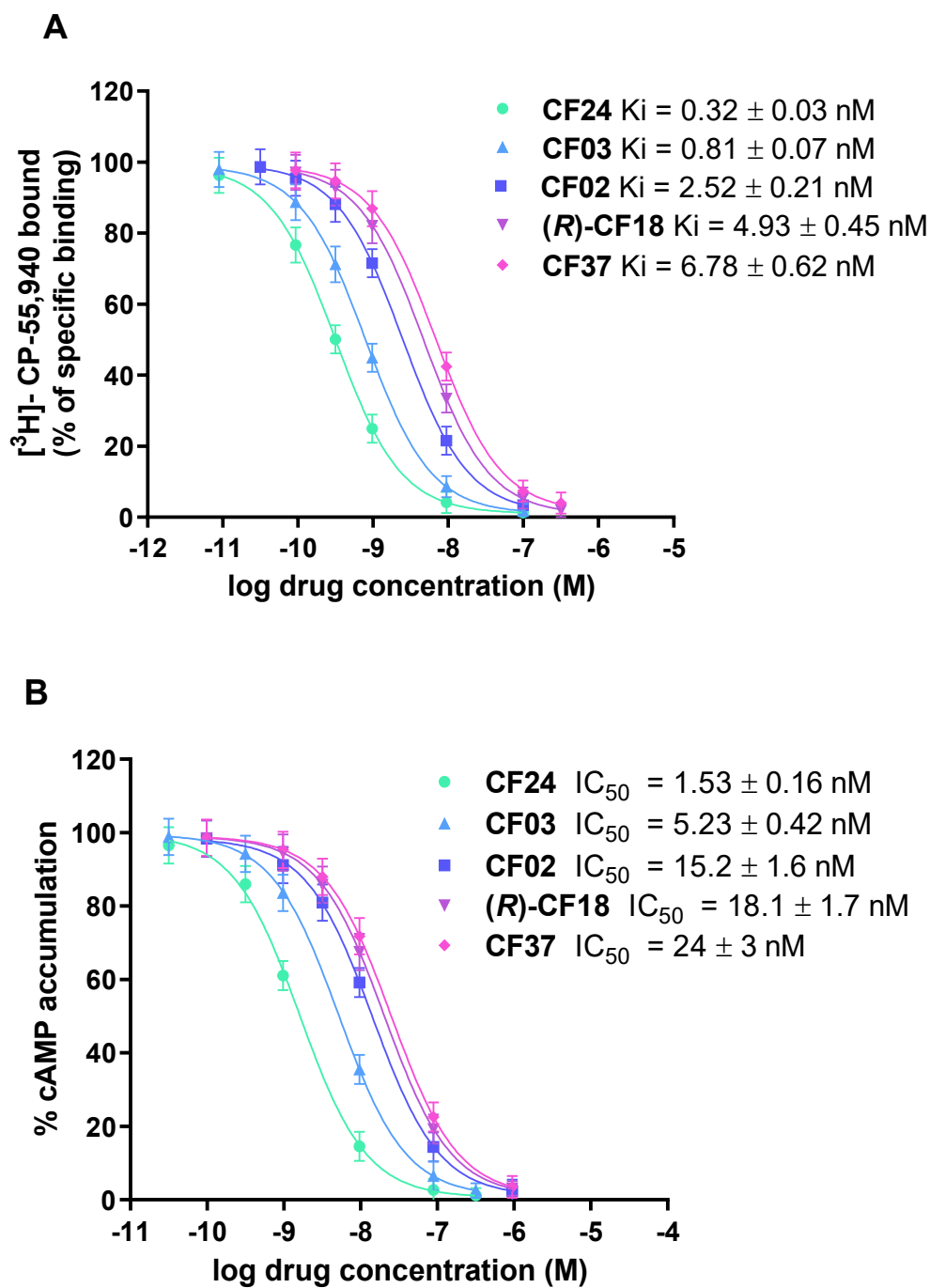
Figure 1 Affinity (K_i, nM) and potency (IC_{50}, nM) of selected novel CB compounds: (A) competition curves on hCB$_2$Rs; (B) inhibition curves of forskolin-stimulated cAMP accumulation in hCB$_2$R CHO cells. Results are mean ± SEM (n=4 independent experiments).

1.2.2 Partial Agonists

All of the newly synthesized compounds were examined in [^{3}H]-CP-55,940 competition binding experiments for their affinity and selectivity toward the rat and human recombinant CB_1Rs and CB_2Rs (Table 4). Interestingly, like above, the measured affinity values of the examined compounds did not significantly change between rat and human CBRs. The compound **CP01** displayed modest affinity and slight selectivity for the cannabinoid receptors (hCB$_2$ K$_i$ = 85 nM; h CB$_1$R K$_i$ = 500 nM, SI = 5.9). **CP01** was taken as a reference compound and subsequently, were prepared analogues by stepwise introduction of structural modifications of this compound to define the correct structural requirements for binding to the CB$_2$R. The first structural modifications of CP01 give a set of compounds (**CP02-CP38**, Table 4). Introducing a shorter alkyl chain on the N^7-position, such as n-butyl, like compound **CP02, (**hK$_i$ = 138 nM) or n-propyl for compound **CP03**, (hK$_i$ = 412 nM), instead of the n-pentyl moiety resulted in reduced affinity for the CB$_2$R. Similarly, extending the aliphatic chain to an n-hexyl substituent resulted in a 3.8-fold reduction of affinity, as shown by **CP07** in comparison with **CP01**. The compounds **CP04, CP05, and CP06** showed a complete loss of affinity for both CBRs. Compounds **CP08** and **CP09** also exhibited a marked decrease or a complete loss of affinity at both CBRs. The structural modification of **CP10** also resulted in an inactive compound at the CB$_2$Rs and CB$_1$Rs. Compound **CP11** showed a 4-fold lower affinity toward the CB$_2$R and lower selectivity when compared with compound **CP01**. Structural modification of **CP12** and **CP13** afforded compounds with a higher affinity at the CB$_2$R (hK$_i$ = 11.4 and 10.6 nM, respectively). Indeed, these compounds proved to have some of the highest CB$_2$R affinities in this series. A stereogenic preference is observed with the *trans*-isomer **CP12** exhibiting better selectivity against the CB$_1$R (SI = 401) compared with the *cis*-isomer **CP13** (SI = 68). A marked increase in affinity was shown by compounds **CP14**, **CP15,** and **CP16**. In addition to compounds **CP12** and **CP13**, these were among the most potent analogs tested, with comparable potencies *(*hK$_i$ values of 11.2, 9.5, and 9.8 nM respectively), although the highest selectivity among the three against the CB$_1$R was observed with the most lipophilic compound **CP16** (SI = 107). The structural modification of compounds CP17, and CP18 induced a dramatic reduction in affinity toward CB$_2$Rs (**CP17**, hK$_i$.= 212 nM CP18 hK$_i$.= 524 nM), with a concomitant reduction in selectivity. The compounds **CP19, CP20, and CP21** showed a complete loss of affinity for both CBRs. The compounds **CP22** and **CP23** displayed lower affinity and poor selectivity at the CBRs when compared with the compounds **CP01** and **CP15**, respectively. Similarly, compounds **CP24**, **CP25**, **CP26**, and **CP27** highlight a decreased affinity (hK$_i$ values of 3526, 363, 237 and 103

nM, respectively). In particular, compound **CP28** was one of the most potent compounds evaluated and the most selective compound in this series (hK$_i$ = 11.6 nM, SI = 432).

Aromatic substituents at the 3-position of the pyrazole, as in compounds **CP29-CP32**, led to a significant loss of affinity at both the CB$_2$Rs and CB$_1$Rs (K$_i$ > 10000 nM for **CP29** and **CP30** K$_i$ = 3620 and 2830 nM for **CP31** and **CP32**). Optimal affinity was obtained for compound **CP33**, (hCB$_2$ K$_i$ = 8.74 nM, SI = 17.7), which showed significantly greater affinity and selectivity than the corresponding compound **CP01**. Compounds **CP34** or **CP35** a good selectivity for CB2Rs (**CP34** hCB$_2$ K$_i$ = 18.5 nM, SI = 7.8 and **CP35** hCB$_2$ K$_i$ = 21 nM, SI = 69.9). Evaluation of the compound **CP36** lost the affinity for the CBRs. Compounds **CP37** and **CP38** proved to have good affinity for the CBRs. In particular, CP42 results in the greatest affinity and selectivity in this group for the CB$_2$R, with a K$_i$ value of 3.58 nM and SI = 146. Figure 2A shows [^{3}H]-CP-55,940 competition binding curves to hCB$_2$Rs of **CP16**, **CP28,** and **CP23** in comparison to the reference compound WIN 55,212-2. Cyclic AMP assays were performed to discriminate between full, partial, and inverse agonism. We also evaluated the efficacy (Emax), expressed as a percentage relative to that of WIN 55,212-2 representing the full CBR agonist with Emax of 100. The majority of the novel compounds (from **CP02** to **CP28** and **CP37**) showed moderate potency, inhibiting adenylate cyclase activity with EC$_{50}$ values between 41 and 3824 nM. Interestingly, most of these compounds reveal a low Emax activity, suggesting they act as partial agonists (Table 5). Figure 2B shows the inhibition curves in cAMP assays to hCB$_2$Rs of **CP16**, **CP28,** and **CP23** compared to the reference full agonist WIN 55,212-2. Figure 3A shows [^{3}H]-CP-55,940 competition binding curves at the hCB$_2$R for compounds **CP33**, **CP37**, and **CP38** compared to the reference compound WIN 55,212-2. Figure 3B shows the dose-dependent effects of **CP33**, **CP37,** and **CP38** in the modulation of forskolin-induced cAMP production. As can be seen from Figures 2B and 3B, as well as the data in Table 5, the different structural classes display different behaviors as full agonists and partial agonists. Thus, it appears that the core structure of these molecules defines the type of activity to be seen, while the substituents around the core structure can be used to modulate the potency of that activity. Considering the results presented, this represents a new class of heterocyclic derivatives acting as potent CB$_2$R partial agonists.

Table 4. Affinity (K_i, nM) and selectivity index (SI) on rat and human CB_1Rs and CB_2Rs, and potency (IC_{50}, nM) and E max % of the novel CB compounds **CP01-CP38** in hCB$_2$R CHO cells on cAMP assays.

CP01-CP32   CP33-CP35   CP36-CP38

Com	R	R^1	R^2	rCB$_1^a$	rCB$_2^b$	hCB$_1^c$	hCB$_2^d$	SI	hCB$_2$ EC$_{50}$ (nM)	Emax (%)
					K_i (nM)					
	R-(+)-WIN 55,212-2			14.4 ± 1.3	7.73 ± 0.68	11.3 ± 1.2	4.95 ± 0.43	2.3	14.8 ± 1.2	100
CP01	Me	Cyclohexyl	Pentyl	1420 ± 138	100 ± 12	500 ± 49	85 ± 9	5.9	323 ± 29	52 ± 5
CP02	Me	Cyclohexyl	Butyl	1533 ± 145	145 ± 13	1256 ± 127	138 ± 12	9.1	1895 ± 193	38 ± 3
CP03	Me	Cyclohexyl	Propyl	832 ± 78	593 ± 18	758 ± 72	412 ± 38	1.8	-	-
CP04	Me	Cyclohexyl	Allyl	> 10000 (27%)	> 10000 (46%)	> 10000 (34%)	> 10000 (42%)	-	587 ± 52	58 ± 4
CP05	Me	Cyclohexyl	2-Ethoxy ethyl	> 10000 (10%)	> 10000 (1%)	> 10000 (14%)	> 10000 (1%)	-	-	-
CP06	Me	Cyclohexyl	4-Cyanobutyl	> 10000 (25%)	> 10000 (5%)	> 10000 (28%)	> 10000 (11%)	-	-	-
CP07	Me	Cyclohexyl	Hexyl	3220 ± 310	480 ± 32	3870 ± 322	325 ± 33	12	1203 ± 117	27 ± 2
CP08	Me	Cyclohexyl	Benzyl	4560 ± 428	1100 ± 58	4248 ± 415	956 ± 94	4.4	3824 ± 392	36 ± 3
CP09	Me	Cyclohexyl	4-CH$_3$-Benzyl	> 10000 (38%)	> 10000 (29%)	> 10000 (35%)	> 10000 (33%)	-	-	-
CP10	Me	Cyclohexyl	2-(Morpholin-4-yl)ethyl-	> 10000 (13%)	> 10000 (32%)	> 10000 (16%)	> 10000 (36%)	-	-	-
CP11	Me	Cyclohexyl-CH$_2$	Pentyl	1040 ± 95	508 ± 22	1124 ± 126	372 ± 35	3	1562 ± 149	41 ± 3

CP12	Me	trans-4-CH$_3$-Cyclohexyl	Pentyl	4800 ± 570	13.3 ± 1.5	4568 ± 422	11.4 ± 1.2	401	58 ± 6	14 ± 1
CP13	Me	cis-4-CH$_3$-Cyclohexyl	Pentyl	750 ± 73	11.8 ± 1.3	723 ± 63	10.6 ± 1.1	68	52 ± 5	16 ± 1
CP14	Me	Cycloheptyl	Pentyl	1620 ± 165	35 ± 3	252 ± 22	11.2 ± 1.2	23	51 ± 6	65 ± 6
CP15	Me	Adamant-1-yl	Pentyl	832 ± 82	11.4 ± 1.7	800 ± 84	9.51 ± 0.93	84	49 ± 5	68 ± 6
CP16	Me	3,5-diMe-Adamant-1-yl	Pentyl	3260 ± 352	16.7 ± 1.8	1050 ± 95	9.83 ± 1.01	107	45 ± 5	71 ± 6
CP17	Me	1,4-diMe-Pentyl	Pentyl	2256 ± 216	262 ± 25	1795 ± 164	212 ± 20	8.5	827 ± 75	46 ± 4
CP18	Me	Phenyl	Pentyl	1020 ± 95	740 ± 38	865 ± 82	524 ± 53	1.7	2159 ± 248	38 ± 3
CP19	Me	4-OCH$_3$-Phenyl	Pentyl	> 10000 (46%)	> 10000 (24%)	> 10000 (38%)	> 10000 (33%)	-	-	-
CP20	Me	4-F-Phenyl	Pentyl	> 10000 (48%)	> 10000 (27%)	> 10000 (44%)	> 10000 (37%)	-	-	-
CP21	Me	Benzyl	Pentyl	> 10000 (42%)	4517 ± 188	> 10000 (38%)	3652 ± 355	>2.7	-	-
CP22	Et	Cyclohexyl	Pentyl	1120 ± 126	516 ± 25	957 ± 92	469 ± 42	2	2348 ± 227	32 ± 2
CP23	Et	Adamant-1-yl	Pentyl	2670 ± 253	97 ± 12	440 ± 35	37 ± 4	12	162 ± 14	51 ± 4
CP24	t-But	Cyclohexyl	Pentyl	>10000 (19%)	4033 ± 260	>10000 (23%)	3526 ± 227	>2.8	-	-
CP25	t-But	Adamant-1-yl	Pentyl	3430 ± 322	417 ± 33	3753 ± 385	363 ± 34	10	1764 ± 167	43 ± 3
CP26	H	Cyclohexyl	Pentyl	5650 ± 525	250 ± 20	5150 ± 480	237 ± 21	22	872 ± 79	48 ± 5
CP27	H	Cycloheptyl	Pentyl	5200 ± 550	130 ± 14	4550 ± 435	103 ± 12	44	404 ± 42	56 ± 5
CP28	H	Adamant-1-yl	Pentyl	5342 ± 493	13.3 ± 1.2	4752 ± 381	11.6 ± 1.1	432	41 ± 4	67 ± 6
CP29	Ph	Cyclohexyl	Pentyl	> 10000 (18%)	> 10000 (1%)	> 10000 (23%)	> 10000 (1%)	-	-	-
CP30	Ph	Cycloheptyl	Pentyl	> 10000 (1%)	> 10000 (1%)	> 10000 (1%)	> 10000(1%)	-	-	-
CP31	p-Cl-Ph	Cyclohexyl	Pentyl	> 10000 (15%)	5017 ± 188	> 10000 (22%)	3620 ± 326	>2.8	-	-
CP32	p-Cl-Ph	Cycloheptyl	Pentyl	> 10000(12%)	4050 ± 132	> 10000 (17%)	2830 ± 264	>3.5	-	-

CP33	-	Cyclohexyl	-	187 ± 15	38 ± 4	155 ± 16	8.74 ± 0.92	17.7	14.3 ± 1.2	98 ± 7
CP34	-	Cycloheptyl	-	184 ± 19	50 ± 4	145 ± 13	18.5 ± 1.7	7.8	35 ± 4	99 ± 6
CP35	-	Adamant-1-yl	-	1495 ± 153	26 ± 3	1468 ± 138	21 ± 2	69.9	83 ± 8	97 ± 8
CP36	H	Cyclohexyl	-	> 10000 (28%)	> 10000 (32%)	> 10000 (25%)	> 10000 (37%)	-	-	-
CP37	H	Adamant-1-yl	-	850 ± 70	21 ± 2	712 ± 64	20 ± 2	35.6	87 ± 9	60 ± 5
CP38	Phenyl	Adamant-1-yl	-	560 ± 52	4.83 ± 0.46	523 ± 47	3.58 ± 0.31	146	89 ± 5	55 ± 3

The data are expressed as the mean $\pm$ SEM of n=4 independent experiments. The affinity values were calculated by using [^{3}H]-CP-55,940 as radioligand on a) rat brain for CB_1Rs, b) rat spleen for CB_2Rs, c) human CB_1R CHO membranes, d) human CB_2R CHO membranes. e) EC_{50} values were calculated on cAMP experiments performed on human CB_2R CHO cells. f) Efficacies (Emax) for CB_2R of the examined compounds are expressed as a percentage relative to the efficacy of the reference compound WIN 55,212-2 at the 10 µM concentration. Emax values around 100% indicated that the compounds behave as full agonists. Emax values between 0 and 100% indicated that the compounds behave as partial agonists.

Figure 2.

A

B
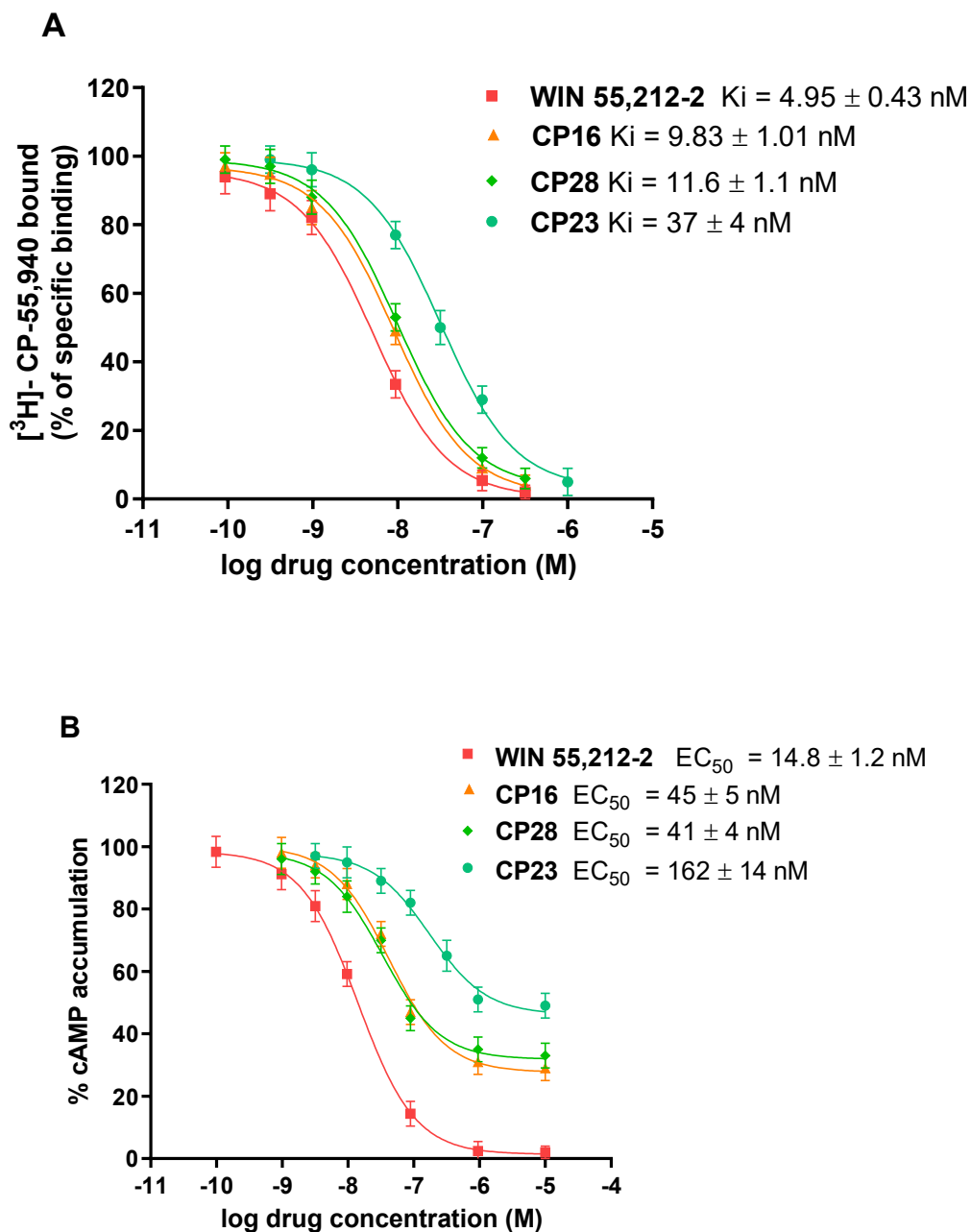
Figure 2. Affinity (K_i, nM) and potency (EC_{50}, nM) of **CP16**, **CP28,** and **CP23** in comparison with WIN-55,2121-2: (A) competition curves on hCB$_2$Rs; (B) inhibition curves of forskolin-stimulated cAMP accumulation in hCB$_2$R CHO cells. Results are mean $\pm$ SEM (n=4 independent experiments).

Figure 3.
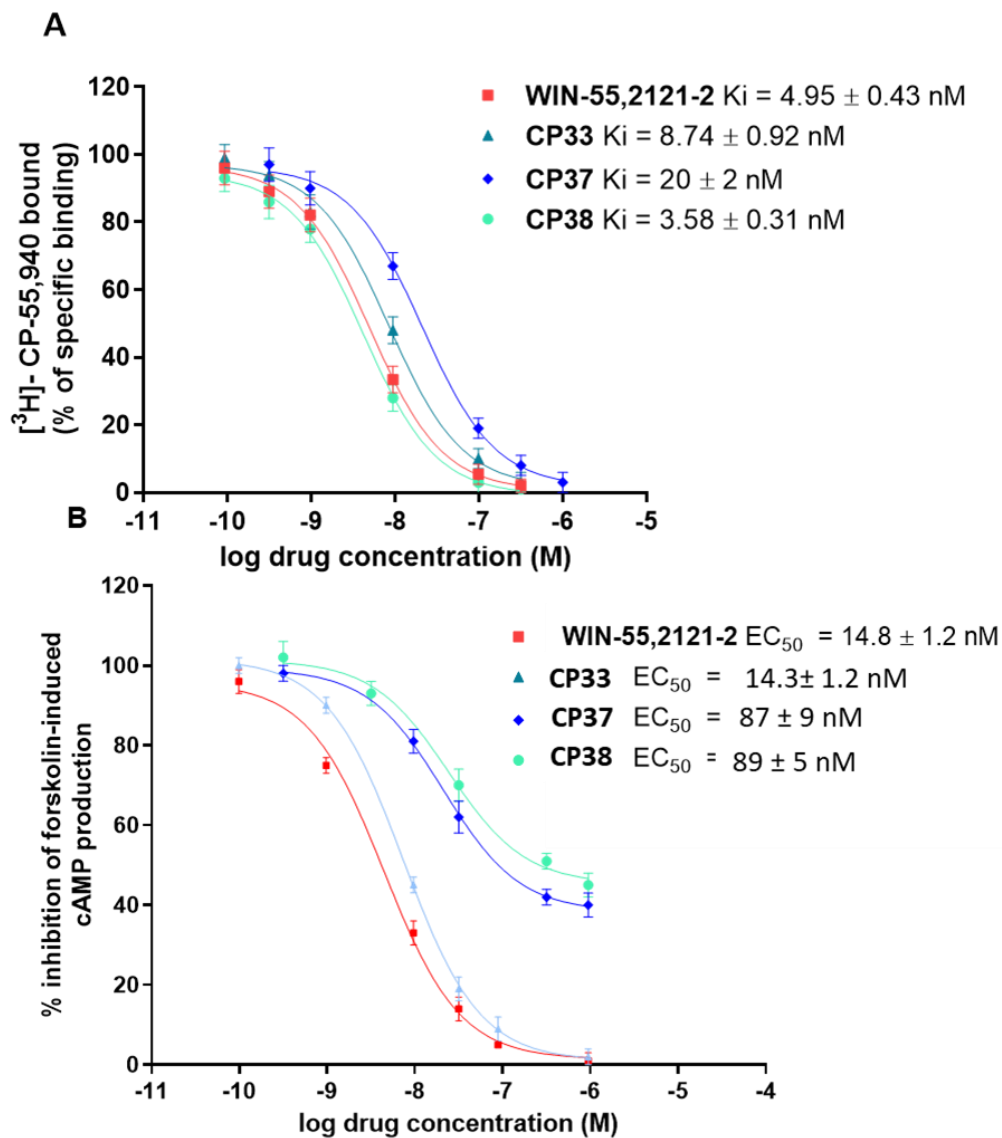
Figure 3. Affinity (K_i, nM) and potency (*EC_{50}*, nM) of **CP33**, **CP37,** and **CP38** in comparison with WIN-55,2121-2: (A) competition curves on *h*CB$_2$Rs; (B) dose-dependent effect of the examined compounds on forskolin-stimulated cAMP accumulation in *h*CB$_2$R CHO cells. Results are mean ± SEM (n=4 independent experiments).

1.2.3 Inverse Agonists

All of the newly synthesized compounds were examined in $[^3H]$-CP-55,940 competition binding experiments for their affinity and selectivity toward the rat and human recombinant CB_1Rs and CB_2Rs. The results, in terms of binding affinities for the two receptors (K_i values), are reported in Table 5.

Good results in terms of both activity and selectivity profiles were found with the compound **CI01** and **CI02** with (hCB_2R $K_i = 22$ nM, SI = 58 and hCB_2R $K_i = 10,3$ nM, SI = 51). Also, the compound CP**03** results with good affinity and selectivity for CB_2R ($K_i = 12.7$ nM, SI = 88). The **CI04** displayed modest affinity and slight selectivity for the CBRs (hCB_2R $K_i = 358$ nM, hCB_1R $K_i = 3290$ nM, SI = 9.2). The compound **CI05** did not enhance affinity (hCB_2R $K_i = 106$ nM; hCB_1R $K_i = 2432$ nM, SI = 23) relative to the compound **CI01**. The compounds **CI06-CI11** showed high affinity for the CB_2R (**CI06-CI08:** 0.84 < nM < 10.4; **CI09-CI11:** 4.95 < nM < 12.3) with remarkable selectivity over the CB_1R (**CI06-CI08**: 38 < SI < 143; **CI09-CI11**: 55 < SI < 124). Replacing the cyclohexyl moiety with a cycloheptyl or adamant moiety led to an increase in affinity, as shown by compounds **CI07, CI08, CI10,** and **CI11.** In addition, the highest selectivity, over the CB_1R was observed with the most lipophilic compounds **CI08** and **CI11** (SI = 143, 124 respectively). Compound **CI08** was found to have the highest CB_2R affinity with a K_i value of 0.84 nM. (Figure 4A). Interestingly, the structural modification of compounds **CI12-CI30** showed that the affinity for the CB_1Rs was completely lost, except for analogs **CI12** and **CI13** which exhibited a moderate affinity for the CB_1R.

The compound **CI14,** improved affinity and selectivity for the CB_2R in comparison to the compounds **CI12** and **CI13**. In contrast, the **CI14** loss of affinity for the CB_1R shows a significant increase in selectivity and suggests a difference between the two receptor subtypes in steric tolerance. In particular, the adamant-1-yl carboxamide **CI14** the most selective compound in this series with high affinity for the target receptor (hCB_2R $K_i = 2.56$ nM, SI > 3906). The compounds **CI15-CI17** highlight a 15- and 41-fold increase of selectivity (SI > 250 and > 1119, respectively) relative to the compounds **CI12** and **CI13**, respectively. Affinity at the CB_2R was also increased, in particular, for the compound **CI16** (hCB_2 $K_i = 8.93$ nM). In contrast, the **CI17** retained affinity and selectivity for the CB_2R equivalent to that of the **CI14**. Structural modification of compounds **CI18-CI20** did not induce a marked alteration in affinity at the CB_2R. The most active compound was the **CI20** (hCB_2R $K_i = 3.41$, SI > 2932), although the **CI19** displayed a high affinity with remarkable selectivity over the CB_1R (hCB_2R $K_i = 10.3$

nM SI > 970). Different compounds, **CI21-CI26**, with chlorine atom substituents, were tested and displayed affinity similar to that of the started compounds **CI15-CI20**. The compounds **CI22-CI26** showed high affinity and selectivity for the CB_2R (**CI22, CI23** hCB_2R K_i = 10.3, 6.21 nM, **CI24** hCB_2R K_i = 55 nM and **CI25, CI26** hCB_2R K_i = 6.31, 3.88 nM respectively, hCB_1R K_i > 10000 nM). The structural modifications of compounds **CI27-CI30** resulted in a significant loss of affinity for the CB_2R in comparison with the corresponding compounds (**CI16-CI17**). The structural modification of compounds **CI31-CI34** mainly induced a marked improvement in affinity at the CB_2R, as seen with compound **CI33** in comparison to the **CI12** (hCB_2R K_i = 9.52 nM *vs* 42 nM, respectively). The compound **CI34** is substantially equivalent to derivative **CI33** in terms of affinity yet endowed with somewhat lower receptor selectivity. The compounds **CI35-CI37** showed a good affinity and selectivity for the CB_2R **CI35** (hCB_2R K_i 6.24 nM, SI > 1602), **CI36** (hCB_2R K_i 15 nM, SI > 666), and **CI37** (hCB_2R K_i 11.6 nM, SI > 862). The structural modifications of the last three compounds **CI38-CI40** show a reduced binding affinity for the CB_2R (**CI38**, hCB_2R K_i = 220 nM, **CI39**, hCB_2R K_i = 181 nM, **CI40**, hCB_2R K_i = 350 nM). The novel compounds were evaluated in functional assays, to study their effects on forskolin-stimulated adenylate cyclase production in hCB_2R CHO cells at the concentrations of 1 µM and 10 µM compared to the maximal effect (set at -100%) achieved with the full CB_2R agonist WIN55,212-2. All of the tested compounds show some level of efficacy, as evidenced by their ability to increase forskolin-induced cAMP production, thus characterizing these compounds as inverse agonists (Table 6).

Interestingly, the highest effect was achieved with the compounds **CI08** and **CI10** which were able to increase forskolin-induced cAMP production by 243% and 213% at 10 Mm respectively (Figure 4B), yet the two compounds display slightly different affinities at the CB_2R (Ki = 0.84 and 7.22 nM, respectively). When tested in the presence of WIN 55,212-2, the novel compound **CI08** was able to completely abrogate the inhibitory effect of the agonist on forskolin-stimulated cAMP production, confirming its opposite effect concerning WIN 55,212-2 (Figure 4B). For the most efficacious compounds **CI08**, **CI10**, and **CI14**, full dose−response curves were measured and EC_{50} values were determined. The obtained results that confirmed the inverse agonism activity relative to the selected compounds are presented in Table 7 and Figure 4C. The potencies of the novel compounds **CI08**, **CI10**, and **CI14** were 95 ± 8, 351 ± 31, and 195 ± 17 nM, respectively, confirming a good correlation with their affinity for CB_2Rs. The compounds **CI14, CI17, CI26,** and **CI20** resulted in the most efficacious, showing 195, 184, 168, and 183%

respectively increases in cAMP levels at 10 μM. These compounds were also found to bind to the CB$_2$R with very good affinities (K$_i$ < 4 nM). Similarly, the compounds **CI12, CI15, CI24, CI18, CI27,** and **CI21** show moderate effects at 10 μM with modest affinity (40 nM <K$_i$ < 57 nM). In the compounds **CI25**, **CI13**, **CI16**, **CI19**, **CI28**, and **CI22** the increase in cAMP levels at 10 μM is correlated with K$_i$ values, while a different trend was observed only for **CI22** that revealed a modest increase in cAMP (69%) despite its good affinity at CB$_2$R (K_i = 10.3 nM). So, the best affinity values associated with high selectivity were obtained with compounds **CI14**, **CI17**, **CI20**, **CI26, CI33,** and **CI35** (2.56 nM < hCB$_2$ K_i < 6.24 nM, 1602 < *SI* < 3906).

These results reveal that the novel series behaved as CB$_2$R inverse agonists. A good correlation between receptor affinity (expressed as K$_i$) and efficacy (represented by a % increase in cAMP levels at different concentrations of test compound), was observed, thus the wide range of relative efficacies seen with this limited series of compounds offers the potential opportunity to more closely examine the structural requirements for delineation between neutral antagonists and potent inverse agonists. Thus, this novel series of compounds offers an attractive starting point for further optimization, representing novel pharmacological tools to evaluate the therapeutic potential of CB$_2$R inverse agonists in various disease settings.

Table 5. Affinity (K_i, nM) and selectivity index (SI) on Rat and Human CB_1Rs and CB_2Rs of the novel CB compounds **CI01-CI40.**
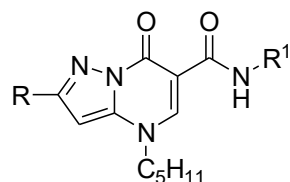
CI01-CI37

CI38-CI40

Compd	R	R^1	rCB$_1$[a]	rCB$_2$[b]	hCB$_1$[c]	hCB$_2$[d]	SI
					K_i (nM)		
R-(+)- WIN 55,212-2			15.3 ± 1.3	7.61 ± 0.68	12.2 ± 1.4	4.56 ± 0.45	2.68
CI01	Me	Cyclohexyl	1578 ± 152	26 ± 2	1278 ± 110	22 ± 2	58
CI02	Me	Cycloheptyl	642 ± 65	12.4 ± 1.1	527 ± 48	10.3 ± 1.2	51
CI03	Me	Adamant-1-yl	1460 ± 148	15.3 ± 1.6	1118 ± 96	12.7 ± 1.3	88
CI04	Me	Benzyl	3688 ± 386	428 ± 17	3290 ± 312	358 ± 32	9.2
CI05	Me	4-Me-cyclohexyl	2600 ± 310	120 ± 11	2432 ± 272	106 ± 9	23
CI06	Et	Cyclohexyl	480 ± 40	11.5 ± 1.2	420 ± 35	10.4 ± 1.2	40
CI07	Et	Cycloheptyl	220 ± 20	5.63 ± 0.57	200 ± 15	5.22 ± 0.45	38
CI08	Et	Adamantyl	150 ± 12	0.96 ± 0.08	120 ± 10	0.84 ± 0.07	143
CI09	t-But	Cyclohexyl	720 ± 70	14.2 ± 1.1	675 ± 54	12.3 ± 1.1	55
CI10	t-But	Cycloheptyl	650 ± 60	7.52 ± 0.68	605 ± 50	7.22 ± 0.63	84
CI11	t-But	Adamant-1-yl	675 ± 65	5.54 ± 0.48	612 ± 57	4.95 ± 0.42	124
CI12	Ph	Cyclohexyl	750 ± 80	50 ± 5	702 ± 68	42 ± 4	17
CI13	Ph	Cycloheptyl	900 ± 100	35 ± 4	825 ± 80	31 ± 3	27
CI14	Ph	Adamant-1-yl	> 10000 (40%)	2.74 ± 0.28	> 10000 (43%)	2.56 ± 0.22	>3906

75

CI15	2-Me-phenyl	Cyclohexyl	> 10000 (30%)	48 ± 4	> 10000 (16%)	40 ± 4	>250
CI16	2-Me-phenyl	Cycloheptyl	> 10000 (45%)	9.53 ± 0.92	> 10000 (34%)	8.93 ± 0.86	>1119
CI17	2-Me-phenyl	Adamant-1-yl	> 10000 (30%)	3.21 ± 0.30	> 10000 (22%)	2.86 ± 0.25	>3496
CI18	4-Me-phenyl	Cyclohexyl	> 10000 (25%)	62 ± 6	> 10000 (20%)	57 ± 5	>175
CI19	4-Me-phenyl	Cycloheptyl	> 10000 (49%)	13.2 ± 1.7	> 10000 (39%)	10.3 ± 1.1	>970
CI20	4-Me-phenyl	Adamant-1-yl	> 10000 (45%)	3.82 ± 0.39	> 10000 (38%)	3.41 ± 0.32	>2932
CI21	2-Cl-phenyl	Cyclohexyl	> 10000 (40%)	52 ± 5	> 10000 (34%)	47 ± 4	>212
CI22	2-Cl-phenyl	Cycloheptyl	> 10000 (42%)	12.3 ± 1.6	> 10000 (35%)	10.3 ± 1.1	>970
CI23	2-Cl-phenyl	Adamant-1-yl	> 10000 (48%)	6.32 ± 0.63	> 10000 (41%)	6.21 ± 0.55	>1610
CI24	4-Cl-phenyl	Cyclohexyl	> 10000 (8%)	58 ± 6	> 10000 (15%)	55 ± 5	>181
CI25	4-Cl-phenyl	Cycloheptyl	> 10000 (47%)	6.53 ± 0.58	> 10000 (40%)	6.31 ± 0.51	>1584
CI26	4-Cl-phenyl	Adamant-1-yl	> 10000 (10%)	4.21 ± 0.42	> 10000 (13%)	3.88 ± 0.31	>2577
CI27	2,4-di-Cl-phenyl	Cyclohexyl	> 10000 (47%)	60 ± 5	> 10000 (38%)	52 ± 5	>192
CI28	2,4-di-Cl-phenyl	Cycloheptyl	> 10000 (49%)	40 ± 4	> 10000 (39%)	37 ± 4	>270
CI29	2,4-di-Cl-phenyl	Adamant-1-yl	> 10000 (40%)	35 ± 3	> 10000 (37%)	30 ± 3	>333
CI30	2,6-di-Cl-phenyl	Adamant-1-yl	> 10000 (18%)	110 ± 10	> 10000 (21%)	98 ± 8	>102
CI31	Furan-2-yl	Cyclohexyl	> 10000 (30%)	10.4 ± 1.8	> 10000 (21%)	9.52 ± 0.92	>1050
CI32	Furan-2-yl	Cycloheptyl	> 10000 (20%)	7.23 ± 0.81	> 10000 (16%)	6.57 ± 0.62	>1522
CI33	Furan-2-yl	Adamant-1-yl	> 10000 (40%)	5.14 ± 0.42	> 10000 (34%)	4.92 ± 0.43	>2032
CI34	Furan-3-yl	Adamant-1-yl	> 10000 (17%)	12.4 ± 1.5	> 10000 (19%)	10.1 ± 1.3	>990
CI35	Thiophen-2-yl	Adamant-1-yl	> 10000 (22%)	7.52 ± 0.71	> 10000 (26%)	6.24 ± 0.61	>1602
CI36	4-Me-thiophen-2-yl	Adamant-1-yl	> 10000 (15%)	18 ± 2	> 10000 (13%)	15 ± 2	>666
CI37	5-Me-thiophen-2-yl	Adamant-1-yl	> 10000 (33%)	12.2 ± 1.8	> 10000 (31%)	11.6 ± 1.7	>862
CI38	Br	-	> 10000 (1%)	272 ± 25	> 10000 (1%)	220 ± 18	>45

CI39	Phenyl	-	> 10000 (15%)	214 ± 17	> 10000 (15%)	181 ± 16	>55
CI40	4-OCH$_3$-Ph	-	> 10000 (5%)	434 ± 41	> 10000 (4%)	350 ± 32	>28

The data are expressed as the mean ± SEM of n=4 independent experiments. The affinity values were calculated by using [^{3}H]-CP-55,940 as radioligand on a) rat brain for CB$_1$Rs, b) rat spleen for CB$_2$Rs, c) human CB$_1$R CHO membranes, d) human CB$_2$R CHO membranes.

Table 6. Effect of the Novel CB Compounds CI01−CI40 in hCB$_2$R CHO Cells on cAMP assays at 1 and 10 μM.

Compd	increase in cAMP production (%)		Compd	increase in cAMP production (%)	
	at 1 μM	at 10 μM		at 1 μM	at 10 μM
R-(+)-WIN 55,212-2	-102 ± 9	-104 ± 8	CI21	37 ± 4	55 ± 5
CI01	42 ± 4	54 ± 5	CI22	53 ± 6	69 ± 7
CI02	44 ± 5	63 ± 6	CI23	114 ± 9	136 ± 12
CI03	56 ± 6	75 ± 8	CI24	79 ± 9	94 ± 10
CI04	38 ± 3	52 ± 4	CI25	121 ± 13	162 ± 14
CI05	48 ± 5	67 ± 5	CI26	144 ± 13	183 ± 15
CI06	121 ± 11	146 ± 12	CI27	45 ± 4	65 ± 6
CI07	137 ± 13	159 ± 16	CI28	61 ± 5	77 ± 8
CI08	173 ± 14	243 ± 22	CI29	87 ± 8	112 ± 10
CI09	85 ± 9	115 ± 10	CI30	38 ± 4	62 ± 6
CI10	151 ± 12	213 ± 18	CI31	73 ± 7	103 ± 9
CI11	114 ± 11	189 ± 16	CI32	42 ± 4	88 ± 9
CI12	92 ± 8	123 ± 11	CI33	107 ± 11	124 ± 13
CI13	103 ± 9	134 ± 12	CI34	56 ± 6	92 ± 8
CI14	163 ± 15	195 ± 17	CI35	89 ± 8	102 ± 9
CI15	73 ± 6	94 ± 8	CI36	71 ± 6	97 ± 8
CI16	107 ± 8	125 ± 10	CI37	38 ± 4	68 ± 5
CI17	155 ± 15	184 ± 17	CI38	32 ± 4	48 ± 4
CI18	63 ± 7	93 ± 9	CI39	34 ± 4	51 ± 6
CI19	81 ± 7	107 ± 11	CI40	36 ± 4	60 ± 6
CI20	138 ± 12	168 ± 16			

The data are expressed as the mean ± SEM of n = 4 independent experiments and represent the % of increase of cAMP production in hCB$_2$R CHO cells stimulated with forskolin (1 μM) obtained by novel CB compounds at 1 or 10 μM in comparison with the full agonist WIN 55,212-2 that completely inhibited the forskolin-stimulated cAMP levels.

Figure 4.
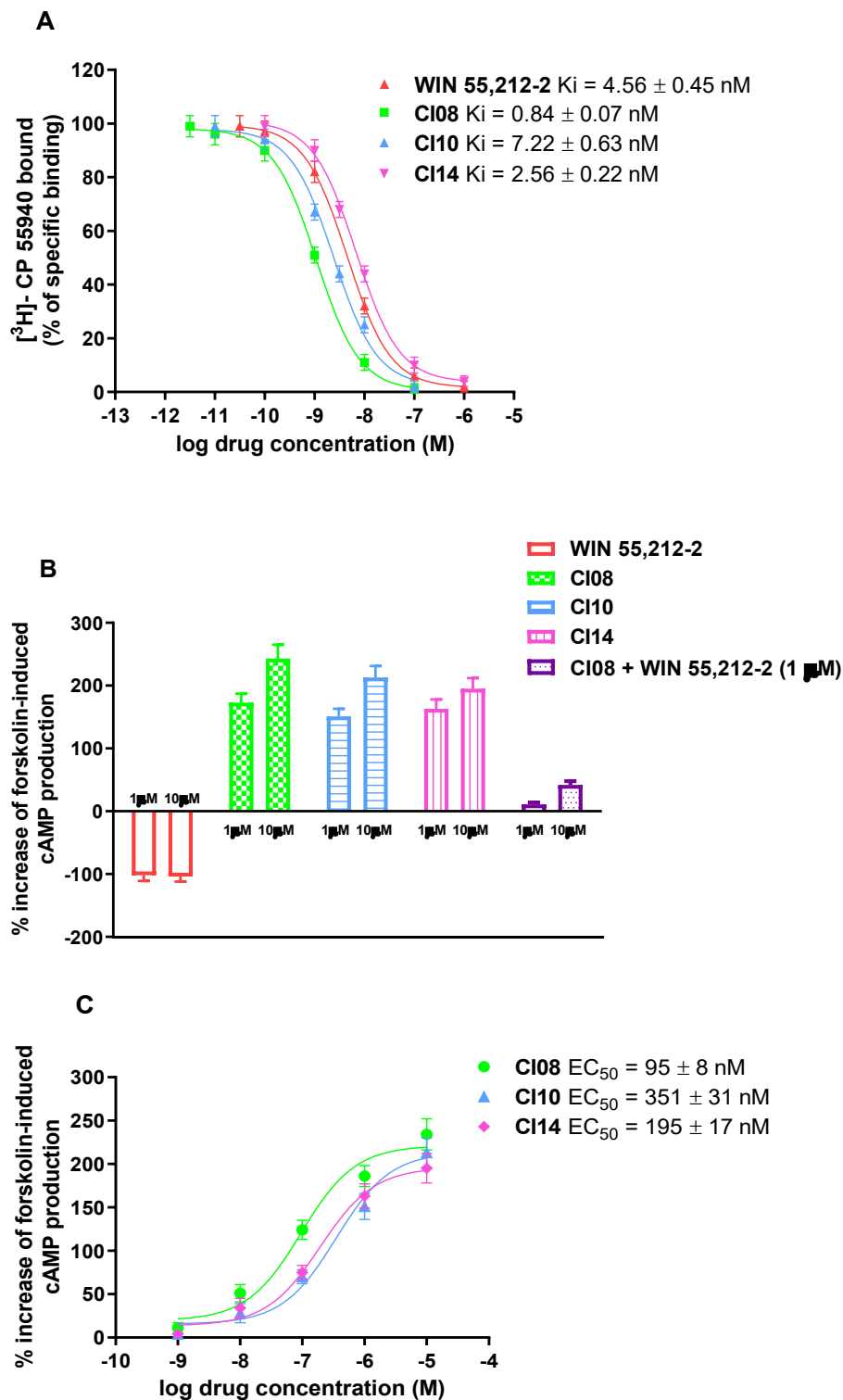
Figure 4. Competition curves on hCB$_2$R of WIN 55,212-2 and selected novel CB compounds (A). Effect of the same compounds expressed as % of increase of forskolin-stimulated cAMP accumulation in hCB$_2$R CHO cells (B). Concentration−response curves of the novel compounds CI08, CI10, and CI14 in cAMP assays (C). Results are the mean ± SEM (n = 4 independent experiments).

CHAPTER 2
PHARMACOLOGICAL CHARACTERIZATION OF NEW SELECTIVE FATTY ACID AMIDE HYDROLASE INHIBITORS

2.1. MATERIALS AND METHODS

Materials

Competition binding experiments were performed by using [^{3}H]-CP-55,940 (specific activity, 180 Ci/mmol) that was obtained from Perkin Elmer Life and Analytical Sciences (USA).
(R)-(+)-WIN 55,212-2 mesylate salt that was obtained from Sigma Aldrich (USA).
3-(4,5-dimethyl-2-thiazolyl)-2,5-diphenyl-2H-tetrazolium bromide (MTT) obtained from Perkin Elmer Life and Analytical Sciences (USA).
tert-Butyl hydroperoxide (TBHP) obtained from Perkin Elmer Life and Analytical Sciences (USA).
N-acetylcysteine (NAC) obtained from Perkin Elmer Life and Analytical Sciences (USA).

Cell culture

Mouse embryo fibroblast (NIH3T3) and human astrocytoma (1321N1) cells (Sigma-Aldrich) were maintained in DMEM (Invitrogen, Grand Island, NY, USA) supplemented with 10% FBS (Thermo Scientific, Waltham, MA, USA), L-glutamine (2 mM), penicillin (100 U/mL) and streptomycin (100 µg/mL) in a humidified atmosphere (5% CO_2) at 37 °C.
CHO cells transfected with human CB_1R or CB_2R (Perkin Elmer) were grown adherently and maintained in Ham's F12 containing 10% FBS, penicillin (100 U/mL), streptomycin (100 µg/mL) and Geneticin (G418, 0.4 mg/mL) at 37 °C in 5% CO_2/95% air.

FAAH inhibition assay

The inhibition activity of the novel compounds towards human FAAH was tested with a fluorescence-based assay, following the manufacturer's instructions (Cayman Chemical, Ann Arbor, MI, USA). Briefly, compounds were pre-incubated at different concentrations with human FAAH for 30 min at 37°C. The reaction was then initiated by the addition of 7-amino-4-methylcoumarin (AMC) arachidonoyl amide (final concentration 1 µM) as a substrate. After an incubation of 30 min at 37 °C, fluorescence due to the release of the AMC product was measured using an excitation wavelength of 355 nm and an emission wavelength of 465 nm in an EnSight Multimode plate reader (Perkin Elmer, MA, USA).

Evaluation of the mechanism of FAAH inhibition by rapid dilution assay

Compounds **FA07**, **FA09**, **FA16,** and **FA21** (10 and 100 nM) were incubated with a 50-fold concentrated solution of human FAAH enzyme for 30 min at 37 °C. Then, the enzyme inhibitor mixtures were diluted 50-fold with assay buffer. After 30 min, aliquots of the mixtures were transferred into empty wells of the plate, and the substrate was added. The enzyme activity was then measured according to the above-described standard procedure.

MAGL inhibition assay

The inhibition activity of the novel compounds towards human MAGL was tested with a fluorescence-based assay, following the manufacturer's instructions (Biovision, Mountain View, CA, USA). Briefly, compounds were pre-incubated at different concentrations with human MAGL for 30 min at 37 °C. After the addition of the substrate 7-hydroxycoumarinyl arachidonate, the assay mixture was incubated for another 30 min at 37 °C and the resulting fluorescence was measured with an excitation at 360 nm and emission at 460 nm using an EnSight Multimode plate reader (Perkin Elmer, MA, USA).

[³H] CP-55,940 competition binding assays.

To obtain membranes, hCB$_1$R and hCB$_2$R CHO cells were washed with PBS and scraped off with ice-cold hypotonic buffer (5 mM Tris HCl, 2 mM EDTA, pH 7.4). The cell suspension was homogenized with a Polytron and then centrifuged for 30 min at 40,000 x g. The membrane pellet was suspended in 50 mM Tris HCl buffer (pH 7.4) containing 2.5 mM EDTA, 5 mM MgCl$_2$, 0.5 mg/mL BSA for CB$_1$R or in 50 mM Tris HCl (pH 7.4), 1 mM EDTA, 5 mM MgCl$_2$, 0.5% BSA for CB$_2$R.

Competition binding experiments were carried out incubating 0.5 nM [³H]-CP-55,940 (Perkin Elmer Life and Analytical Sciences, USA) and different concentrations of the tested compounds for 90 or 60 min at 30 °C with hCB$_1$R or hCB$_2$R CHO membranes (2 µg protein/100 µL), respectively. Non-specific binding was determined in the presence of 1 µM WIN 55,212-2. Bound and free radioactivity were separated by filtering the assay mixture through Whatman GF/C glass fiber filters using a Brandel cell harvester (Brandel Instruments, Unterföhring,

Germany). The filter-bound radioactivity was counted using a Tri-Carb 2810TR liquid scintillation analyzer (Perkin Elmer).

MTT assay

NIH3T3 and 1321N1 cell viability was determined using a MTT assay. For this purpose, cells were harvested from culture flasks by trypsinization and seeded into 96-well microculture plates at a cell density of $1x10^4$ cells/150 µL and incubated overnight in a humidified atmosphere (5% CO_2) at 37 °C. Cells were then exposed to different concentrations (10 nM – 30 µM) of selected novel compounds for 24 h. After the incubation time, 15 µL of a 5 mg/mL MTT solution in PBS was added to each well and incubated for 4 h in the dark. During this time MTT is converted to formazan by the mitochondrial dehydrogenase in viable cells. At the end of the incubation, the formazan crystals are solubilized by adding 150 µL of an acidified isopropanolol solution. Optical densities at 570 nm were measured with the EnSight multimode plate reader (Perkin Elmer).

ROS production assay

1321N1 cells were seeded in 6-well plates at a density of 2.5×10^5 cells/2 mL and incubated overnight in a humidified atmosphere (5% CO_2) at 37 °C. Cells were pre-treated with selected novel compounds (1 nM – 1 µM) for 24 h before exposure to 50 µM TBHP for one additional hour at 37°C. NAC (2 mM) was used as a reference antioxidant compound. At the end of the treatment period, 1 µM CellROX™ Green Reagent (Thermo-Fisher Scientific, Paisley, UK) was added to the cells followed by an incubation of 45 min at 37°C. Immediately after cell detachment, data were acquired on an Attune NxT Flow Cytometer (Thermo-Fisher Scientific, Paisley, UK) equipped with a 488 nm laser for excitation, and fluorescence emission was collected using a 530/30 BP filter. 1321N1 cells were gated according to physical parameters and cell aggregates were removed from the analysis.

Ex vivo studies in hippocampal slices

All media and sera for OHSCs were purchased from Gibco (Milan, Italy). All animal experiments and handling and care were by the ARRIVE guidelines and the Guide for the Care and Use of Laboratory Animals. Female Wistar rats (14-day timed pregnant) were obtained from Charles River Laboratories (Italy) and maintained at a constant temperature (22 + 1 °C) on a 12

h light/dark cycle (lights on at 7 AM) with food and water ad libitum. The pregnant dams were allowed to deliver their pups naturally; 7-9 days postpartum littermates were used for the preparation of organotypic explants. All efforts were made to minimize animal suffering and to reduce the number of animals used.

Rat hippocampal organotypic explants

Briefly, 400-μm-thick parasagittal slices were obtained from hippocampi of P7- to P9-day-old Wistar rat pups (Charles River Laboratories, Calco, Italy) using a McIlwain tissue chopper (Campden Instruments, Leicester, UK) and placed into ice-cold Hank's balanced salt solution (HBSS, Gibco, Italy) supplemented with 5 mg/mL glucose and 1.5% (v/v) Fungizone. Cultures were then transferred to a humidified semi-porous membrane (30-mm Millicell tissue culture plate inserts of 0.4 mm pore size from Millipore, Italy) in six-well tissue culture plates (4 slices per membrane). Each well contained 1.2 mL of tissue culture medium consisting of 50% minimal essential medium (MEM, Gibco, Monza, Italy), 25% HBSS, 25% heat-inactivated horse serum, 6.5 mg/mL glucose, 1 mM glutamine, and 1.5% Fungizone. Cultures were maintained at a 37 °C and 5% CO_2-conditioned atmosphere. All experiments were performed on cultures kept in vitro for 10-12 days (DIV).

Lipopolysaccharide (LPS) plus interferon-gamma (INF-ɣ) exposure and pharmacological treatments

Hippocampal explants were removed from normal serum-containing medium (NM) and exposed to a combined application of 10 μg/mL LPS plus 100 ng/mL INFɣ for 96 h in serum-free medium SFM (SFM, consisting of NM with serum replaced with MEM). This model triggers the release of massive proinflammatory and cytotoxic factors and promotes inflammatory neurodegeneration. The appropriate concentration of each FAAH inhibitor: 0.3 nM -0.1 μM FA07; 0.3 nM-0.1 μM FA09; 3 nM-1 μM FA16; 0.1-10 μM FA21; or vehicle (DMSO ≤ 0.1%) were added to the medium at the beginning of the LPS+IFN-ɣ exposure and were kept in the culture medium during the entire duration of the experiment. Control culture explants, in the absence or the presence of compounds, were kept in SFM.

Assessment of cell death and image analysis.

Cell injury was assessed in explants by live incorporation of a marker of compromised membrane integrity, propidium iodide (PI, 5 μg/mL, Molecular Probes), that emits a bright red

fluorescence when exposed to blue-green light. For densitometric measurements, the digital pictures were analyzed with the Image Pro-Plus software (Media Cybernetics), after freehand outlining of the CA1 neuronal layer.

Statistical analysis.

Statistical analysis was performed by using one-way ANOVA followed by Bonferroni post-hoc test as indicated in the legends of figures. Analysis was done using the software Graphpad Prism 8.0.1. Values represent the mean ± SEM of at least three independent experiments. Differences were considered statistically significant at * $p < 0.05$.

2.2. *RESULTS AND DISCUSSION*

2.2.1. *Enzymatic assays and SAR discussion*

FAAH activity was measured on a human recombinant purified enzyme following a 30-minute pre-incubation with the tested compounds. IC_{50} values for compounds **FA03-FA22** are reported in Table 1, along with that of the reference phenylpyrrole **FA01** and phenylfurane **FA02**. The goal of our investigation was the identification of compounds with balanced potency on FAAH, solubility, chemical stability, and lack of activity on MAGL. Given the distinct localization of FAAH and MAGL, along with the fact that FAAH predominantly cleaves AEA while MAGL targets 2-AG, developing selective FAAH inhibitors could prove useful in selectively enhancing the AEA signal at the post-synaptic level with therapeutic potential for neuroinflammation, pain, and conditions associated with depression and anxiety. The compounds **FA01** and **FA02** were taken as a starting point for the development of the new compounds. The two reference compounds are selective inhibitors of the enzyme FAAH but have poor water solubility. To improve this property, new compounds were synthesized based on the structure of **FA02**. In particular, the substitutions made on the **FA02** compound to obtain the **FA03** compound were found to be suboptimal as they worsened the inhibitory potency of the FAAH enzyme by 10 times. On the other hand, the substitutions made in the compounds **FA04** and **FA05**, also starting from the reference compound **FA02**, showed IC_{50} values of 188 and 407 nM, respectively. Tertiarization of the carbamate group of **FA06** had a different impact on inhibitory potency, with direct methylation of the nitrogen dramatically reducing activity (**FA06**, $IC_{50} = 6556$ nM),

and its inclusion in a piperazine ring leading to a single-digit nanomolar compound (**FA07**, IC$_{50}$ = 8.3 nM). Compound **FA07** thus emerged as a key inhibitor deserving further investigation, considering our multiparametric optimization aimed at finding inhibitors with good potency and balanced physicochemical properties. Compounds **FA08**-**FA22** were all synthesized by modifying the structure of the new reference compound **FA07**. In particular, it was found that compounds **FA08**, **FA09**, **FA13**, **FA16**, **FA17**, **FA18**, **FA19**, and **FA21** are excellent selective inhibitors of the FAAH enzyme with inhibitory potencies of 11.7, 26, 15.6, 10.1, 15.8, 47, 10.5, and 7.54 nM, respectively. Two compounds showed low inhibition potency for the enzyme, namely **FA12** with an IC$_{50}$ of 8450 and **FA15** with an IC$_{50}$ greater than 10000 nM. Compounds **FA10**, **FA11**, **FA14**, **FA20**, and **FA22** exhibited inhibitory potencies of 165 nM, 194 nM, 315 nM, 128 nM, and 253 nM, respectively.

The present exploration allowed to identification of several candidates with fair potency (IC$_{50}$ < 100 nM) potentially endowed with higher solubility and/or enhanced chemical stability compared to reference inhibitors **FA02** and **FA01**, and devoid of significant activity on MAGL.

2.2.2. *Mechanism of action of carbamate-based FAAH inhibitors FA07, FA09, FA16 and FA21*.

To investigate the inhibitory mechanism of the compounds **FA07**, **FA09**, **FA16,** and **FA21**, were conducted rapid dilution experiments. These compounds were exposed to two different concentrations (10 and 100 nM) in the presence of FAAH levels 50 times higher than standard conditions. Following a 50-fold dilution, we introduced the substrate and assessed enzymatic activity. In the case of reversible inhibitors, rapid dilution disrupts the equilibrium between the inhibitor and the enzyme, leading to the recovery of enzymatic activity. In contrast, dilution of the assay mixture containing the enzyme and an irreversible inhibitor does not result in the restoration of enzymatic activity. Subsequent to rapid dilution, we observed a near-complete recovery of FAAH activity for both **FA07** (Figure 1A), **FA09** (Figure 1B), **FA16** (Figure 1C) and **FA21** (Figure 1D) when compared to standard incubation conditions. These findings indicate that derivatives **FA07**, **FA09**, **FA16,** and **FA21** inhibit FAAH through a reversible mechanism. Conversely, when employing URB597, a known irreversible FAAH inhibitor, no restoration of enzyme activity was noted following rapid dilution (Figure 1E).

2.2.3. Selectivity and Toxicity Profile

For the most promising compounds, the selectivity profile against CB_1R and CB_2R was evaluated, and the potential cytotoxicity was investigated in murine fibroblast cell lines NIH3T3 and human astrocyte cell lines 1321N1. We investigated the affinity of FAAH inhibitors **FA04**, **FA05**, **FA07**, **FA08**, **FA09**, **FA10**, **FA11**, **FA13**, **FA14**, **FA16**, **FA17**, **FA18**, **FA19**, **FA20**, **FA21**, and **FA22** towards human CB_1R and CB_2R. To this aim, competition binding experiments were performed using $[^3H]$-CP-55,940 as radioligand in membranes obtained from CHO cells transfected with human CB_1R or CB_2R. As reported in Table 2, none of the selected analogs showed an K_i less than 10 µM for either CBR subtype. The cytotoxicity profile of compounds **FA07**, **FA09**, **FA16**, and **FA21** was evaluated in the murine fibroblast cell lines (NIH3T3) and human astrocytes (1321N1) after 24 h of incubation. The results, reported in Table 3, showed the low toxicity of all the selected analogs that, except for compound **FA07**, nicely challenged the IC_{50} of the reference phenylfurane-based analog **FA02** by almost doubling it. The results, reported in Table 4 showed that selected analogs displayed notable safety profiles at all tested concentrations. No toxicity was detected at all the tested concentrations.

2.2.4. Evaluation of the anti-inflammatory profile

While neurodegenerative diseases may have diverse origins and pathways, a common characteristic of these conditions is the presence of neuroinflammatory processes, which trigger various biological mechanisms, such as oxidative stress and glial responses. Glial cells, including astrocytes, play a role in maintaining the balance of the central nervous system by either exacerbating inflammatory reactions or promoting tissue repair. In this context, inhibiting the catabolic enzymes of the endocannabinoid system, either through pharmacological means or genetic approaches, has been shown to reduce both neuroinflammatory and neurodegenerative states in various animal models. Building on these findings, we investigated the impact of our newly developed FAAH inhibitors on reducing oxidative stress in human astrocytes of the 1321N1 cell line. We also assessed the protective effects of our selected analogs in ex vivo cultures of rat hippocampal explants exposed to inflammation-induced neurodegeneration. Then the effects of selected compound on TBHP-induced ROS production were tested. When administered to 1321N1 astrocytes, FAAH inhibitors **FA07**, **FA09**, **FA16**, and **FA21** resulted effective in the prevention of TBHP-induced ROS production as shown in Figure 2. **FA07** and **FA21** significantly reduced ROS production starting from the 10 nM

concentration, while compound **FA09** and **FA16** from the 100 nM concentration. All the tested compounds at 1 μM exerted an effect similar to that of 2 mM NAC, used as a reference antioxidant compound (Figure 2).

To study the neuroprotective actions of selective FAAH inhibitors on neuroinflammatory damage, 10-12 DIV organotypic explants (ex vivo cultures of rat hippocampal explants) were exposed to a combined application of 10 μg/mL LPS and recombinant 100 ng/mL IFN-ɣ for 96 h, and cell death was assessed with propidium iodide (PI) staining. Densitometric analysis of PI uptake revealed that when hippocampal explants were exposed to the inflammatory injury, cell death selectively occurred after 96 h in the CA1 pyramidal cell layer. The presence of **FA07** (0.3 nM – 0.1 μM), **FA09** (0.3 nM – 0.1 μM), **FA16** (3 nM – 1 μM) and **FA21** (0.1–10 μM) in the incubation media throughout the experiment did not affect the viability of organotypic cultures, while significantly prevented the increase in PI uptake occurring in the CA1 region 96 hours after LPS+IFN-ɣ exposure (Figure 3 A-D). The compound **FA07** (0.3 nM – 0.1 μM) exerted dose-dependent and marked neuroprotective action in the CA1 region (70-80%) after LPS+IFN-ɣ exposure with an $EC_{50} \sim 3$ nM (EC_{50} 4e = 2.913 nM). **FA09** significantly attenuated cell death at 3 nM – 0.1 μM concentrations. **FA16** significantly prevented PI uptake at concentrations of 30 nM – 1 μM. **FA21** showed significant dose-dependent protection at 1 μM and 10 μM concentrations.

Table 1. Inhibitory activity towards *human* FAAH and *human* MAGL (expressed as IC$_{50}$ nM) for title compounds **FA03**–**FA22**, and reference compounds **URB597, FA01, FA02**.

Compounds	Structure	IC$_{50}$ (nM) *h*FAAH	IC$_{50}$ (nM) *h*MAGL
URB597		31.1 ± 1.8	9384 ± 652
FA01		3.72 ± 0.21	8754 ± 473
FA02		102 ± 9	>10000
FA03		1044 ± 73	>10000
FA04		188 ± 11	>10000
FA05		407 ± 32	>10000
FA06		6556 ± 412	>10000
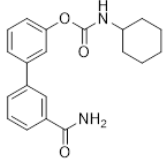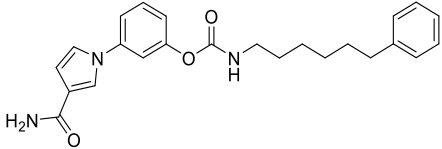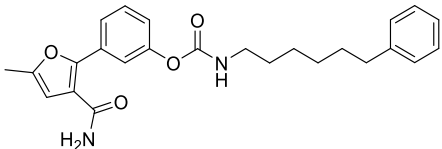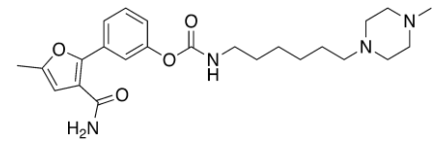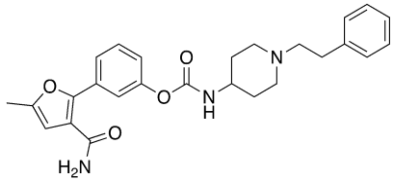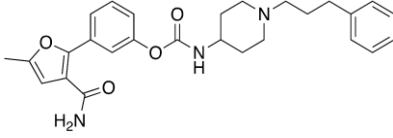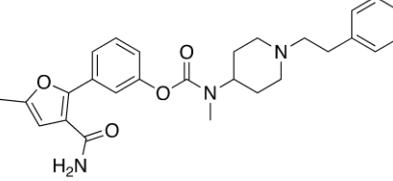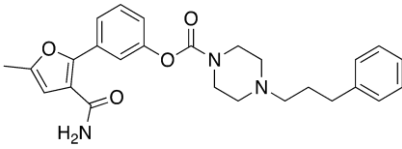
FA07		8.29 ± 0.58	5061 ± 387
FA08		11.7 ± 0.8	4116 ± 314
FA09		26 ± 2	>10000
FA10		165 ± 12	9878 ± 677
FA11		194 ± 13	>10000
FA12		8450 ± 523	>10000
FA13		15.6 ± 0.9	>10000
FA14		315 ± 19	>10000
FA15		>10000	>10000
FA16		10.1 ± 0.6	>10000
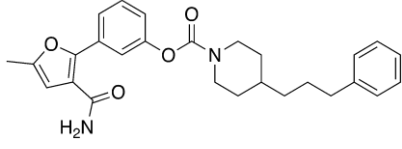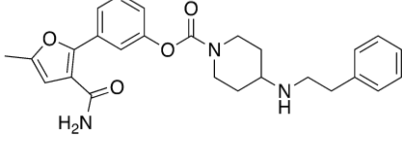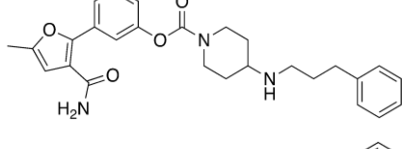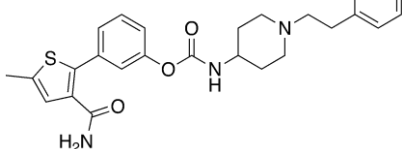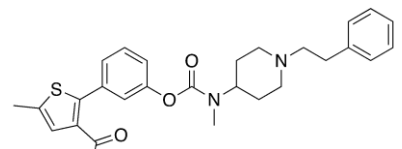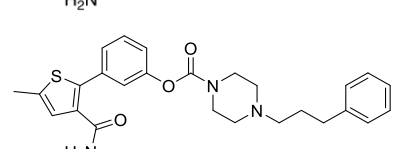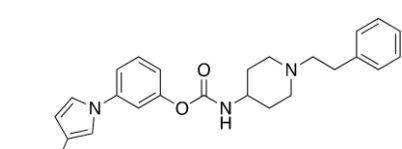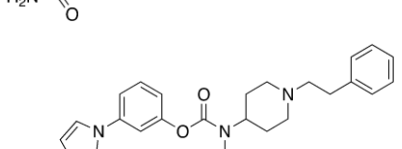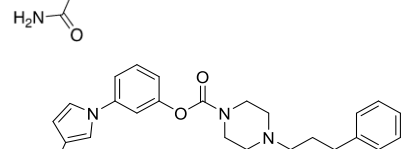
90
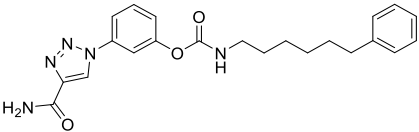
FA17		15.8 ± 1.1	479 ± 28
FA18		47 ± 3	2899 ± 193
FA19		10.5 ± 0.8	2437 ± 178
FA20		128 ± 9	>10000
FA21		7.54 ± 0.51	8396 ± 621
FA22		253 ± 13	>10000
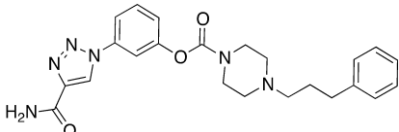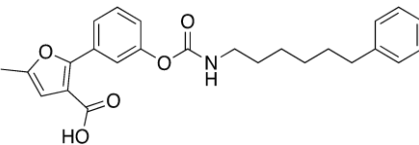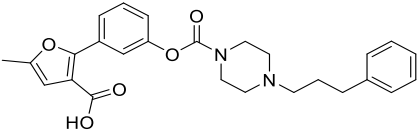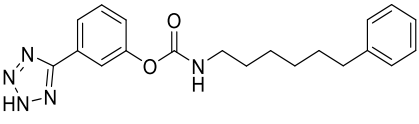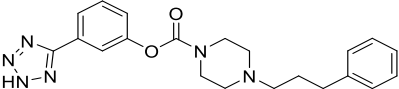
Each value is the mean ± SEM of three independent experiments; FAAH and MAGL inhibition was measured after 30 min of pre-incubation.
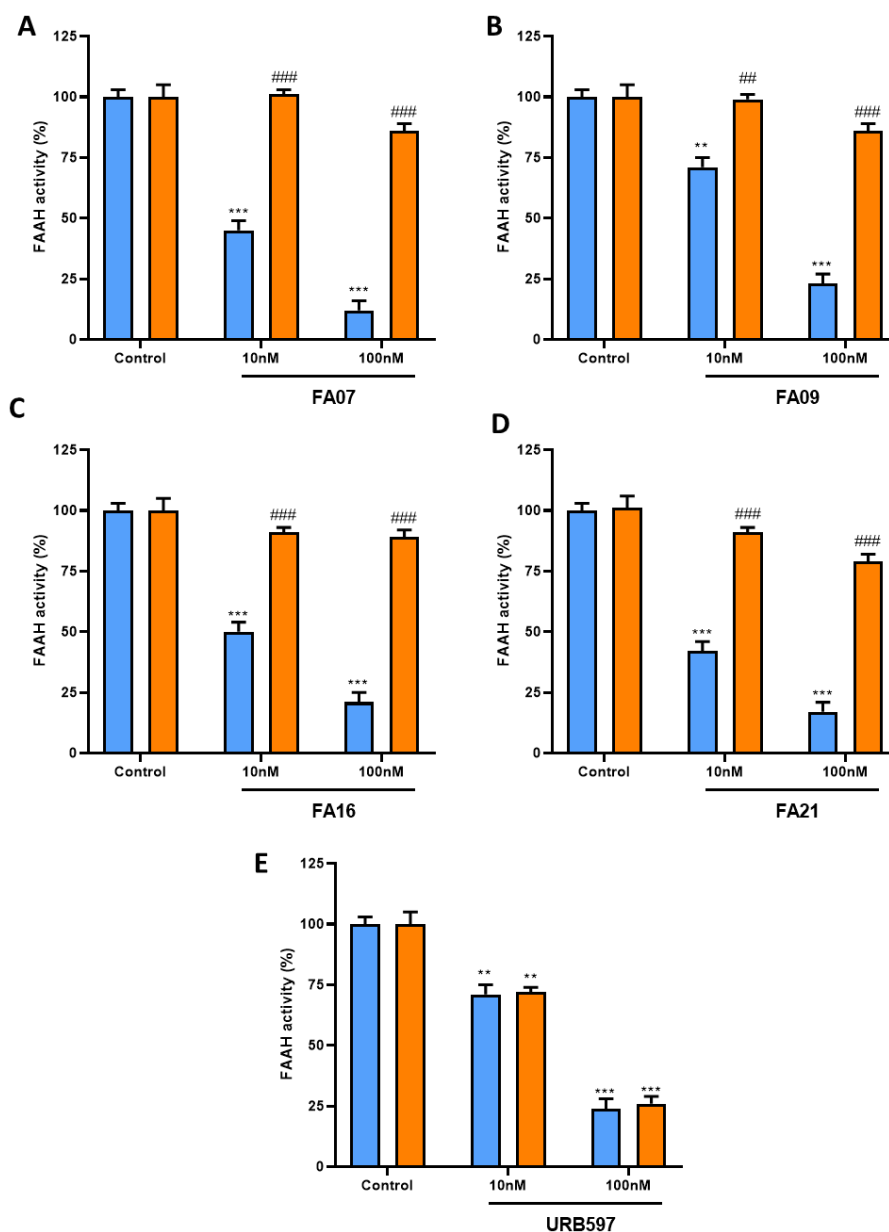
Figure 1. Reversibility of FAAH inhibition by compounds **FA07** (**A**), **FA09** (**B**) **FA16** (**C**), and **FA21** (**D**) in comparison to reference compound **URB597** (**E**). Rapid dilution assay (orange histograms), standard protocol (blue histograms). The complete recovery of the enzymatic activity following rapid dilution demonstrates the reversible nature of the inhibition of compounds **FA07, FA09, FA16,** and **FA21**. Conversely, the lack of recovery of FAAH activity confirms that the reference compound URB597 acts as an irreversible inhibitor.

**, $p < 0.01$ vs control; ***, $p < 0.001$ vs control; ##, $p < 0.01$ vs standard protocol; ###, $p < 0.001$ vs standard protocol (two-way ANOVA followed by Tuckey's multiple comparison test).

Table 2. Inhibition potency of selected analogs for *human* cannabinoid receptors CBR_1 and CBR_2 expressed as K_i (nM).

Compound	[³H]-CP 55,940 binding *h*CBR₁ cells K_i (nM)	[³H]-CP 55,940 binding *h*CBR₂ cells K_i (nM)
FA04	>10000 (5%)	>10000 (2%)
FA05	>10000 (1%)	>10000 (4%)
FA07	>10000 (3%)	>10000 (1%)
FA08	>10000 (7%)	>10000 (10%)
FA09	>10000 (1%)	>10000 (2%)
FA10	>10000 (12%)	>10000 (10%)
FA11	>10000 (1%)	>10000 (2%)
FA13	>10000 (1%)	>10000 (1%)
FA14	>10000 (4%)	>10000 (5%)
FA16	>10000 (12%)	>10000 (1%)
FA17	>10000 (7%)	>10000 (3%)
FA18	>10000 (1%)	>10000 (4%)
FA19	>10000 (9%)	>10000 (15%)
FA20	>10000 (12%)	>10000 (14%)
FA21	>10000 (18%)	>10000 (22%)
FA22	>10000 (1%)	>10000 (11%)

Data are obtained from three independent experiments performed in duplicate. In parentheses, the percentage of inhibition at the 10 µM concentration is indicated.

Table 3. Viability of *mouse* fibroblasts NIH3T3 after compounds **FA07**, **FA09**, **FA16,** and **FA21** and reference compounds **FA01** and **FA02** administration.

Compound	Cell viability (%) at different concentrations					IC$_{50}$ (nM)
	10 nM	100 nM	1 µM	10 µM	30 µM	
FA07	100.1 ± 5.3	89.7 ± 3.7	65.4 ± 3.2	41.7 ± 2.2	32.3 ± 1.1	6330 ± 260
FA09	98.2 ± 5.8	85.3 ± 4.7	59.1 ± 3.2	40.3 ± 2.5	27.8 ± 2.3	4296 ± 173
FA16	99.8 ± 6.2	86.2 ± 4.8	58.2 ± 3.5	40.1 ± 3.2	30.1 ± 2.4	4724 ± 190
FA21	96.2 ± 6.1	84.2 ± 5.8	55.2 ± 4.2	39.2 ± 2.6	29.1 ± 1.2	3376 ± 141
FA01	101.2 ± 6.1	89.0 ± 5.8	74.2 ± 5.1	46.3 ± 3.3	32.2 ± 2.1	8783 ± 389
FA02	95.4 ± 5.8	79.7 ± 4.8	52.3 ± 3.1	34.5 ± 2.5	25.9 ± 1.9	1694 ± 101

Each value is the mean ± SEM of at least three experiments.

Table 4. Viability of 1321N1 *human* astrocytes after compounds **FA07**, **FA09**, **FA16,** and **FA21** and reference compounds **FA01** and **FA02** administration.

Compound	Cell viability (%) at different concentrations					IC$_{50}$ (nM)
	10 nM	100 nM	1 µM	10 µM	30 µM	
FA07	99.3 ± 5.1	97.0 ± 4.8	100.0 ± 5.5	101.0 ± 4.0	96.0 ± 6.5	>30000
FA09	101.3 ± 5.3	98.8 ± 4.1	99.2 ± 6.0	97.5 ± 5.5	98.2 ± 4.8	>30000
FA16	100.5 ± 5.6	99.5 ± 4.8	100.3 ± 4.7	100.0 ± 5.4	101.5 ± 4.8	>30000
FA21	100.8 ± 1.5	98.5 ± 1.4	98.8 ± 1.7	99.8 ± 2.0	97.0 ± 1.5	>30000
FA01	100.2 ± 6.2	90.5 ± 5.8	79.4 ± 5.1	56.5 ± 4.3	42.8 ± 2.9	15983 ± 789
FA02	97.1 ± 5.8	81.3 ± 4.8	54.2 ± 3.4	35.3 ± 2.5	28.8 ± 2.9	2345 ± 124

Each value is the mean ± SEM of at least three experiments.
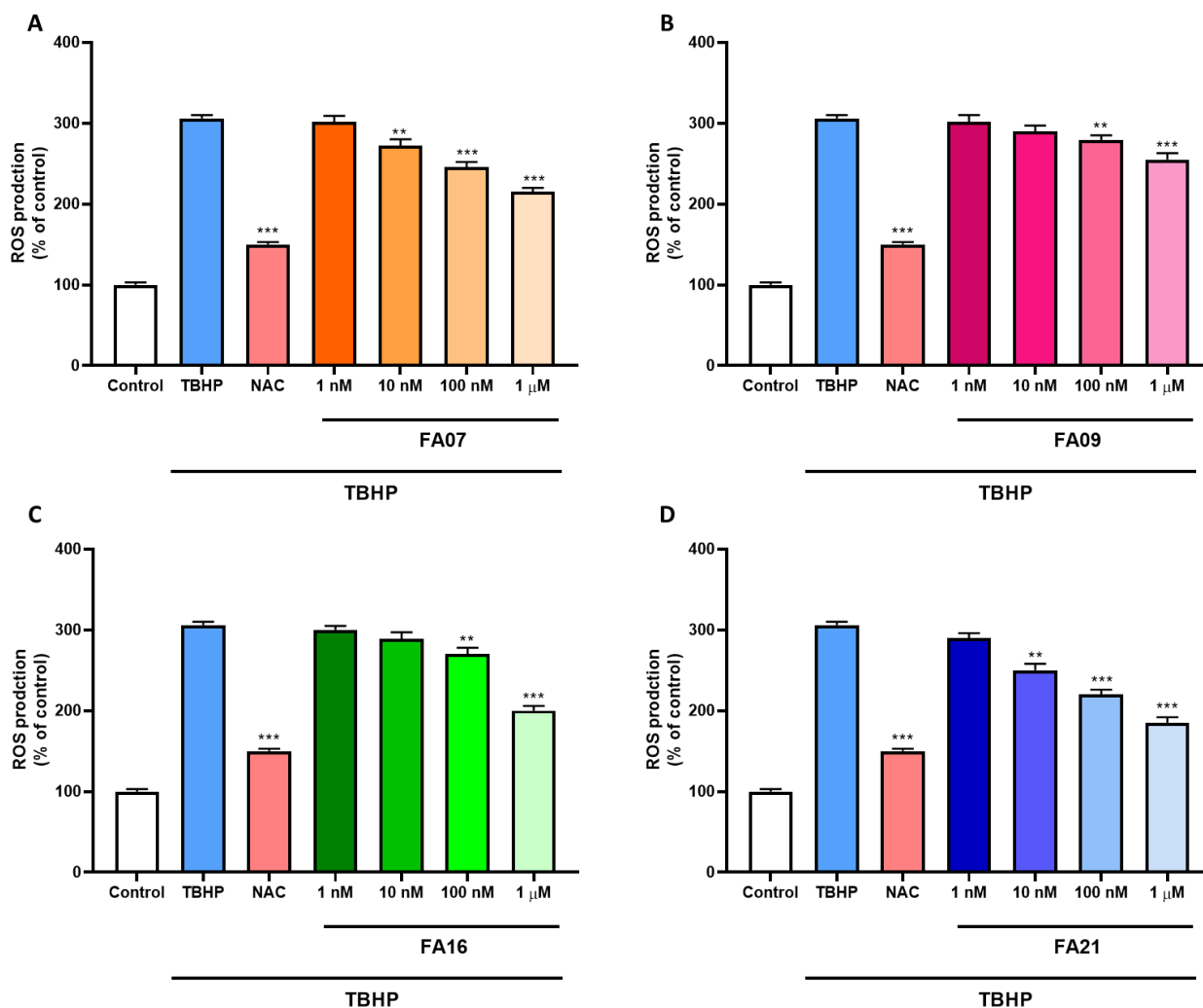
Figure 2. Effect of novel FAAH inhibitors on TBHP-induced ROS production in 1321N1 astrocytes in comparison to NAC, 2 mM. Compound **FA07** (A), **FA09** (B), **FA16** (C), and **FA21** (D) significantly reduced ROS levels induced by 50 μM TBHP. NAC (2 mM) was used as a reference antioxidant compound. $**p < 0.01$ versus TBHP; $*** p < 0.001$ versus TBHP.
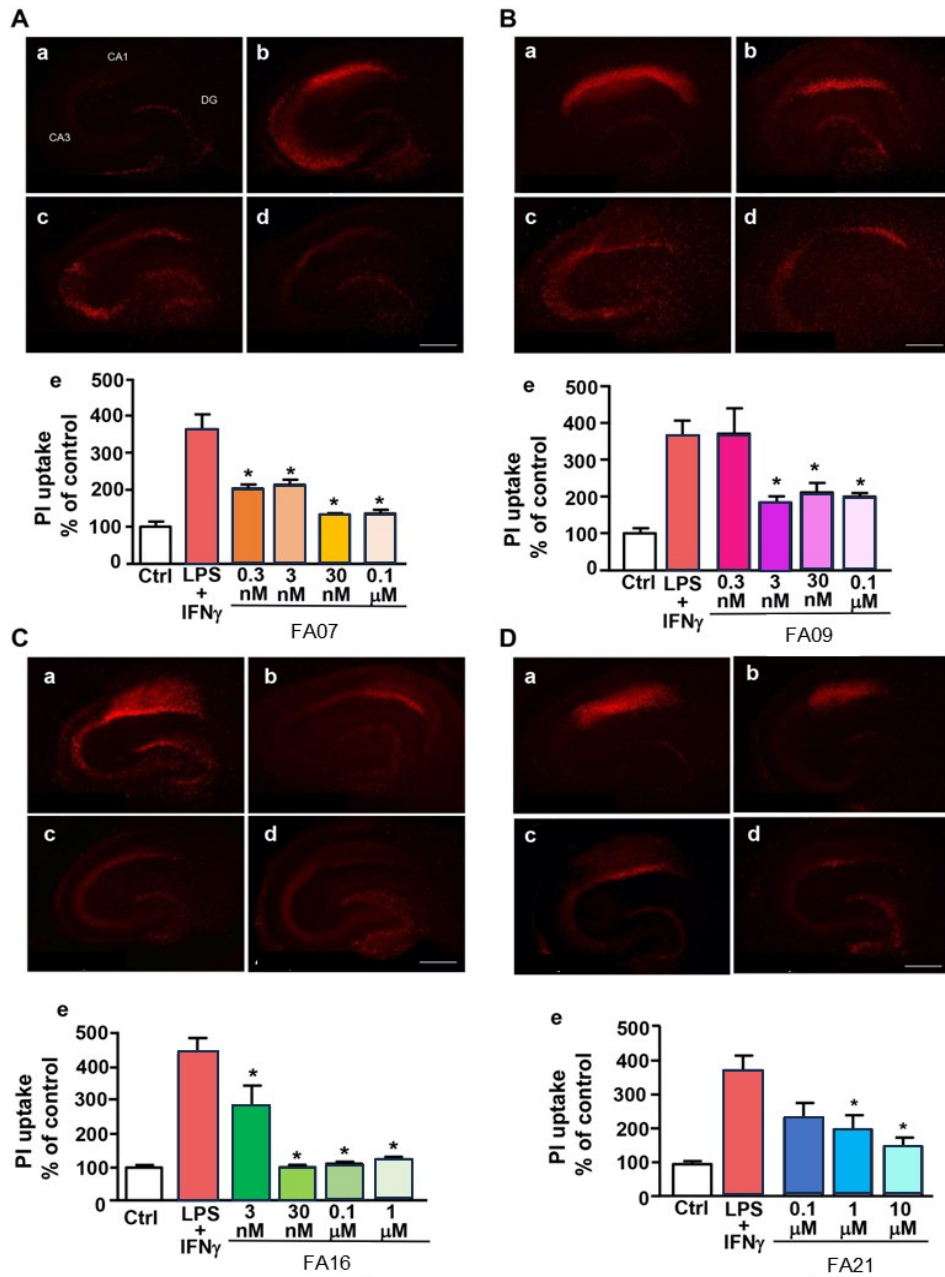
Figure 3. Effects of FAAH inhibitors against LPS+IFNɣ induced inflammatory damage in hippocampal organotypic cultures. A–D, a-d; PI fluorescence staining patterns observed in representative hippocampal organotypic slices under control conditions (A, a) and following 96 h of LPS + IFNɣ exposure in the absence of drug exposure (A, b; B-D, a) or the presence of 0.3 nM – 30 nM **FA07 (**A, c-d); 0.3 nM – 0.1 μM **FA09 (**B, b-d); 3 nM – 1 μM **FA16** (C, b-d); 0.1 μM – 10 μM **FA21** (D, b-d). Scale bars in a-d: 500 μm. A-D, e; Quantification of cell damage in the CA1 subfield evaluated by densitometric analysis of PI fluorescence and normalized to that recorded in the CA1 subregion of untreated hippocampal slices. *p < 0.05 versus LPS+ IFNɣ.

CHAPTER 3

PHARMACOLOGICAL CHARACTERIZATION OF NEW

FATTY ACID AMIDE HYDROLASE INHIBITORS AND

MELATONIN RECEPTOR LIGANDS

3.1. MATERIALS AND METHODS

Materials

Competition binding experiments were performed by using 2- [^{125}I]iodomelatonin (specific activity 2200 Ci/mmol) that was obtained from Perkin Elmer Life and Analytical Sciences (USA).

Melatonin salt was obtained from Sigma Aldrich (USA).

7β-acetossi-8,13-epossi-1α,6β,9α-triidrossilabd-14-en-11-one or Forskolin that was obtained from Sigma Aldrich (USA).

4-(3-butoxy-4-methoxybenzyl)-2-imidazolidinone (Ro 20-1724) that was obtained from Sigma Aldrich (USA).

Lipopolysaccharide (LPS) obtained from Sigma Aldrich (USA).

Interferon-gamma (INF-ɣ) obtained from Sigma Aldrich (USA).

Cell culture

CHO cells stably transfected with human MT_1Rs and MT_2Rs were cultured in Ham's F-12K medium supplemented with 10% FBS, 1% glutamine, 600 µg/mL geneticin, and 10 µg/mL puromycin.

Rat hippocampal organotypic explants

Organotypic explants were prepared as previously described. Postnatal P7- to P9-day-old Wistar rat pups were killed by cervical dislocation and 400-µm-thick parasagittal slices were obtained from dissected hippocampi using a McIlwain tissue chopper (Campden Instruments, Leicester, UK) and placed into ice-cold Hank's balanced salt solution (HBSS, Gibco, Milan, Italy, Cat# 24020117) supplemented with 5 mg·ml−1 glucose and 1.5% (v/v) fungizone. Cultures were then transferred to a humidified semi-porous membrane (30 mm Millicell tissue culture plate inserts of 0.4 m pore size from Millipore, Milan, Italy, Cat# PICM03050) in six-well tissue culture plates (five slices per membrane). Each well contained 1.2 ml of tissue culture medium consisting of 50% minimal essential medium (MEM, Gibco, Milan, Italy, Cat# 11095080), 25% HBSS, 25% heat-inactivated horse serum (HS, Gibco, Italy, Cat# 26050088), 6.5 mg·ml−1 glucose, 1 mM glutamine and 1.5% fungizone (Thermo Fisher Scientific, Italy, Cat# 15290018) (normal medium [NM]). Cultures were maintained at a 37°C and 5% CO2-conditioned

atmosphere. Experiments were performed on cultures kept in vitro for 7 days (7 DIV) or 10 days (10 DIV). Therapeutic screens in organotypic explant cultures prepared from rodent postnatal P7–P9 brains provide a valuable system to study candidate lead compounds for neuroprotection and their mechanism of action in a multicellular CNS context. Brains of postnatal animals are commonly used for slice cultures because they are more resistant to mechanical trauma that occurs during slice preparation compared to adult brains. Preparing organotypic brain slice cultures from adult brains is more challenging and requires to be optimized for long-term culturing such as culturing at lower temperatures, optimizing culture medium components, or reducing the thickness because the cell survival is very limited and cytoarchitectural organization of the tissue is not retained for a long time.

LPS + IFN-γ-induced neurodegeneration and drug exposure

Hippocampal explants were removed from normal serum-containing medium, washed in SFM (consisting of NM with serum replaced with MEM, plus 1% HS), and exposed to a combined application of $10\ \mu g \cdot ml^{-1}$ LPS + $100\ ng \cdot ml^{-1}$ IFN-γ for 72–96 h in SFM. This model, by mimicking microglial interaction with infiltrating peripheral immune T cells, triggers the release of large amounts of pro-inflammatory and cytotoxic factors and promotes inflammatory neurodegeneration. Appropriate concentrations of FM15 (0.1–10 μM), URB597 (10 μM), melatonin (10 μM), or vehicle (DMSO ≤ 0.1%) were added to the medium at the beginning of the treatment and were kept in the culture medium during the entire duration of the experiment.

[^{125}I] iodomelatonin competition binding assays.

To obtain membranes, hMT$_1$R and hMT$_2$R CHO cells were washed with PBS and scraped off with ice-cold hypotonic buffer (5 mM Tris HCl, 2 mM EDTA, pH 7.4). The cell suspension was homogenized using a Polytron, followed by centrifugation for 30 minutes at 40,000 × g at 4°C. The resulting pellets were resuspended in binding buffer (50 mM Tris-HCl, pH 7.4, 5 mM MgCl$_2$) and then utilized for binding experiments. Protein concentration was determined according to the Bradford method using the Bio-Rad Protein Assay (Bio-Rad Laboratories). Competition binding experiments were performed incubating 2-[^{125}I]iodomelatonin (30 pM for MT$_1$Rand 80 pM for MT$_2$R) and different concentrations of the examined compounds in binding buffer (50 mM Tris-HCl, pH 7.4, 5 mM MgCl$_2$) with hMT$_1$R CHO or hMT$_2$R CHO cell membranes for 120 min or 20 h at 37°C. The pK$_i$ values were calculated from the IC$_{50}$ values

in accordance with the Cheng− Prusoff equation. The pK$_i$ values are the mean of at least three independent determinations performed in duplicate. Bound and free radioactivity were separated by filtering the assay mixture through Whatman GF/C glass fiber filters using a Brandel cell harvester (Brandel Instruments, Unterföhring, Germany). The filter-bound radioactivity was counted using a Tri-Carb 2810TR liquid scintillation analyzer (Perkin Elmer).

cAMP assays

hMT$_1$R CHO or hMT$_2$R CHO cells were washed with phosphate-buffered saline, detached with trypsin, and centrifuged for 10 min at 200×g. Cells were seeded in a 96-well white half-area microplate in stimulation buffer composed of Hank Balanced Salt Solution, 5 mM HEPES, 0.5 mM Ro 20–1724, and 0.1% BSA. To assess potency, agonists were used in the presence of 1 µM forskolin to stimulate cAMP production. The antagonist's effect was evaluated based on its ability to counteract the melatonin-induced reduction of forskolin-stimulated cAMP production. Melatonin (MLT) concentrations used in this experiment were 0.3 nM for the MT$_1$R and 1 nM for the MT$_2$R. The cAMP levels were quantified by using the AlphaScreen cAMP Detection Kit (Perkin Elmer), following the manufacturer's instructions. The Alpha signal was read with a Perkin Elmer EnSight Multimode Plate Reader.

Enzymatic assays on human FAAH

The inhibition activity of the novel compounds against human FAAH was assessed using a fluorescence-based assay, following the manufacturer's instructions (Cayman Chemical, Ann Arbor, MI, USA). Briefly, the compounds were preincubated at various concentrations with human FAAH for 30 minutes at 37°C. The reaction was initiated by adding 7-Amino-4-methylcoumarin (AMC) arachidonoyl amide (final concentration 1 µM) as the substrate. After a 30-minute incubation at 37°C, the fluorescence resulting from the release of the AMC product was measured using an excitation wavelength of 355 nm and an emission wavelength of 465 nm, utilizing an EnSight Multimode plate reader (Perkin Elmer, MA, USA).

IL-6, IL-10 and TNFα quantification

IL-6 and L-10 levels were measured by using specific AlphaLISA detection kits (Perkin Elmer Life and Analytical Sciences, Boston, MA, USA). Briefly, aliquots of the samples were incubated in the presence of biotinylated anti-analyte antibody and anti-analyte antibody-

conjugated acceptor beads. After 60 min incubation, streptavidin-coated donor beads were added. Upon excitation at 680 nm, a photosensitizer inside the donor beads converts ambient oxygen to an excited singlet state that produces a chemiluminescent reaction in the acceptor beads. The resulting light emission, proportional to the amount of analyte, was read at 615 nm with a Perkin Elmer EnSight Multimode Plate Reader.

TNFα levels were determined with a quantitative sandwich ELISA kit (Elabsciences, Houston, TX, USA) following manufacturer instructions. The reaction was developed with streptavidin-horseradish peroxidase and the optical density was measured spectrophotometrically at a wavelength of 450 nm in a Perkin Elmer EnSight Multimode Plate Reader.

Data and statistical analysis

IC_{50} data are expressed as mean ± SEM of three independent experiments performed in triplicate. All statistical analyses were performed with GraphPad Prism 8.0.1. Differences between groups were analyzed using one-way analysis of variance (ANOVA) followed by Tukey's multiple comparisons test.

3.2. *RESULTS AND DISCUSSION*

3.2.1. *Enzymatic assays and SAR discussion*

Binding affinity and intrinsic activity at MT_1Rs and MT_2Rs and FAAH inhibitory potency obtained for the newly synthesized compounds are reported in Table 1. N-Cyclohexylcarbamic acid O-phenyl esters **FM03** and **FM04** showed only moderate binding affinity at human MT_1Rs and MT_2Rs, about one hundred times lower than that of MLT. Compounds **FM01** and **FM02**, which could be produced in vivo from hydrolysis of carbamates **FM03** and **FM04**, showed reduced binding affinity that may be attributed to lower lipophilicity of their chains. These two compounds also showed poor potency on FAAH. The compounds FM05 and FM06 result in a low binding affinity at MT_1Rs and MT_2Rs. The compounds **FM07-FM12** showed binding affinities at MT_1Rs and MT_2Rs similar to or slightly higher than the previous **FM03** and **FM04**. These compounds showed a remarkable ability to inhibit FAAH activity, with a subnanomolar IC_{50} value observed for compound **FM09**. The compounds **FM11** and **FM12** showed improved inhibitor potencies with IC_{50} respectively of 0.436 and 0.369 nM. These substituents were

tolerated at melatonin receptors and led to an increase in intrinsic activity at both receptor subtypes. The compound **FM07-FM12** demonstrated that it is possible to fuse the structural elements required for FAAH inhibition and MLT receptor binding and activation in the same molecule. However, activity at the two targets of these compounds appeared rather unbalanced as FAAH inhibitory potency is about 10−100 times higher than binding affinity at MLT receptors. To increase MT_1Rs and MT_2Rs binding affinity, the N- anilinoethylamide portion was replaced by the N-indolylethy-lamide scaffold of MLT. This bioisosteric replacement allowed to increase in MLT receptor binding affinity of about 1 order of magnitude as observed for compounds **FM13** and **FM14**, with maintenance of FAAH inhibitory potency in the nanomolar range. Moreover, the introduction of a bromine atom in position 2 of the indole ring in compound **FM15** allowed a further increase of MT_1Rs and MT_2Rs binding affinity similar to the reference compound Melatonin (Figure 1), consistent with SAR for indole derivatives. Furthermore, the compound **FM15** was found agonist for the MT_1Rs and MT_2Rs similar to the reference compound Melatonin (Figure 2). The bromine atom slightly improved FAAH inhibitory potency leading to a subnanomolar IC_{50} value (0.853 nM), consistent with the hypothesis that this substituent can be favorably positioned in the lipophilic acyl chain binding pocket of FAAH. The inhibitor potency of **FM15** for FAAH results better even than the reference compound URB597 (Figure 3). Compound **FM15** represents therefore a potent dual-acting melatonergic agonist and FAAH inhibitor with balanced potency at the two targets. Subsequently, functional assays were conducted to characterize the pharmacological behavior of these compounds. The assay used allows the measurement of cAMP levels produced in CHO cells transfected with the MT_1Rs and MT_2Rs and the determination of the IC_{50}, which represents a measure of the compound's potency. IC_{50} values are reported in Table 1. All the compounds tested are agonists for the MT_1Rs and MT_2Rs.

3.2.2. *FM15 prevented TNFα release in hippocampal explants*

To address the effects of drug treatment on inflammatory response, we analyzed the expression of pro-inflammatory cytokines as well as markers of anti-inflammatory pathways. Quantitative alphaLISA analysis showed that LPS + IFN-γ exposure for 24–72 h progressively increased the release of pro-inflammatory (IL-6) and anti-inflammatory (IL-10) cytokines (Figure 4 A-B). Interestingly, although the levels of IL-6 and IL-10 were not affected by drug treatment (Figure 4 A-B), **FM15** prevented the release of TNFα, in both the medium and tissue lysates after 72 h

(Figure 5). The hippocampal explants subjected to the LPS+IFN-γ treatment released significantly higher levels of TNFα into the medium compared to the control. Hippocampal explants treated with the compound **FM15**, in addition to the inflammatory stimulus (induced by LPS+IFN-γ), showed significantly lower levels of TNFα, bringing them back to control levels (figure 5).

Table 1. Molecules structure
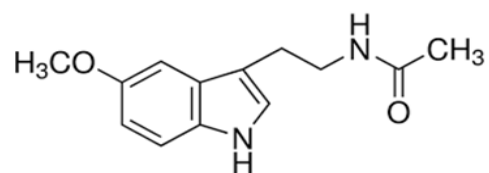
Melatonin
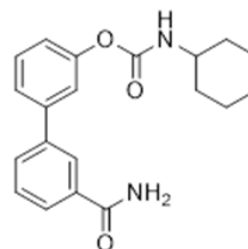
URB597
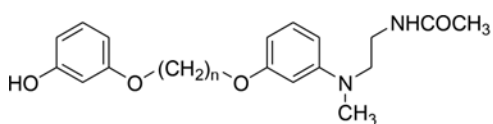
FM01-FM02
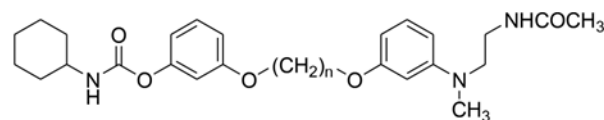
FM03-FM04
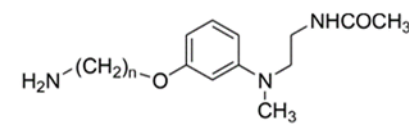
FM05-FM06
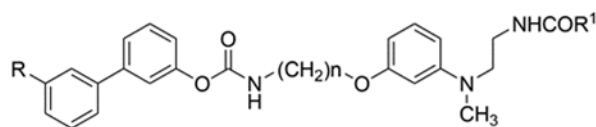
FM07-FM12
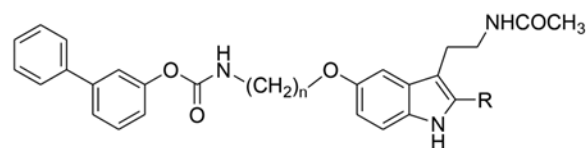
FM13-FM15

Table 2. Affinity (K_i, nM), potency (IC_{50}, nM) of the reference compounds MLT, URB597, and the novel compounds **FM01-FM15** and inhibitory activity (IC_{50}, nM) on hFAAH enzyme.

	n	R	R^1	MT_1 $K_i(nM) \pm SEM$	MT_1 $IC_{50}(nM) \pm SEM$	MT_2 $K_i(nM) \pm SEM$	MT_2 $IC_{50}(nM) \pm SEM$	FAAH $IC_{50}(nM) \pm SEM$
MLT				0.205 ± 0.008	0.699 ± 0.027	0.291 ± 0.011	0.803 ± 0.034	N.T.
URB597				N.T.	N.T.	N.T.	N.T.	4.61 ± 0.15
FM01	4			186 ± 7	540 ± 25	603 ± 24	1269 ± 51	N.T.
FM02	6			58.9 ± 2.4	232 ± 10	331 ± 13	863 ± 35	N.T.
FM03	4			34.7 ± 1.6	105 ± 4	53.7 ± 2.4	119 ± 5	184 ± 7
FM04	6			27.5 ± 1.1	100 ± 3	295 ± 12	785 ± 33	197 ± 9
FM05	4			3090 ± 124	5601 ± 225	>10000	N.T.	N.T.
FM06	6			467 ± 19	837 ± 34	398 ± 16	1065 ± 42	N.T.
FM07	4	H	CH_3	12.9 ± 0.5	27.8 ± 1.2	46.7 ± 1.9	93.4 ± 3.8	1.45 ± 0.05
FM08	6	H	CH_2CH_3	16.2 ± 0.7	41.3 ± 1.8	19.1 ± 0.7	52.3 ± 2.2	3.07 ± 0.12
FM09	8	H	CH_3	31.6 ± 1.5	65.4 ± 2.7	32.4 ± 1.3	87.1 ± 3.4	0.635 ± 0.025
FM10	6	H	CH_3	21.4 ± 0.8	56.7 ± 2.3	33.1 ± 1.4	95.4 ± 3.8	1.34 ± 0.06
FM11	6	$CONH_2$	CH_3	38.9 ± 1.6	99.8 ± 3.9	15.5 ± 0.7	40.8 ± 1.6	0.436 ± 0.018
FM12	6	OH	CH_3	29.5 ± 1.2	79.4 ± 3.1	26.9 ± 1.1	66.7 ± 2.7	0.369 ± 0.015
FM13	6	H		6.03 ± 0.21	15.6 ± 0.8	4.57 ± 0.19	10.5 ± 0.5	2.38 ± 0.11
FM14	8	H		4.90 ± 0.19	11.2 ± 0.4	6.31 ± 0.22	15.6 ± 0.8	4.00 ± 0.17
FM15	6	Br		0.786 ± 0.037	2.58 ± 0.10	1.70 ± 0.07	3.97 ± 0.16	0.853 ± 0.041

The data are expressed as the mean ± SEM of n=4 independent experiments. N.T. not tested
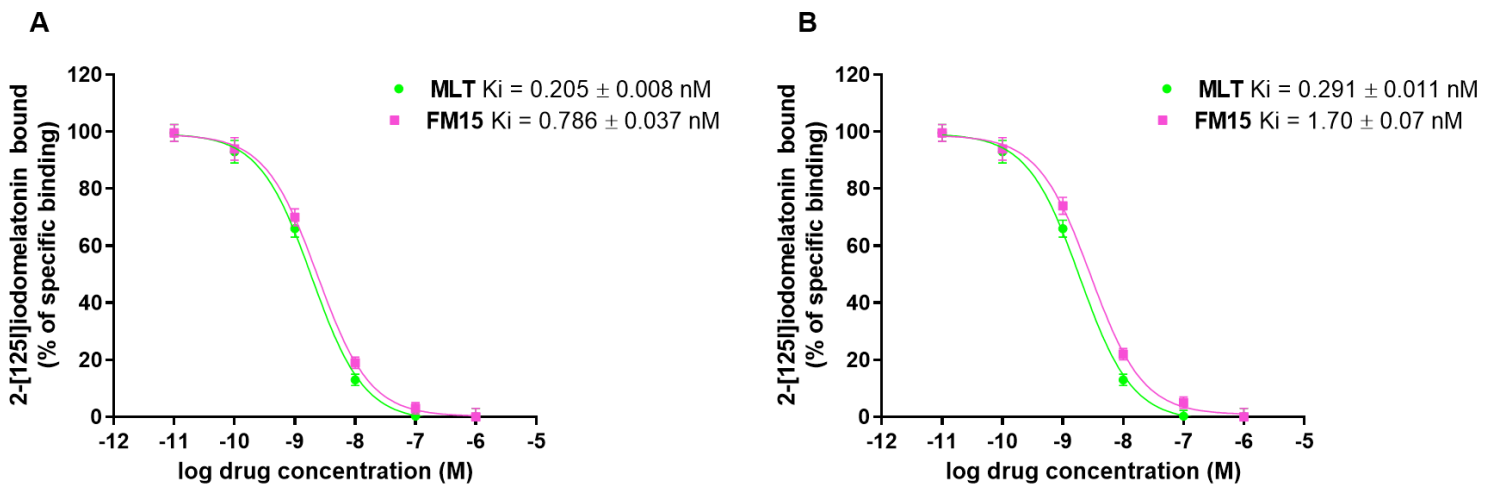
Figure 1 Competition binding curves of the newly synthesized compound **FM15** compared to the reference compound MLT in membranes of cells expressing the melatonin MT_1Rs (A) and MT_2Rs (B). Concentrations of the compounds are plotted on the x-axis in a logarithmic scale, while the percentage of specific binding.
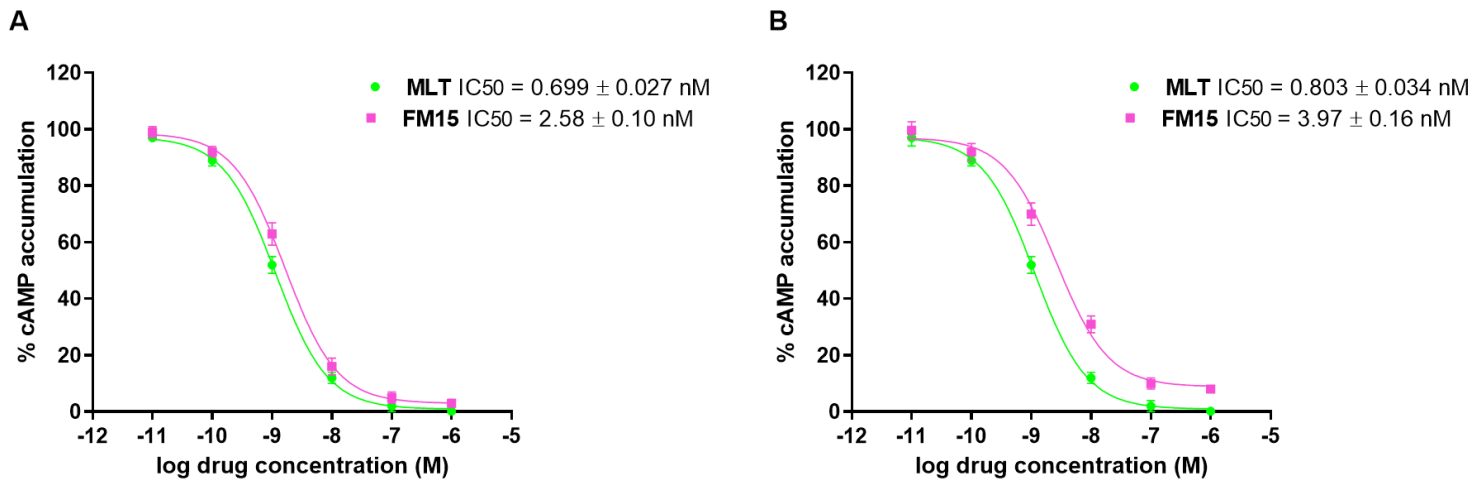
Figure 2 Functional assay curves for the quantification of cAMP levels of the newly synthesized compound **FM15** compared to the reference compound MLT in membranes of cells expressing the melatonin MT_1Rs (A) and MT_2Rs (B). The percentage of cAMP levels is shown on the y-axis.

106
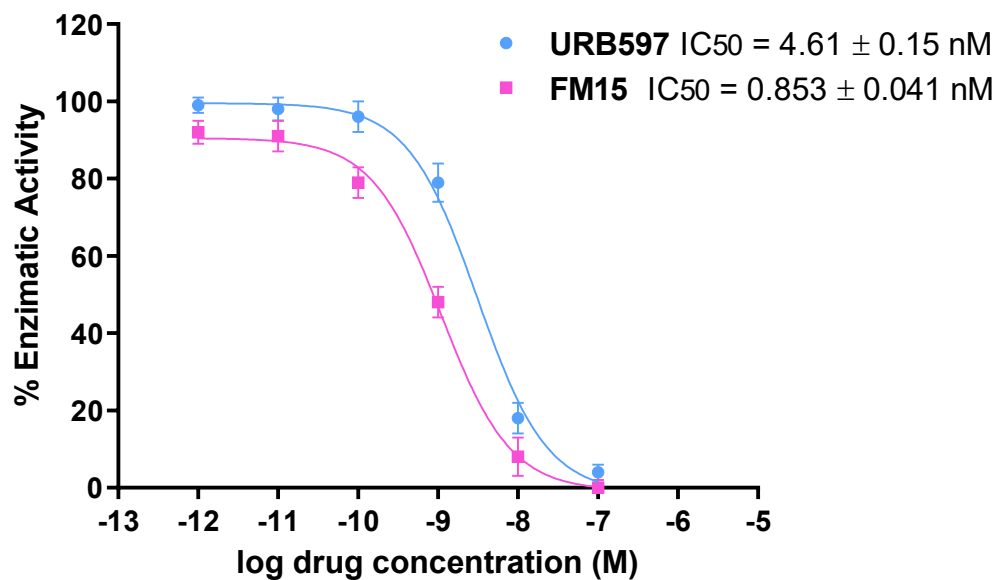
Figure 3 Inhibition curve of the known compound URB597 and the newly synthesized compound **FM15** on the FAAH enzyme. Compound concentrations are shown on the x-axis in a logarithmic scale, while the percentage of FAAH enzyme activity is displayed on the y-axis.
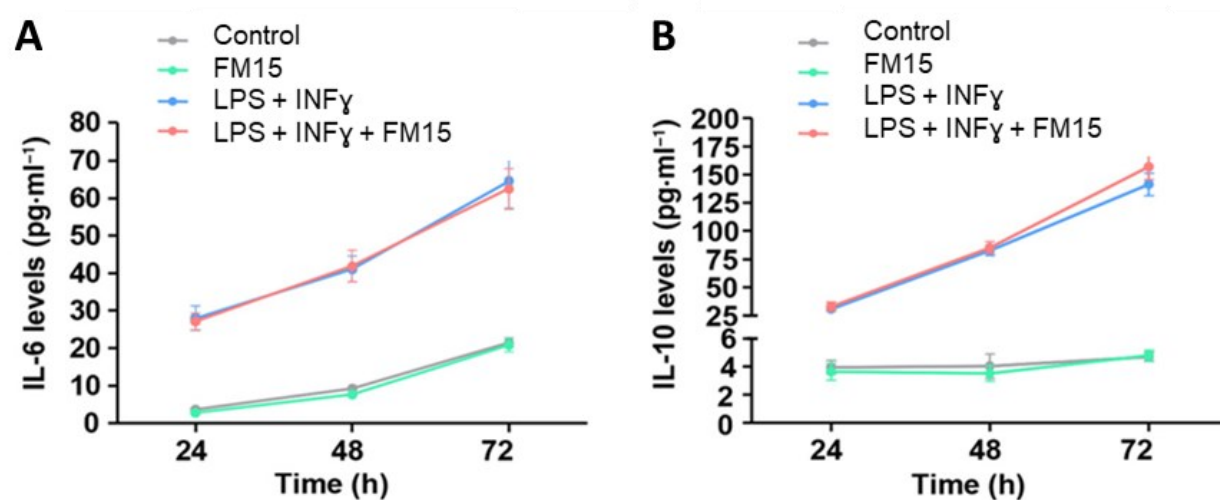
Figure 4 Time-dependent production of IL-6 (A) and IL-10 (B) in the medium of explants cultures under control conditions or LPS+IFN-γ exposure in the absence or the presence of 10 μM **FM15** for 24-72 hours. Results are expressed as mean values ± SEM (n=3).
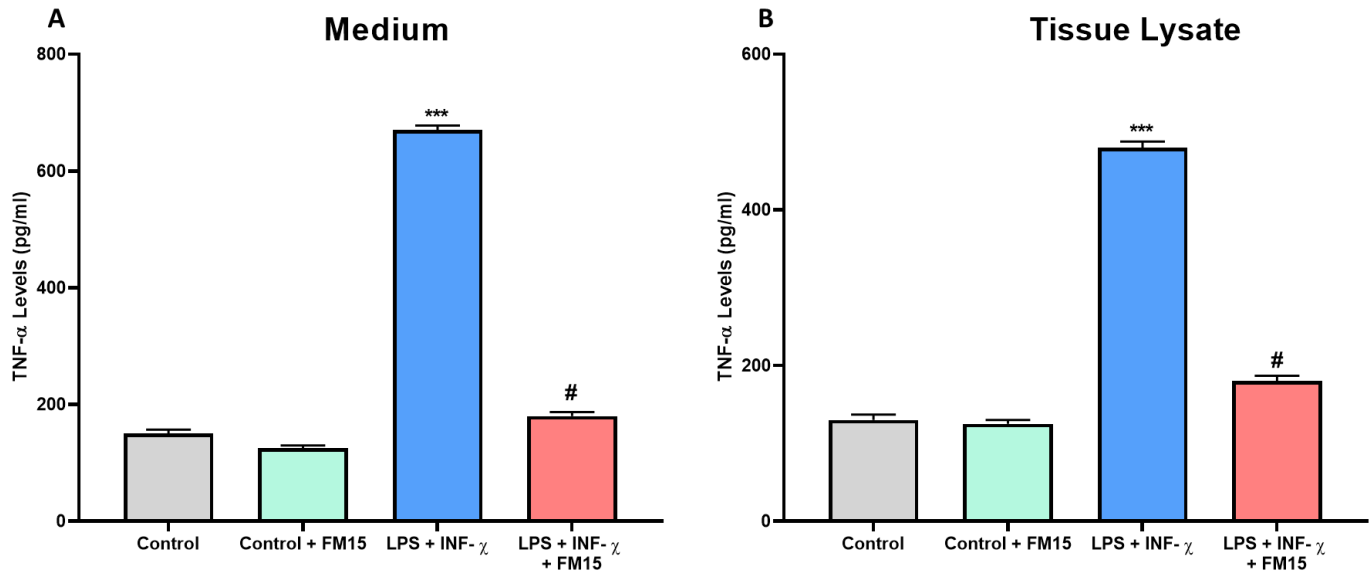
Figure 5 TNFα determination in the medium (A) and tissue lysates (B) of hippocampal cultures under control conditions, and LPS+IFN-γ exposure in the absence or the presence of 10 μM **FM15** for 72 hours. Results are expressed as mean values ± S.E.M. (n=2). *** p<0.01 vs control #, p<0.05 vs LPS+IFN-γ

CHAPTER 4

PHARMACOLOGICAL CHARACTERIZATION OF NEW

FATTY ACID AMIDE HYDROLASE AND HISTONE

DEACETYLASE 6 INHIBITORS

4.1. MATERIALS AND METHODS

Materials

3-(4,5-dimethyl-2-thiazolyl)-2,5-diphenyl-2H-tetrazolium bromide (MTT) obtained from Perkin Elmer Life and Analytical Sciences (USA).

tert-Butyl hydroperoxide (TBHP) obtained from Perkin Elmer Life and Analytical Sciences (USA).

N-acetylcysteine (NAC) obtained from Perkin Elmer Life and Analytical Sciences (USA).

Glutamate was obtained from Perkin Elmer Life and Analytical Sciences (USA).

Cell culture

1321N1 astrocyte cell line (Sigma-Aldrich) was maintained in DMEM (Invitrogen, Grand Island, NY, USA) supplemented with 10% FBS (Thermo Scientific, Waltham, MA, USA), L-glutamine (2 mM), penicillin (100 U/ml) and streptomycin (100 µg/ml) in a humidified atmosphere (5% CO_2) at 37°C. Human neuroblastoma (SH-SY5Y) cells were purchased from American Type Culture Collection (Manassas, VA, USA) and maintained in a 1:1 mixture of Eagle's Minimum Essential Medium and F12 Medium supplemented with 10% FBS, penicillin (100 U/mL), and streptomycin (100 µg/mL) at 37 °C in a humidified atmosphere with 5% CO_2.

Enzymatic assays on human HDACs

For the evaluation of their inhibitory activity, different concentrations of the novel compounds were incubated in a low-binding black 96-well plate with 30 ng of human recombinant HDAC6 (BPS Bioscience, San Diego, CA, USA; Cat. # 50056), human recombinant HDAC1 (BPS Bioscience; Cat. # 50051), human recombinant HDAC8 (BPS Bioscience; Cat. # 50008), or 500 ng of human recombinant HDAC10 (BPS Bioscience; Cat. # 50060) in an assay buffer composed of 25 mM Tris/HCl, pH 8.0, 137 mM NaCl, 2.7 mM KCl, 1 mM $MgCl_2$, and 0.1 mg/mL bovine serum albumin for 30 min at 37 °C. At the end of the incubation, the deacetylation reaction was initiated by adding 200 µM of the fluorogenic acetylated HDAC substrate 3 (BPS Bioscience; Cat. # 50037) for HDAC6, HDAC1 and HDAC10 assays, or of the fluorogenic HDAC substrate class 2A (BPS Bioscience; Cat. # 50040) for HDAC8 assays. After 30 min at 37 °C, the reaction was stopped by the addition of an HDAC assay developer (BPS Bioscience; Cat. # 50060). Following an incubation of 15 min at RT, fluorescence was

measured in an EnSight multimodal plate reader (PerkinElmer, Boston, MA, USA) with an excitation wavelength of 360 nm and an emission wavelength of 450 nm.

Enzymatic assays on human FAAH

The inhibition activity of the novel compounds against human FAAH was assessed using a fluorescence-based assay, following the manufacturer's instructions (Cayman Chemical, Ann Arbor, MI, USA). Briefly, the compounds were preincubated at various concentrations with human FAAH for 30 minutes at 37°C. The reaction was initiated by adding 7-Amino-4-methylcoumarin (AMC) arachidonoyl amide (final concentration 1 µM) as the substrate. After a 30-minute incubation at 37°C, the fluorescence resulting from the release of the AMC product was measured using an excitation wavelength of 355 nm and an emission wavelength of 465 nm, utilizing an EnSight Multimode plate reader (Perkin Elmer, MA, USA).

Enzymatic assays on human MAGL

The inhibitory activity of the novel compounds against human MAGL was evaluated using a fluorescence-based assay, following the manufacturer's instructions (Biovision, Mountain View, CA, USA). Briefly, the compounds were preincubated at various concentrations with human MAGL for 30 minutes at 37°C. After adding the substrate, 7-hydroxycoumarinyl-arachidonate, the assay mixture was further incubated for 30 minutes at 37°C, and the resulting fluorescence was measured using an excitation wavelength of 360 nm and an emission wavelength of 460 nm, employing an EnSight Multimode plate reader (Perkin Elmer, MA, USA).

ROS production assay

ROS production was evaluated through the Total Reactive Oxygen Species Assay Kit (Thermo-Fisher, cat. n. 88-5930-74). 1321N1 or SH-SY5Y were seeded into 96-well microculture plates at a density of 1×10^4 cells/well and incubated overnight in a humidified atmosphere (5% CO_2) at 37°C. Afterward, the cells were treated for 24 hours with the novel selected compounds or NAC. Subsequently, 10 µl of ROS Assay Stain was added directly to the culture media, and the cells were incubated for 60 minutes at 37°C. The cells were then exposed to 50 µM TBHP to induce the production of ROS. After a 1-hour incubation at 37°C, fluorescence was measured

with an excitation wavelength of 488 nm and an emission wavelength of 520 nm, employing an EnSight Multimode plate reader (Perkin Elmer, MA, USA).

Cell viability assay

1321N1 or SH-SY5Y cell viability was assessed using a 3-(4,5-dimethyl-2-thiazolyl)-2,5-diphenyl-2H-tetrazolium bromide (MTT) assay. The cells were harvested from culture flasks through trypsinization and then seeded into 96-well microculture plates at a density of 1×10^4 cells/well. Subsequently, they were incubated overnight in a humidified atmosphere (5% CO_2) at 37 °C. After the incubation with the novel compounds, TBHP or glutamate, 15 µl of a 5 mg/ml MTT solution in PBS was added to each well, followed by a 4-hour incubation in the dark. During this time, MTT is transformed into formazan by mitochondrial dehydrogenase in viable cells. After the incubation, formazan crystals were solubilized by adding 150 µl of an acidified isopropanol solution. Optical densities at 570 nm were measured using the EnSight multimode plate reader (Perkin Elmer).

Data and statistical analysis

IC_{50} data are expressed as mean ± SEM of three independent experiments performed in triplicate. All statistical analyses were performed with GraphPad Prism 8.0.1. Differences between groups were analyzed using one-way analysis of variance (ANOVA) followed by Tukey's multiple comparisons test.

4.2. RESULTS AND DISCUSSION

4.2.1. Enzymatic assays and SAR discussion

The multi-target inhibitory profile of the newly synthesized compounds was primarily assessed by evaluating their IC_{50} values against *human* FAAH and HDAC6 *in vitro*. FAAH inhibition activity was measured on a *human* recombinant purified enzyme following a 30-minute pre-incubation with the tested compounds. The IC_{50} values versus the target enzymes are reported in Table 1 for derivatives **FH04-FH13**, taking compounds **FH01-FH03** as the reference compounds. The purpose of our screening was to identify a compound with a balanced inhibitory profile against both targets. The selective FAAH inhibitory activity of compounds **FH04, FH05**, **FH08**, and **FH10** (*h*FAAH IC_{50} 6.75, 28.3, 1817 and 30.7 nM respectively and

hHDAC6 >10000 nM for all these compounds) could be attributed to the lack of a ZBG or the presence of a weak ZBG. Also, compound **FH07** exhibited the same inhibitory profile (hFAAH IC$_{50}$ 65.6 and hHDAC6 >10000 nM). Unexpectedly, compounds **FH12** and **FH13** completely lost their activity against FAAH and were only able to inhibit HDAC6 (hHDAC6 IC50 78.4, 112 nM respectively and hFAAH >10000 nM). Compound **FH06** showed a good inhibitory profile for FAAH and micromolar potency for HDAC6 (hFAAH IC$_{50}$ 15.9 nM and hHDAC6 IC$_{50}$ 3999 nM). Compounds **FH09** and **FH11** emerged as the most promising multi-target directed ligands as their IC$_{50}$ on both targets lay in the nanomolar or low-micromolar range. In particular, **FH11** showed comparable potencies against the two enzymes (hFAAH IC50 297 nM and hHDAC6 370 nM). Thus, were selected compounds **FH04**, **FH09,** and **FH11** as the hit compounds for further investigation of their selectivity profile, as reported in Table 2, and their potential antioxidant and neuroprotective effects.

4.2.2. *Assessment of neuroprotective and antioxidant effects and toxicity evaluation*

In the context of neurodegeneration, ROS play a pivotal role in cell homeostasis. An imbalanced production or an ineffective disposal of ROS can trigger damaging signaling cascades, often leading to impaired functions and cell death. Therefore, we selected the most promising multi-target directed ligands (**FH09**, **FH11**) and the selective FAAH inhibitors **FH04** to investigate their efficacy in acute models of TBHP-induced oxidative stress in both 1321N1 human astrocytes and SH-SY5Y human neuronal cell lines. On 1321N1 cells, compounds **FH11** and **FH09**, the first-in-class FAAH-HDAC multi-target directed ligands, reduced TBHP-stimulated ROS production in a concentration-dependent manner and showed a greater effect compared to the reference antioxidant NAC (Figure 1A). In contrast, compound **FH04**, which solely inhibits FAAH, did not show any significant effect on ROS levels, highlighting the value of the polypharmacological approach. When tested on neuron-like cells SH-SY5Y, compounds **FH11** and **FH09** also exhibited an effect on reducing TBHP-stimulated ROS production, although to a lesser extent than NAC, while compound **FH04** remained ineffective (Figure 1B). Furthermore, the toxicity profile of the newly developed compounds was evaluated on the same cell lines. Compounds **FH11** and **FH09** showed no significant cytotoxicity at the concentrations used, indicating their safety within the tested range, both in 1321N1 astrocytes (Figure 2A) and SH-SY5Y neuron-like cells (Figure 2B). Compound **FH04** significantly reduced 1321N1 and SH-SY5Y cell viability although only at the concentration of 30 µM. Astrocytes serve a crucial

function in protecting the CNS from oxidative damage and glutamate-induced toxicity. Given their vital role, we examined the potential of newly synthesized compounds to mitigate the damage induced by TBHP or glutamate in 1321N1 cells. Compounds **FH11**, **FH09**, and **FH04** significantly prevented a decrease in cell viability triggered by 1 mM TBHP (Figure 3A). Furthermore, the multi-target FAAH-HDAC inhibitors **FH11** and **FH09**, but not the selective FAAH inhibitor **FH04** (tested at 10 µM), counteracted the toxic effects of 200 mM glutamate (Figure 3B). These findings suggest an enhanced oxidative stress resistance and ability for glutamate clearance by astrocytes, emphasizing the potential therapeutic role of these compounds in protecting the CNS.

Table 1. Inhibitory activity of the reference compounds **FH01-FH03** and the novel compounds **FH04-FH13** on *human* (*h*) FAAH and *human* (*h*) HDAC6 enzymes.

Compound	Structure	hFAAH IC$_{50}$ (nM)	hHDAC6 IC$_{50}$ (nM)
FH01	-	3.72± 0.21	-
FH02	-	10.1± 0.6	-
FH03	-	-	36.0 ± 2.9
FH04		6.75 ± 0.47	>10000 (1%)
FH05		28.3 ± 1.8	>10000 (8%)
FH06		15.9 ± 1.2	3999 ± 312
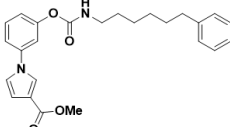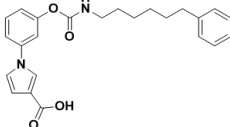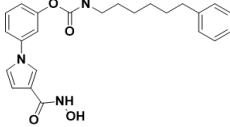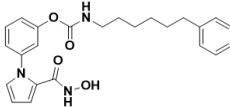
FH07		65.6 ± 4.7	>10000 (6%)
FH08		1817 ± 154	>10000 (3%)
FH09		36.2 ± 3.2	1387 ± 108
FH10		30.7 ± 2.2	>10000 (1%)
FH11		297 ± 17	370 ± 23
FH12		>10000 (21%)	78.4 ± 5.1
FH13		>10000 (17%)	112 ± 7
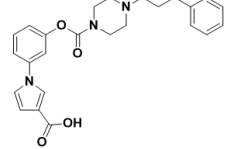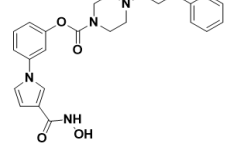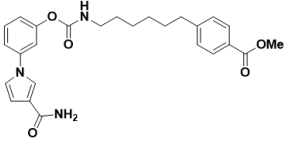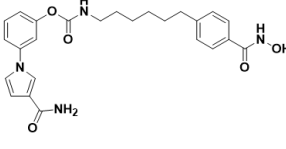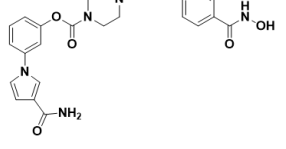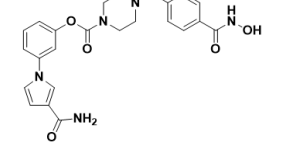
Data are expressed as mean ± SEM of three independent experiments performed in triplicate. Data in parentheses indicates inhibition at the 10 μM concentration. Incubation time = 30 min.

Table 2. Selectivity profile of compounds **FH04, FH09, FH11** on isoforms 1,8,10 of human HDAC and human MAGL enzymes.

Compound	*h*MAGL IC$_{50}$ (nM)	*h*HDAC1 IC$_{50}$ (nM)	*h*HDAC8 IC$_{50}$ (nM)	*h*HDAC10 IC$_{50}$ (nM)
FH04	8347 ± 412	>10000	>10000	>10000
FH09	>10000	>10000	>10000	9050 ± 651
FH11	>10000	531 ± 26	1410 ± 116	659 ± 37

Data are expressed as mean $\pm$ SEM of three independent experiments performed in triplicate. Incubation time = 30 min.
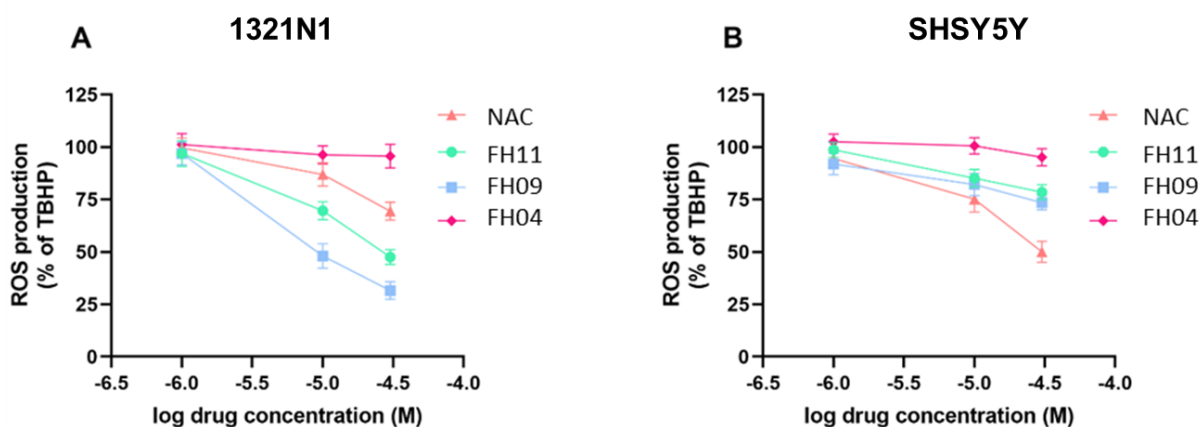
Figure 1 Evaluation of the antioxidant profile of the FAAH-HDAC inhibitors **FH11**, **and FH09** in comparison to the selective FAAH inhibitor **FH04** and NAC. The effect of newly developed compounds **FH11**, **FH09,** and **FH04** in comparison to NAC on the reduction of ROS production induced by 50 μM TBHP was evaluated in 1321N1 *human* astrocytes (**A**) and SH-SY5Y *human* neuronal (**B**) cell lines.
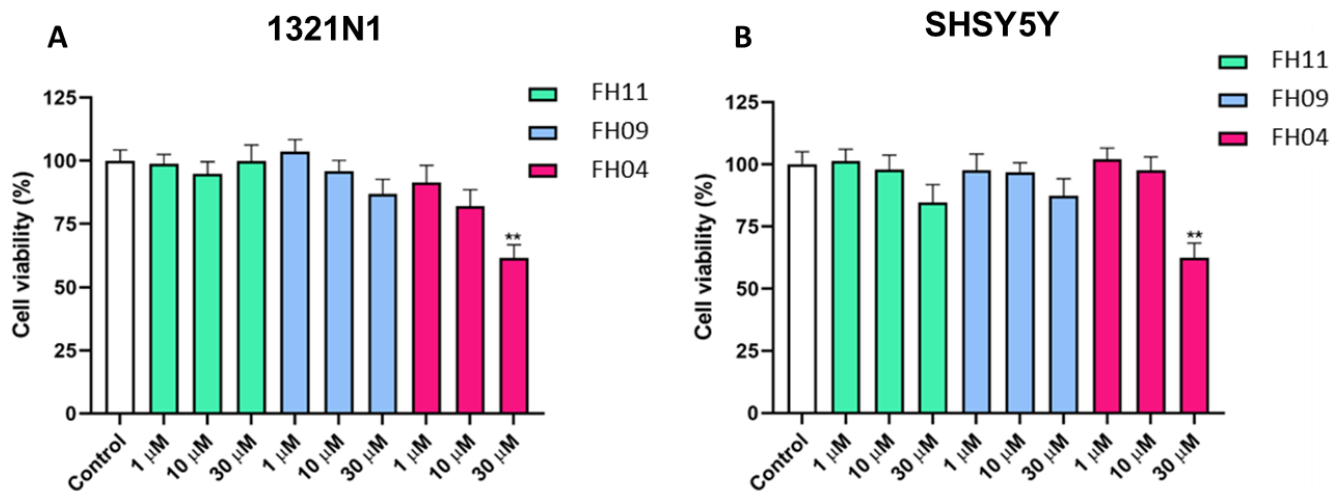
Figure 2 Cell viability was assessed after 24-hour incubation with the new dual inhibitors compounds **FH11**, **FH09,** and the selective FAAH inhibitor **FH04** in both 1321N1 (**A**) and SH-SY5Y (**B**) cells. **, $p < 0.01$ vs control
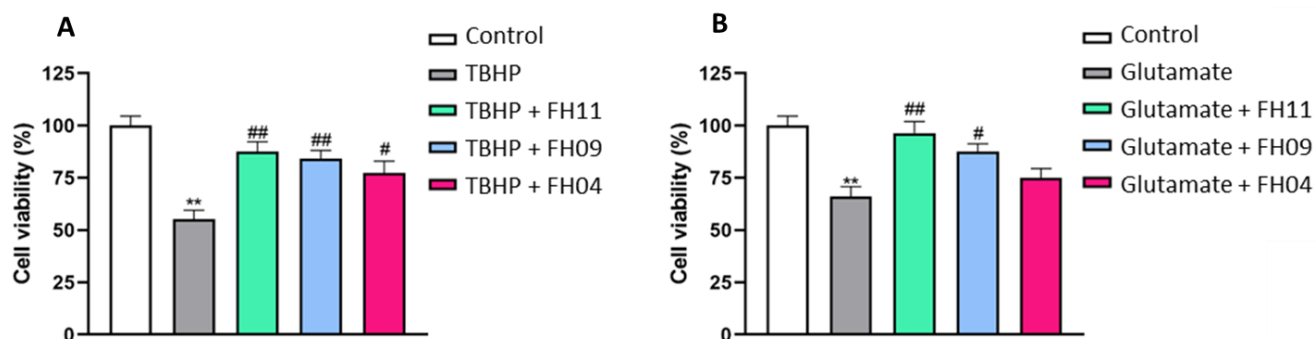
Figure 3 The ability of the new compounds to protect 1321N1 cells from damage induced by 24 hours of 1 mM TBHP (**A**) or 200 mM glutamate (**B**) was evaluated by pre-incubating the compounds (10 µM) for 24 hours before exposure to the noxious stimuli. **, $p < 0.01$ vs control; #, $p < 0.05$ vs TBHP or glutamate; ##, $p < 0.01$ vs TBHP or glutamate.

CONCLUSIONS

The extensive presence of CBRs indicates the involvement of the ECS in numerous physiological processes, encompassing motor control, memory and learning, pain perception, energy balance regulation, and behaviors such as food intake. Moreover, the ECS plays a role in endocrine and vascular system functions, immune system modulation, and neuroprotection. Within each tissue, the ECS undertakes specific functions to uphold homeostasis, ensuring stability in the internal environment despite external fluctuations (Lu & Mackie, 2021). Consequently, this study aimed to characterize novel ligands for modulating this system. **Chapter 1** specifically focused on investigating new selective CB_2R ligands capable of activating the ECS without inducing the side effects associated with CB_1R ligands. Multiple series of compounds were examined in $[^3H]$-CP-55,940 competition binding experiments to assess their affinity and selectivity toward rat and human recombinant CB_1Rs and CB_2Rs. Some compounds exhibited characteristics as full agonists, displaying high selectivity for the CB_2Rs. Notably, compounds **CF02**, **CF03**, **CF04,** and **CF05** demonstrated high affinity at the CB_2Rs while displaying low affinity at CB_1Rs. Specifically, **CF03** and **CF05** proved to be potent and selective agonists. Derivatives **CF14-CF15** showed a good affinity and selectivity for the CB_2Rs. Compounds **CF20** and **CF38** displayed high affinity and remarkable selectivity at the CB_2Rs. Among these, **CF40** emerged as the most promising compound, binding to CB_2R with exceptional affinity and selectivity. Additionally, some ligands acted as partial agonists for the CB_2Rs. Compounds **CP12** and **CP13** showed affinity for CB_2Rs, although the highest selectivity for the CB_1R was observed with the compound **CP16**. These molecules resulted as a partial agonist according to the cyclic AMP assay used to distinguish between full, partial, and inverse agonism. **CP28** emerged as one of the most potent and selective compounds in this series, also acting as a partial agonist. Moreover, some ligands were identified as inverse agonists for CB_2Rs. Compound **CI08** demonstrated the highest affinity for CB_2R, while **CI14** emerged as the most selective compound in this series, possessing a higher affinity for the target receptor. Notably, the most significant effects were observed in compounds **CI08** and **CI10** which increased forskolin-induced cAMP production by 243% and 213% at 10 mM respectively. When tested in the presence of WIN 55,212-2, the novel compounds **CI08** and **CI10** were able to completely abrogate the inhibitory effect of the agonist on forskolin-

stimulated cAMP production, confirming their opposite effect to WIN 55,212-2. Similar inhibitory effect were observed for **CI14**, **CI15**, **CI16**, **CI17**, **CI20**, **CI23**, **CI25**, and **CI26**.

The cross-link between neuroinflammation and neurodegeneration is a common characteristic observed in several CNS diseases such as AD, PD, ALS, and MS. The ECS plays a central role in regulating neuroinflammatory conditions and its indirect activation by using FAAH inhibitors can represent an attractive therapeutic approach to treating neuroinflammatory-based disorders (Papa et al., 2022). **Chapter 2** focused on identifying new carbamate-based FAAH inhibitors (compounds **FA03-FA22**). These tested compounds revealed themselves as highly potent FAAH inhibitors with an excellent selectivity profile evaluated against MAGL, CB_1R, and CB_2R. Moreover, selected analogs demonstrated no cellular toxicity in normal fibroblast cell lines. The most promising ligands were further investigated for their anti-neuroinflammatory properties. Derivatives **FA07**, **FA16**, and **FA21** effectively prevented TBHP-induced ROS production in human astrocytes, in particular, **FA07** and **FA21** significantly reduced ROS production starting from the 10 nM concentration, while **FA16** exhibited the same effect starting from a concentration of 100 nM. All tested compounds at 1 μM showed effects comparable to the reference antioxidant compound NAC used at 2mM. Furthermore, these compounds did not exhibit any toxic effects in the same cell line as demonstrated by an MTT assay. Selected analogs **FA07**, **FA09**, **FA16**, and **FA21** resulted in an effective reduction of neuroinflammation induced by LPS + IFN-ɣ in hippocampal explants.

The melatoninergic system could be implicated, like the ECS, in several neurodegenerative conditions. Moreover, melatonin serves a protective role against ischemic damage through its receptors and can promote neurogenesis (Cammarota et al., 2023). Consequently, in **Chapter 3** a new series of compounds were tested to determine if they exhibited a multitarget effect on the melatoninergic system and ECS. This testing involved assessing the binding affinity at MT_1Rs and MT_2Rs and the intrinsic activity evaluating FAAH inhibitory potency for the newly synthesized compounds. Compound **FM07-FM15** displayed a good affinity for MT_1Rs and MT_2Rs, along with significant inhibitory potency against FAAH. Notably, compound **FM15** emerged as the most potent dual-acting compound, resulting as a melatoninergic agonist and FAAH inhibitor with well-balanced efficacy at both targets. Subsequent functional assays were conducted to characterize the pharmacological behavior of these compounds. Additionally, the anti-inflammatory effect of the compound was evaluated. **FM15** exhibited a significant reduction in TNFα production induced by LPS. However, no significant reductions were

observed in the production of IL-6 and IL-10. Therefore, **FM15**, by enhancing signaling in both the endocannabinoid and melatoninergic systems, appears to promote neuroprotection and stimulate pathways involved in resolving inflammation.

Considering the widespread presence and significant function of FAAH-HDAC in various pathological conditions, research aimed to develop potentially greater neuroprotective agents by combining the established neuroprotective effects of FAAH inhibitors with the recently discovered therapeutic advantages of HDAC inhibitors in CNS diseases related to oxidative stress (Kumar et al., 2022). In **Chapter 4**, a group of FAAH/HDAC multi-target directed ligands was examined. Following initial enzymatic assays, the most effective compounds were identified as **FH09** and **FH11**. These analogs were tested in different TBHP-induced oxidative stress cellular models to assess their neuroprotective effect. Among them, compound **FH11** not only exhibited well-balanced nanomolar inhibitory activity against the selected targets, but also outperformed NAC on 1321N1 astrocytes, showing no significant cytotoxic effects. Further assessments were carried out to determine the effectiveness of the newly synthesized multi-target directed ligands **FH09**, and **FH11** in mitigating glutamate-induced toxicity in 1321N1 cells. Collectively, these preliminary studies suggest that these compounds possess substantial therapeutic potential, as they have demonstrated remarkable capabilities in mitigating TBHP or glutamate-induced harm, successfully preventing a reduction in cell viability in the same cell line.

In conclusion, substantial evidence suggests that modulating the ECS, using new full selective agonists, partial agonists, and inverse agonists could offer therapeutic benefits for a wide range of conditions, including neurodegenerative diseases such as AD, PD, MS, HD, mood disorders, pain management, inflammation, autoimmune diseases, cancer, cardiovascular and respiratory ailments, metabolic disorders, migraines, glaucoma, and even osteoporosis avoiding the side effects deviates for the activations of CB_1Rs. Moreover, the use of new selective FAAH inhibitors could be useful as pharmacological tools for treating inflammatory CNS disorders by raising the eCBs tone without resorting to CBR agonists, known for their potential side effects. The multitarget compounds like **FM15** or **FH09 FH11** represent an innovative approach for addressing multifactorial conditions, particularly those associated with neurodegenerative diseases. These compounds may pave the way for the development of additional libraries of multi-target ligands acting on the ECS. This could provide an innovative pharmacological approach for treating inflammation or CNS diseases related to oxidative stress.

BIBLIOGRAPHY

Adamson Barnes, N. S., Mitchell, V. A., Kazantzis, N. P., & Vaughan, C. W. (2016). Actions of the dual FAAH/MAGL inhibitor JZL195 in a murine neuropathic pain model. *British Journal of Pharmacology*, *173*(1), 77–87. https://doi.org/10.1111/bph.13337

Adermark, L., & Lovinger, D. M. (2007). Retrograde endocannabinoid signaling at striatal synapses requires a regulated postsynaptic release step. *Proceedings of the National Academy of Sciences*, *104*(51), 20564–20569. https://doi.org/10.1073/pnas.0706873104

Aiello, F., Carullo, G., Badolato, M., & Brizzi, A. (2016). TRPV1–FAAH–COX: The *Couples Game* in Pain Treatment. *ChemMedChem*, *11*(16), 1686–1694. https://doi.org/10.1002/cmdc.201600111

Anand, P., Whiteside, G., Fowler, C. J., & Hohmann, A. G. (2009). Targeting CB2 receptors and the endocannabinoid system for the treatment of pain. *Brain Research Reviews*, *60*(1), 255–266. https://doi.org/10.1016/j.brainresrev.2008.12.003

Anderson, W. B., Gould, M. J., Torres, R. D., Mitchell, V. A., & Vaughan, C. W. (2014). Actions of the dual FAAH/MAGL inhibitor JZL195 in a murine inflammatory pain model. *Neuropharmacology*, *81*, 224–230. https://doi.org/10.1016/j.neuropharm.2013.12.018

Angelia, J., Weng, X., Solomatov, A., Chin, C., Fernandez, A., Hudson, P. K., Morisseau, C., Hammock, B. D., Kandasamy, R., & Pecic, S. (2023). Structure-activity relationship studies of benzothiazole-phenyl analogs as multi-target ligands to alleviate pain without affecting normal behavior. *Prostaglandins & Other Lipid Mediators*, *164*, 106702. https://doi.org/10.1016/j.prostaglandins.2022.106702

Bab, I., Zimmer, A., & Melamed, E. (2009). Cannabinoids and the skeleton: From marijuana to reversal of bone loss. *Annals of Medicine*, *41*(8), 560–567. https://doi.org/10.1080/07853890903121025

Bacci, A., Huguenard, J. R., & Prince, D. A. (2004). Long-lasting self-inhibition of neocortical interneurons mediated by endocannabinoids. *Nature*, *431*(7006), 312–316. https://doi.org/10.1038/nature02913

Baggelaar, M. P., Maccarrone, M., & Van Der Stelt, M. (2018). 2-Arachidonoylglycerol: A signaling lipid with manifold actions in the brain. *Progress in Lipid Research*, *71*, 1–17. https://doi.org/10.1016/j.plipres.2018.05.002

Barrie, N., & Manolios, N. (2017). The endocannabinoid system in pain and inflammation: Its relevance to rheumatic disease. *European Journal of Rheumatology*, *4*(3), 210–218. https://doi.org/10.5152/eurjrheum.2017.17025

Basavarajappa, B. S., Shivakumar, M., Joshi, V., & Subbanna, S. (2017). Endocannabinoid system in neurodegenerative disorders. *Journal of Neurochemistry*, *142*(5), 624–648. https://doi.org/10.1111/jnc.14098

Bedse, G., Romano, A., Lavecchia, A. M., Cassano, T., & Gaetani, S. (2014). The Role of Endocannabinoid Signaling in the Molecular Mechanisms of Neurodegeneration in Alzheimer's Disease. *Journal of Alzheimer's Disease*, *43*(4), 1115–1136. https://doi.org/10.3233/JAD-141635

Biegon, A., & Kerman, I. A. (2001). Autoradiographic Study of Pre- and Postnatal Distribution of Cannabinoid Receptors in Human Brain. *NeuroImage*, *14*(6), 1463–1468. https://doi.org/10.1006/nimg.2001.0939

Blankman, J. L., Simon, G. M., & Cravatt, B. F. (2007). A Comprehensive Profile of Brain Enzymes that Hydrolyze the Endocannabinoid 2-Arachidonoylglycerol. *Chemistry & Biology*, *14*(12), 1347–1356. https://doi.org/10.1016/j.chembiol.2007.11.006

Blázquez, C., Chiarlone, A., Sagredo, O., Aguado, T., Pazos, M. R., Resel, E., Palazuelos, J., Julien, B., Salazar, M., Börner, C., Benito, C., Carrasco, C., Diez-Zaera, M., Paoletti, P., Díaz-Hernández, M., Ruiz, C., Sendtner, M., Lucas, J. J., De Yébenes, J. G., … Guzmán, M. (2011). Loss of striatal type 1 cannabinoid receptors is a key pathogenic factor in Huntington's disease. *Brain*, *134*(1), 119–136. https://doi.org/10.1093/brain/awq278

Blessing, E. M., Steenkamp, M. M., Manzanares, J., & Marmar, C. R. (2015). Cannabidiol as a Potential Treatment for Anxiety Disorders. *Neurotherapeutics*, *12*(4), 825–836. https://doi.org/10.1007/s13311-015-0387-1

Butini, S., Gemma, S., Brindisi, M., Maramai, S., Minetti, P., Celona, D., Napolitano, R., Borsini, F., Cabri, W., Fezza, F., Merlini, L., Dallavalle, S., Campiani, G., & Maccarrone, M. (2013). Identification of a novel arylpiperazine scaffold for fatty acid amide hydrolase inhibition with improved drug disposition properties. *Bioorganic & Medicinal Chemistry Letters*, *23*(2), 492–495. https://doi.org/10.1016/j.bmcl.2012.11.035

Cabral, G. A., Raborn, E. S., Griffin, L., Dennis, J., & Marciano-Cabral, F. (2008). CB $_2$ receptors in the brain: Role in central immune function. *British Journal of Pharmacology*, *153*(2), 240–251. https://doi.org/10.1038/sj.bjp.0707584

Cairns, E. A., Baldridge, W. H., & Kelly, M. E. M. (2016). The Endocannabinoid System as a Therapeutic Target in Glaucoma. *Neural Plasticity*, *2016*, 1–10. https://doi.org/10.1155/2016/9364091

Callén, L., Moreno, E., Barroso-Chinea, P., Moreno-Delgado, D., Cortés, A., Mallol, J., Casadó, V., Lanciego, J. L., Franco, R., Lluis, C., Canela, E. I., & McCormick, P. J. (2012). Cannabinoid Receptors CB1 and CB2 Form Functional Heteromers in Brain. *Journal of Biological Chemistry*, *287*(25), 20851–20865. https://doi.org/10.1074/jbc.M111.335273

Cammarota, M., Ferlenghi, F., Vacondio, F., Vincenzi, F., Varani, K., Bedini, A., Rivara, S., Mor, M., & Boscia, F. (2023). Combined targeting of fatty acid amide hydrolase and melatonin receptors promotes neuroprotection and stimulates inflammation resolution in rats. *British Journal of Pharmacology*, *180*(10), 1316–1338. https://doi.org/10.1111/bph.16014

Carta, F., Supuran, C. T., & Scozzafava, A. (2012). Novel therapies for glaucoma: A patent review 2007 – 2011. *Expert Opinion on Therapeutic Patents*, *22*(1), 79–88. https://doi.org/10.1517/13543776.2012.649006

Castillo, P. E., Younts, T. J., Chávez, A. E., & Hashimotodani, Y. (2012). Endocannabinoid Signaling and Synaptic Function. *Neuron*, *76*(1), 70–81. https://doi.org/10.1016/j.neuron.2012.09.020

Celorrio, M., Fernández-Suárez, D., Rojo-Bustamante, E., Echeverry-Alzate, V., Ramírez, M. J., Hillard, C. J., López-Moreno, J. A., Maldonado, R., Oyarzábal, J., Franco, R., & Aymerich, M. S. (2016). Fatty acid amide hydrolase inhibition for the symptomatic relief of Parkinson's disease. *Brain, Behavior, and Immunity*, *57*, 94–105. https://doi.org/10.1016/j.bbi.2016.06.010

Chakravarti, B., Ravi, J., & Ganju, R. K. (2014). Cannabinoids as therapeutic agents in cancer: Current status and future implications. *Oncotarget*, *5*(15), 5852–5872. https://doi.org/10.18632/oncotarget.2233

Chen, J., Matias, I., Dinh, T., Lu, T., Venezia, S., Nieves, A., Woodward, D. F., & Di Marzo, V. (2005). Finding of endocannabinoids in human eye tissues: Implications for glaucoma. *Biochemical and Biophysical Research Communications*, *330*(4), 1062–1067. https://doi.org/10.1016/j.bbrc.2005.03.095

Chicca, A., Marazzi, J., Nicolussi, S., & Gertsch, J. (2012). Evidence for Bidirectional Endocannabinoid Transport across Cell Membranes. *Journal of Biological Chemistry*, *287*(41), 34660–34682. https://doi.org/10.1074/jbc.M112.373241

Chiurchiù, V., Cencioni, M. T., Bisicchia, E., De Bardi, M., Gasperini, C., Borsellino, G., Centonze, D., Battistini, L., & Maccarrone, M. (2013). Distinct modulation of human myeloid and plasmacytoid dendritic cells by anandamide in multiple sclerosis: Anandamide Modulates DCs in MS. *Annals of Neurology*, *73*(5), 626–636. https://doi.org/10.1002/ana.23875

Chiurchiù, V., Lanuti, M., Catanzaro, G., Fezza, F., Rapino, C., & Maccarrone, M. (2014). Detailed characterization of the endocannabinoid system in human macrophages and foam cells, and anti-inflammatory role of type-2 cannabinoid receptor. *Atherosclerosis*, *233*(1), 55–63. https://doi.org/10.1016/j.atherosclerosis.2013.12.042

Choi, S.-H., Mou, Y., & Silva, A. C. (2019). Cannabis and Cannabinoid Biology in Stroke: Controversies, Risks, and Promises. *Stroke*, *50*(9), 2640–2645. https://doi.org/10.1161/STROKEAHA.118.023587

Cipriano, M., Björklund, E., Wilson, A. A., Congiu, C., Onnis, V., & Fowler, C. J. (2013). Inhibition of fatty acid amide hydrolase and cyclooxygenase by the N-(3-methylpyridin-2-yl)amide derivatives of flurbiprofen and naproxen. *European Journal of Pharmacology*, *720*(1–3), 383–390. https://doi.org/10.1016/j.ejphar.2013.09.065

Clouse, G., Penman, S., Hadjiargyrou, M., Komatsu, D. E., & Thanos, P. K. (2022). Examining the role of cannabinoids on osteoporosis: A review. *Archives of Osteoporosis*, *17*(1), 146. https://doi.org/10.1007/s11657-022-01190-x

Colangeli, R., Teskey, G. C., & Di Giovanni, G. (2021). Endocannabinoid-serotonin systems interaction in health and disease. In *Progress in Brain Research* (Vol. 259, pp. 83–134). Elsevier. https://doi.org/10.1016/bs.pbr.2021.01.003

Covey, D. P., Mateo, Y., Sulzer, D., Cheer, J. F., & Lovinger, D. M. (2017). Endocannabinoid modulation of dopamine neurotransmission. *Neuropharmacology*, *124*, 52–61. https://doi.org/10.1016/j.neuropharm.2017.04.033

Crocq, M.-A. (2020). History of cannabis and the endocannabinoid system. *Dialogues in Clinical Neuroscience*, *22*(3), 223–228. https://doi.org/10.31887/DCNS.2020.22.3/mcrocq

De Icco, R., Greco, R., Demartini, C., Vergobbi, P., Zanaboni, A., Tumelero, E., Reggiani, A., Realini, N., Sances, G., Grillo, V., Allena, M., & Tassorelli, C. (2021). Spinal nociceptive sensitization and plasma palmitoylethanolamide levels during experimentally induced migraine attacks. *Pain*, *162*(9), 2376–2385. https://doi.org/10.1097/j.pain.0000000000002223

De Simone, A., Russo, D., Ruda, G. F., Micoli, A., Ferraro, M., Di Martino, R. M. C., Ottonello, G., Summa, M., Armirotti, A., Bandiera, T., Cavalli, A., & Bottegoni, G. (2017). Design, Synthesis, Structure–Activity Relationship Studies, and Three-Dimensional Quantitative Structure–Activity Relationship (3D-QSAR)

Modeling of a Series of *O*-Biphenyl Carbamates as Dual Modulators of Dopamine D3 Receptor and Fatty Acid Amide Hydrolase. *Journal of Medicinal Chemistry*, *60*(6), 2287–2304. https://doi.org/10.1021/acs.jmedchem.6b01578

Di Filippo, C., Rossi, F., Rossi, S., & D'Amico, M. (2004). Cannabinoid CB2 receptor activation reduces mouse myocardial ischemia-reperfusion injury: Involvement of cytokine/chemokines and PMN. *Journal of Leukocyte Biology*, *75*(3), 453–459. https://doi.org/10.1189/jlb.0703303

Di Marzo, V., & De Petrocellis, L. (2012). Why do cannabinoid receptors have more than one endogenous ligand? *Philosophical Transactions of the Royal Society B: Biological Sciences*, *367*(1607), 3216–3228. https://doi.org/10.1098/rstb.2011.0382

Di Sabatino, A., Battista, N., Biancheri, P., Rapino, C., Rovedatti, L., Astarita, G., Vanoli, A., Dainese, E., Guerci, M., Piomelli, D., Pender, S. L. F., MacDonald, T. T., Maccarrone, M., & Corazza, G. R. (2011). The endogenous cannabinoid system in the gut of patients with inflammatory bowel disease. *Mucosal Immunology*, *4*(5), 574–583. https://doi.org/10.1038/mi.2011.18

Dong, B., Shilpa, B. M., Shah, R., Goyal, A., Xie, S., Bakalian, M. J., Suckow, R. F., Cooper, T. B., Mann, J. J., Arango, V., & Vinod, K. Y. (2020). Dual pharmacological inhibitor of endocannabinoid degrading enzymes reduces depressive-like behavior in female rats. *Journal of Psychiatric Research*, *120*, 103–112. https://doi.org/10.1016/j.jpsychires.2019.10.010

Fantauzzi, M. F., Aguiar, J. A., Tremblay, B. J.-M., Mansfield, M. J., Yanagihara, T., Chandiramohan, A., Revill, S., Ryu, M. H., Carlsten, C., Ask, K., Stämpfli, M., Doxey, A. C., & Hirota, J. A. (2020). Expression of endocannabinoid system components in human airway epithelial cells: Impact of sex and chronic respiratory disease status. *ERJ Open Research*, *6*(4), 00128–02020. https://doi.org/10.1183/23120541.00128-2020

Farran, B. (2017). An update on the physiological and therapeutic relevance of GPCR oligomers. *Pharmacological Research*, *117*, 303–327. https://doi.org/10.1016/j.phrs.2017.01.008

Fechtner, S., Singh, A. K., Srivastava, I., Szlenk, C. T., Muench, T. R., Natesan, S., & Ahmed, S. (2019). Cannabinoid Receptor 2 Agonist JWH-015 Inhibits Interleukin-1β-Induced Inflammation in Rheumatoid Arthritis Synovial Fibroblasts and in Adjuvant Induced Arthritis Rat via Glucocorticoid Receptor. *Frontiers in Immunology*, *10*, 1027. https://doi.org/10.3389/fimmu.2019.01027

Fernández-Ruiz, J., Moro, M. A., & Martínez-Orgado, J. (2015). Cannabinoids in Neurodegenerative Disorders and Stroke/Brain Trauma: From Preclinical Models to Clinical Applications. *Neurotherapeutics*, *12*(4), 793–806. https://doi.org/10.1007/s13311-015-0381-7

Florencio-Silva, R., Sasso, G. R. D. S., Sasso-Cerri, E., Simões, M. J., & Cerri, P. S. (2015). Biology of Bone Tissue: Structure, Function, and Factors That Influence Bone Cells. *BioMed Research International*, *2015*, 1–17. https://doi.org/10.1155/2015/421746

Fowler, C., Naidu, P., Lichtman, A., & Onnis, V. (2009). The case for the development of novel analgesic agents targeting both fatty acid amide hydrolase and either cyclooxygenase or TRPV1. *British Journal of Pharmacology*, *156*(3), 412–419. https://doi.org/10.1111/j.1476-5381.2008.00029.x

Franco, R., Martínez-Pinilla, E., Lanciego, J. L., & Navarro, G. (2016). Basic Pharmacological and Structural Evidence for Class A G-Protein-Coupled Receptor Heteromerization. *Frontiers in Pharmacology*, *7*. https://doi.org/10.3389/fphar.2016.00076

Franco, R., Villa, M., Morales, P., Reyes-Resina, I., Gutiérrez-Rodríguez, A., Jiménez, J., Jagerovic, N., Martínez-Orgado, J., & Navarro, G. (2019). Increased expression of cannabinoid CB2 and serotonin 5-HT1A heteroreceptor complexes in a model of newborn hypoxic-ischemic brain damage. *Neuropharmacology*, *152*, 58–66. https://doi.org/10.1016/j.neuropharm.2019.02.004

Fu, Q., Zheng, Y., Dong, X., Wang, L., & Jiang, C. G. (2017). Activation of cannabinoid receptor type 2 by JWH133 alleviates bleomycin-induced pulmonary fibrosis in mice. *Oncotarget*, *8*(61), 103486–103498. https://doi.org/10.18632/oncotarget.21975

Fulmer, M. L., & Thewke, D. P. (2018). The Endocannabinoid System and Heart Disease: The Role of Cannabinoid Receptor Type 2. *Cardiovascular & Hematological Disorders-Drug Targets*, *18*(1), 34–51. https://doi.org/10.2174/1871529X18666180206161457

Giannini, L., Nistri, S., Mastroianni, R., Cinci, L., Vannacci, A., Mariottini, C., Passani, M. B., Mannaioni, P. F., Bani, D., & Masini, E. (2008). Activation of cannabinoid receptors prevents antigen-induced asthma-like reaction in guinea pigs. *Journal of Cellular and Molecular Medicine*, *12*(6a), 2381–2394. https://doi.org/10.1111/j.1582-4934.2008.00258.x

Glass, C. K., Saijo, K., Winner, B., Marchetto, M. C., & Gage, F. H. (2010). Mechanisms Underlying Inflammation in Neurodegeneration. *Cell*, *140*(6), 918–934. https://doi.org/10.1016/j.cell.2010.02.016

Goadsby, P. J., Holland, P. R., Martins-Oliveira, M., Hoffmann, J., Schankin, C., & Akerman, S. (2017). Pathophysiology of Migraine: A Disorder of Sensory Processing. *Physiological Reviews*, *97*(2), 553–622. https://doi.org/10.1152/physrev.00034.2015

Gowran, A., McKayed, K., & Campbell, V. A. (2013). The Cannabinoid Receptor Type 1 Is Essential for Mesenchymal Stem Cell Survival and Differentiation: Implications for Bone Health. *Stem Cells International*, *2013*, 1–8. https://doi.org/10.1155/2013/796715

Grabiec, U., & Dehghani, F. (2017). *N* -Arachidonoyl Dopamine: A Novel Endocannabinoid and Endovanilloid with Widespread Physiological and Pharmacological Activities. *Cannabis and Cannabinoid Research*, *2*(1), 183–196. https://doi.org/10.1089/can.2017.0015

Greco, R., Demartini, C., Francavilla, M., Zanaboni, A. M., & Tassorelli, C. (2021). Dual Inhibition of FAAH and MAGL Counteracts Migraine-like Pain and Behavior in an Animal Model of Migraine. *Cells*, *10*(10), 2543. https://doi.org/10.3390/cells10102543

Greco, R., Demartini, C., Zanaboni, A., Casini, I., De Icco, R., Reggiani, A., Misto, A., Piomelli, D., & Tassorelli, C. (2021). Characterization of the peripheral FAAH inhibitor, URB937, in animal models of acute and chronic migraine. *Neurobiology of Disease*, *147*, 105157. https://doi.org/10.1016/j.nbd.2020.105157

Greco, R., Demartini, C., Zanaboni, A. M., Francavilla, M., De Icco, R., Ahmad, L., & Tassorelli, C. (2022). The endocannabinoid system and related lipids as potential targets for the treatment of migraine-related pain. *Headache: The Journal of Head and Face Pain*, *62*(3), 227–240. https://doi.org/10.1111/head.14267

Greco, R., Demartini, C., Zanaboni, A. M., Piomelli, D., & Tassorelli, C. (2018). Endocannabinoid System and Migraine Pain: An Update. *Frontiers in Neuroscience*, *12*, 172. https://doi.org/10.3389/fnins.2018.00172

Greco, R., Demartini, C., Zanaboni, A. M., Tumelero, E., Icco, R. D., Sances, G., Allena, M., & Tassorelli, C. (2021). Peripheral changes of endocannabinoid system components in episodic and chronic migraine patients: A pilot study. *Cephalalgia*, *41*(2), 185–196. https://doi.org/10.1177/0333102420949201

Greco, R., Mangione, A. S., Sandrini, G., Maccarrone, M., Nappi, G., & Tassorelli, C. (2011). Effects of anandamide in migraine: Data from an animal model. *The Journal of Headache and Pain*, *12*(2), 177–183. https://doi.org/10.1007/s10194-010-0274-4

Haspula, D., & Clark, M. A. (2020). Cannabinoid Receptors: An Update on Cell Signaling, Pathophysiological Roles and Therapeutic Opportunities in Neurological, Cardiovascular, and Inflammatory Diseases. *International Journal of Molecular Sciences*, *21*(20), 7693. https://doi.org/10.3390/ijms21207693

Heier, C., Taschler, U., Radulovic, M., Aschauer, P., Eichmann, T. O., Grond, S., Wolinski, H., Oberer, M., Zechner, R., Kohlwein, S. D., & Zimmermann, R. (2016). Monoacylglycerol Lipases Act as Evolutionarily Conserved Regulators of Non-oxidative Ethanol Metabolism. *Journal of Biological Chemistry*, *291*(22), 11865–11875. https://doi.org/10.1074/jbc.M115.705541

Hillard, C. J. (2018). Circulating Endocannabinoids: From Whence Do They Come and Where are They Going? *Neuropsychopharmacology*, *43*(1), 155–172. https://doi.org/10.1038/npp.2017.130

Huang, W.-J., Chen, W.-W., & Zhang, X. (2016). Endocannabinoid system: Role in depression, reward and pain control (Review). *Molecular Medicine Reports*, *14*(4), 2899–2903. https://doi.org/10.3892/mmr.2016.5585

Iannotti, F. A., Di Marzo, V., & Petrosino, S. (2016). Endocannabinoids and endocannabinoid-related mediators: Targets, metabolism and role in neurological disorders. *Progress in Lipid Research*, *62*, 107–128. https://doi.org/10.1016/j.plipres.2016.02.002

Idris, A. I., & Ralston, S. H. (2010). Cannabinoids and Bone: Friend or Foe? *Calcified Tissue International*, *87*(4), 285–297. https://doi.org/10.1007/s00223-010-9378-8

Idris, A. I., Van 'T Hof, R. J., Greig, I. R., Ridge, S. A., Baker, D., Ross, R. A., & Ralston, S. H. (2005). Regulation of bone mass, bone loss and osteoclast activity by cannabinoid receptors. *Nature Medicine*, *11*(7), 774–779. https://doi.org/10.1038/nm1255

Intranuovo, F., Brunetti, L., DelRe, P., Mangiatordi, G. F., Stefanachi, A., Laghezza, A., Niso, M., Leonetti, F., Loiodice, F., Ligresti, A., Kostrzewa, M., Brea, J., Loza, M. I., Sotelo, E., Saviano, M., Colabufo, N. A., Riganti, C., Abate, C., & Contino, M. (2023). Development of *N* -(1-Adamantyl)benzamides as Novel Anti-Inflammatory Multitarget Agents Acting as Dual Modulators of the Cannabinoid CB2 Receptor and Fatty Acid Amide Hydrolase. *Journal of Medicinal Chemistry*, *66*(1), 235–250. https://doi.org/10.1021/acs.jmedchem.2c01084

Jockers, R., Delagrange, P., Dubocovich, M. L., Markus, R. P., Renault, N., Tosini, G., Cecon, E., & Zlotos, D. P. (2016). Update on melatonin receptors: IUPHAR Review 20. *British Journal of Pharmacology*, *173*(18), 2702–2725. https://doi.org/10.1111/bph.13536

Jourdan, T., Godlewski, G., Cinar, R., Bertola, A., Szanda, G., Liu, J., Tam, J., Han, T., Mukhopadhyay, B., Skarulis, M. C., Ju, C., Aouadi, M., Czech, M. P., & Kunos, G. (2013). Activation of the Nlrp3

inflammasome in infiltrating macrophages by endocannabinoids mediates beta cell loss in type 2 diabetes. *Nature Medicine*, *19*(9), 1132–1140. https://doi.org/10.1038/nm.3265

Julius, D. (2013). TRP Channels and Pain. *Annual Review of Cell and Developmental Biology*, *29*(1), 355–384. https://doi.org/10.1146/annurev-cellbio-101011-155833

Jung, K.-M., Astarita, G., Yasar, S., Vasilevko, V., Cribbs, D. H., Head, E., Cotman, C. W., & Piomelli, D. (2012). An amyloid β42-dependent deficit in anandamide mobilization is associated with cognitive dysfunction in Alzheimer's disease. *Neurobiology of Aging*, *33*(8), 1522–1532. https://doi.org/10.1016/j.neurobiolaging.2011.03.012

Jung, K.-M., Sepers, M., Henstridge, C. M., Lassalle, O., Neuhofer, D., Martin, H., Ginger, M., Frick, A., DiPatrizio, N. V., Mackie, K., Katona, I., Piomelli, D., & Manzoni, O. J. (2012). Uncoupling of the endocannabinoid signalling complex in a mouse model of fragile X syndrome. *Nature Communications*, *3*(1), 1080. https://doi.org/10.1038/ncomms2045

Justinova, Z., Panlilio, L. V., Moreno-Sanz, G., Redhi, G. H., Auber, A., Secci, M. E., Mascia, P., Bandiera, T., Armirotti, A., Bertorelli, R., Chefer, S. I., Barnes, C., Yasar, S., Piomelli, D., & Goldberg, S. R. (2015). Effects of Fatty Acid Amide Hydrolase (FAAH) Inhibitors in Non-Human Primate Models of Nicotine Reward and Relapse. *Neuropsychopharmacology*, *40*(9), 2185–2197. https://doi.org/10.1038/npp.2015.62

Karpińska, O., Baranowska-Kuczko, M., Kloza, M., Ambroz˙ewicz, E., Kozłowski, T., Kasacka, I., Malinowska, B., & Kozłowska, H. (2017). Activation of CB $_1$ receptors by 2-arachidonoylglycerol attenuates vasoconstriction induced by U46619 and angiotensin II in human and rat pulmonary arteries. *American Journal of Physiology-Regulatory, Integrative and Comparative Physiology*, *312*(6), R883–R893. https://doi.org/10.1152/ajpregu.00324.2016

Katchan, V., David, P., & Shoenfeld, Y. (2016). Cannabinoids and autoimmune diseases: A systematic review. *Autoimmunity Reviews*, *15*(6), 513–528. https://doi.org/10.1016/j.autrev.2016.02.008

Katz, D., Katz, I., Porat-Katz, B., & Shoenfeld, Y. (2017). Medical cannabis: Another piece in the mosaic of autoimmunity? *Clinical Pharmacology & Therapeutics*, *101*(2), 230–238. https://doi.org/10.1002/cpt.568

Kicman, A., Pędzińska-Betiuk, A., & Kozłowska, H. (2021). The potential of cannabinoids and inhibitors of endocannabinoid degradation in respiratory diseases. *European Journal of Pharmacology*, *911*, 174560. https://doi.org/10.1016/j.ejphar.2021.174560

Klein, M. O., Battagello, D. S., Cardoso, A. R., Hauser, D. N., Bittencourt, J. C., & Correa, R. G. (2019). Dopamine: Functions, Signaling, and Association with Neurological Diseases. *Cellular and Molecular Neurobiology*, *39*(1), 31–59. https://doi.org/10.1007/s10571-018-0632-3

Kodani, S. D., Wan, D., Wagner, K. M., Hwang, S. H., Morisseau, C., & Hammock, B. D. (2018). Design and Potency of Dual Soluble Epoxide Hydrolase/Fatty Acid Amide Hydrolase Inhibitors. *ACS Omega*, *3*(10), 14076–14086. https://doi.org/10.1021/acsomega.8b01625

Kohnz, R. A., & Nomura, D. K. (2014). Chemical approaches to therapeutically target the metabolism and signaling of the endocannabinoid 2-AG and eicosanoids. *Chem. Soc. Rev.*, *43*(19), 6859–6869. https://doi.org/10.1039/C4CS00047A

Kokona, D., Spyridakos, D., Tzatzarakis, M., Papadogkonaki, S., Filidou, E., Arvanitidis, K. I., Kolios, G., Lamani, M., Makriyannis, A., Malamas, M. S., & Thermos, K. (2021). The endocannabinoid 2-arachidonoylglycerol and dual ABHD6/MAGL enzyme inhibitors display neuroprotective and anti-inflammatory actions in the in vivo retinal model of AMPA excitotoxicity. *Neuropharmacology*, *185*, 108450. https://doi.org/10.1016/j.neuropharm.2021.108450

Koob, G. F., & Volkow, N. D. (2010). Neurocircuitry of Addiction. *Neuropsychopharmacology*, *35*(1), 217–238. https://doi.org/10.1038/npp.2009.110

Kubajewska, I., & Constantinescu, C. S. (2010). Cannabinoids and experimental models of multiple sclerosis. *Immunobiology*, *215*(8), 647–657. https://doi.org/10.1016/j.imbio.2009.08.004

Kumar, V., Kundu, S., Singh, A., & Singh, S. (2022). Understanding the Role of Histone Deacetylase and their Inhibitors inNeurodegenerative Disorders: Current Targets and Future Perspective. *Current Neuropharmacology*, *20*(1), 158–178. https://doi.org/10.2174/1570159X19666210609160017

Laksmidewi, A. A. A. P., & Soejitno, A. (2021). Endocannabinoid and dopaminergic system: The pas de deux underlying human motivation and behaviors. *Journal of Neural Transmission*, *128*(5), 615–630. https://doi.org/10.1007/s00702-021-02326-y

Lamens, A., & Bajorath, J. (2023). Explaining Accurate Predictions of Multitarget Compounds with Machine Learning Models Derived for Individual Targets. *Molecules*, *28*(2), 825. https://doi.org/10.3390/molecules28020825

Liu, J., Wang, L., Harvey-White, J., Huang, B. X., Kim, H.-Y., Luquet, S., Palmiter, R. D., Krystal, G., Rai, R., Mahadevan, A., Razdan, R. K., & Kunos, G. (2008). Multiple pathways involved in the biosynthesis of anandamide. *Neuropharmacology*, *54*(1), 1–7. https://doi.org/10.1016/j.neuropharm.2007.05.020

Liu, J., Wang, L., Harvey-White, J., Osei-Hyiaman, D., Razdan, R., Gong, Q., Chan, A. C., Zhou, Z., Huang, B. X., Kim, H.-Y., & Kunos, G. (2006). A biosynthetic pathway for anandamide. *Proceedings of the National Academy of Sciences*, *103*(36), 13345–13350. https://doi.org/10.1073/pnas.0601832103

Liu, L., Labani, N., Cecon, E., & Jockers, R. (2019). Melatonin Target Proteins: Too Many or Not Enough? *Frontiers in Endocrinology*, *10*, 791. https://doi.org/10.3389/fendo.2019.00791

López-Carballo, G., Moreno, L., Masiá, S., Pérez, P., & Barettino, D. (2002). Activation of the Phosphatidylinositol 3-Kinase/Akt Signaling Pathway by Retinoic Acid Is Required for Neural Differentiation of SH-SY5Y Human Neuroblastoma Cells. *Journal of Biological Chemistry*, *277*(28), 25297–25304. https://doi.org/10.1074/jbc.M201869200

Lowe, H., Toyang, N., Steele, B., Bryant, J., & Ngwa, W. (2021). The Endocannabinoid System: A Potential Target for the Treatment of Various Diseases. *International Journal of Molecular Sciences*, *22*(17), 9472. https://doi.org/10.3390/ijms22179472

Lu, H.-C., & Mackie, K. (2021). Review of the Endocannabinoid System. *Biological Psychiatry: Cognitive Neuroscience and Neuroimaging*, *6*(6), 607–615. https://doi.org/10.1016/j.bpsc.2020.07.016

Lunerti, V., Li, H., Benvenuti, F., Shen, Q., Domi, A., Soverchia, L., Concetta Di Martino, R. M., Bottegoni, G., Haass-Koffler, C. L., & Cannella, N. (2022). The multitarget FAAH inhibitor/D3 partial agonist ARN15381 decreases nicotine self-administration in male rats. *European Journal of Pharmacology*, *928*, 175088. https://doi.org/10.1016/j.ejphar.2022.175088

Maccarrone, M., Bari, M., Lorenzon, T., Bisogno, T., Di Marzo, V., & Finazzi-Agrò, A. (2000). Anandamide Uptake by Human Endothelial Cells and Its Regulation by Nitric Oxide. *Journal of Biological Chemistry*, *275*(18), 13484–13492. https://doi.org/10.1074/jbc.275.18.13484

Maione, S., De Petrocellis, L., De Novellis, V., Moriello, A. S., Petrosino, S., Palazzo, E., Rossi, F. S., Woodward, D. F., & Di Marzo, V. (2007). Analgesic actions of *N*-arachidonoyl-serotonin, a fatty acid amide hydrolase inhibitor with antagonistic activity at vanilloid TRPV1 receptors. *British Journal of Pharmacology*, *150*(6), 766–781. https://doi.org/10.1038/sj.bjp.0707145

Maleki, M. F., Nadri, H., Kianfar, M., Edraki, N., Eisvand, F., Ghodsi, R., Mohajeri, S. A., & Hadizadeh, F. (2021). Design and synthesis of new carbamates as inhibitors for fatty acid amide hydrolase and cholinesterases: Molecular dynamic, in vitro and in vivo studies. *Bioorganic Chemistry*, *109*, 104684. https://doi.org/10.1016/j.bioorg.2021.104684

Maresz, K., Pryce, G., Ponomarev, E. D., Marsicano, G., Croxford, J. L., Shriver, L. P., Ledent, C., Cheng, X., Carrier, E. J., Mann, M. K., Giovannoni, G., Pertwee, R. G., Yamamura, T., Buckley, N. E., Hillard, C. J., Lutz, B., Baker, D., & Dittel, B. N. (2007). Direct suppression of CNS autoimmune inflammation via the cannabinoid receptor CB1 on neurons and CB2 on autoreactive T cells. *Nature Medicine*, *13*(4), 492–497. https://doi.org/10.1038/nm1561

Maroso, M., Szabo, G. G., Kim, H. K., Alexander, A., Bui, A. D., Lee, S.-H., Lutz, B., & Soltesz, I. (2016). Cannabinoid Control of Learning and Memory through HCN Channels. *Neuron*, *89*(5), 1059–1073. https://doi.org/10.1016/j.neuron.2016.01.023

Martínez-Pinilla, E., Rico, A. J., Rivas-Santisteban, R., Lillo, J., Roda, E., Navarro, G., Franco, R., & Lanciego, J. L. (2020). Expression of cannabinoid CB$_1$R–GPR55 heteromers in neuronal subtypes of the *Macaca fascicularis* striatum. *Annals of the New York Academy of Sciences*, *1475*(1), 34–42. https://doi.org/10.1111/nyas.14413

Marzo, V., & Petrocellis, L. (2010). Endocannabinoids as Regulators of Transient Receptor Potential (TRP)Channels: A Further Opportunity to Develop New Endocannabinoid-Based Therapeutic Drugs. *Current Medicinal Chemistry*, *17*(14), 1430–1449. https://doi.org/10.2174/092986710790980078

Mechoulam, R., & Parker, L. A. (2013). The Endocannabinoid System and the Brain. *Annual Review of Psychology*, *64*(1), 21–47. https://doi.org/10.1146/annurev-psych-113011-143739

Micale, V., Cristino, L., Tamburella, A., Petrosino, S., Leggio, G. M., Drago, F., & Di Marzo, V. (2009). Anxiolytic Effects in Mice of a Dual Blocker of Fatty Acid Amide Hydrolase and Transient Receptor Potential Vanilloid Type-1 Channels. *Neuropsychopharmacology*, *34*(3), 593–606. https://doi.org/10.1038/npp.2008.98

Milian, L., Mata, M., Alcacer, J., Oliver, M., Sancho-Tello, M., Martín De Llano, J. J., Camps, C., Galbis, J., Carretero, J., & Carda, C. (2020). Cannabinoid receptor expression in non-small cell lung cancer. Effectiveness of tetrahydrocannabinol and cannabidiol inhibiting cell proliferation and epithelial-mesenchymal transition in vitro. *PLOS ONE*, *15*(2), e0228909. https://doi.org/10.1371/journal.pone.0228909

Miller, P. D. (2016). Management of severe osteoporosis. *Expert Opinion on Pharmacotherapy*, *17*(4), 473–488. https://doi.org/10.1517/14656566.2016.1124856

Morales, P., & Reggio, P. H. (2017). An Update on Non-CB 1 , Non-CB 2 Cannabinoid Related G-Protein-Coupled Receptors. *Cannabis and Cannabinoid Research*, *2*(1), 265–273. https://doi.org/10.1089/can.2017.0036

Moreno, E., Chiarlone, A., Medrano, M., Puigdellívol, M., Bibic, L., Howell, L. A., Resel, E., Puente, N., Casarejos, M. J., Perucho, J., Botta, J., Suelves, N., Ciruela, F., Ginés, S., Galve-Roperh, I., Casadó, V., Grandes, P., Lutz, B., Monory, K., … Guzmán, M. (2018). Singular Location and Signaling Profile of Adenosine A2A-Cannabinoid CB1 Receptor Heteromers in the Dorsal Striatum. *Neuropsychopharmacology*, *43*(5), 964–977. https://doi.org/10.1038/npp.2017.12

Morisseau, C., & Hammock, B. D. (2013). Impact of Soluble Epoxide Hydrolase and Epoxyeicosanoids on Human Health. *Annual Review of Pharmacology and Toxicology*, *53*(1), 37–58. https://doi.org/10.1146/annurev-pharmtox-011112-140244

Morphy, R. (2010). Selectively Nonselective Kinase Inhibition: Striking the Right Balance. *Journal of Medicinal Chemistry*, *53*(4), 1413–1437. https://doi.org/10.1021/jm901132v

Muller, C., Morales, P., & Reggio, P. H. (2019). Cannabinoid Ligands Targeting TRP Channels. *Frontiers in Molecular Neuroscience*, *11*, 487. https://doi.org/10.3389/fnmol.2018.00487

Nagarkatti, P., Pandey, R., Rieder, S. A., Hegde, V. L., & Nagarkatti, M. (2009). Cannabinoids as novel anti-inflammatory drugs. *Future Medicinal Chemistry*, *1*(7), 1333–1349. https://doi.org/10.4155/fmc.09.93

Nagy, I., Friston, D., Valente, J. S., Perez, J. V. T., & Andreou, A. P. (2014). Pharmacology of the Capsaicin Receptor, Transient Receptor Potential Vanilloid Type-1 Ion Channel. In O. M. E. Abdel-Salam (A c. Di), *Capsaicin as a Therapeutic Molecule* (pp. 39–76). Springer Basel. https://doi.org/10.1007/978-3-0348-0828-6_2

Narushima, M., Uchigashima, M., Fukaya, M., Matsui, M., Manabe, T., Hashimoto, K., Watanabe, M., & Kano, M. (2007). Tonic Enhancement of Endocannabinoid-Mediated Retrograde Suppression of Inhibition by Cholinergic Interneuron Activity in the Striatum. *The Journal of Neuroscience*, *27*(3), 496–506. https://doi.org/10.1523/JNEUROSCI.4644-06.2007

Navarria, A., Tamburella, A., Iannotti, F. A., Micale, V., Camillieri, G., Gozzo, L., Verde, R., Imperatore, R., Leggio, G. M., Drago, F., & Di Marzo, V. (2014). The dual blocker of FAAH/TRPV1 N-arachidonoylserotonin reverses the behavioral despair induced by stress in rats and modulates the HPA-axis. *Pharmacological Research*, *87*, 151–159. https://doi.org/10.1016/j.phrs.2014.04.014

Nicolussi, S., & Gertsch, J. (2015). Endocannabinoid Transport Revisited. In *Vitamins & Hormones* (Vol. 98, pp. 441–485). Elsevier. https://doi.org/10.1016/bs.vh.2014.12.011

Nikolaev, G., Robeva, R., & Konakchieva, R. (2021). Membrane Melatonin Receptors Activated Cell Signaling in Physiology and Disease. *International Journal of Molecular Sciences*, *23*(1), 471. https://doi.org/10.3390/ijms23010471

Nomura, D. K., Lombardi, D. P., Chang, J. W., Niessen, S., Ward, A. M., Long, J. Z., Hoover, H. H., & Cravatt, B. F. (2011). Monoacylglycerol Lipase Exerts Dual Control over Endocannabinoid and Fatty Acid Pathways to Support Prostate Cancer. *Chemistry & Biology*, *18*(7), 846–856. https://doi.org/10.1016/j.chembiol.2011.05.009

Nomura, D. K., Morrison, B. E., Blankman, J. L., Long, J. Z., Kinsey, S. G., Marcondes, M. C. G., Ward, A. M., Hahn, Y. K., Lichtman, A. H., Conti, B., & Cravatt, B. F. (2011). Endocannabinoid Hydrolysis Generates Brain Prostaglandins That Promote Neuroinflammation. *Science*, *334*(6057), 809–813. https://doi.org/10.1126/science.1209200

Nucci, C., Gasperi, V., Tartaglione, R., Cerulli, A., Terrinoni, A., Bari, M., De Simone, C., Agro`, A. F., Morrone, L. A., Corasaniti, M. T., Bagetta, G., & Maccarrone, M. (2007). Involvement of the Endocannabinoid System in Retinal Damage after High Intraocular Pressure–Induced Ischemia in Rats. *Investigative Opthalmology & Visual Science*, *48*(7), 2997. https://doi.org/10.1167/iovs.06-1355

Ofek, O., Karsak, M., Leclerc, N., Fogel, M., Frenkel, B., Wright, K., Tam, J., Attar-Namdar, M., Kram, V., Shohami, E., Mechoulam, R., Zimmer, A., & Bab, I. (2006). Peripheral cannabinoid receptor, CB2, regulates bone mass. *Proceedings of the National Academy of Sciences*, *103*(3), 696–701. https://doi.org/10.1073/pnas.0504187103

Ohno-Shosaku, T., & Kano, M. (2014). Endocannabinoid-mediated retrograde modulation of synaptic transmission. *Current Opinion in Neurobiology*, *29*, 1–8. https://doi.org/10.1016/j.conb.2014.03.017

Palazuelos, J., Aguado, T., Pazos, M. R., Julien, B., Carrasco, C., Resel, E., Sagredo, O., Benito, C., Romero, J., Azcoitia, I., Fernández-Ruiz, J., Guzmán, M., & Galve-Roperh, I. (2009). Microglial CB2 cannabinoid receptors are neuroprotective in Huntington's disease excitotoxicity. *Brain*, *132*(11), 3152–3164. https://doi.org/10.1093/brain/awp239

Papa, A., Pasquini, S., Contri, C., Gemma, S., Campiani, G., Butini, S., Varani, K., & Vincenzi, F. (2022). Polypharmacological Approaches for CNS Diseases: Focus on Endocannabinoid Degradation Inhibition. *Cells*, *11*(3), 471. https://doi.org/10.3390/cells11030471

Parsons, L. H., & Hurd, Y. L. (2015). Endocannabinoid signalling in reward and addiction. *Nature Reviews Neuroscience*, *16*(10), 579–594. https://doi.org/10.1038/nrn4004

Patrono, C., & Baigent, C. (2009). Low-Dose Aspirin, Coxibs, and other NSAIDS: A Clinical Mosaic Emerges. *Molecular Interventions*, *9*(1), 31–39. https://doi.org/10.1124/mi.9.1.8

Pertwee, R. (2010). Receptors and Channels Targeted by Synthetic Cannabinoid Receptor Agonists and Antagonists. *Current Medicinal Chemistry*, *17*(14), 1360–1381. https://doi.org/10.2174/092986710790980050

Peters, J.-U. (2013). Polypharmacology – Foe or Friend? *Journal of Medicinal Chemistry*, *56*(22), 8955–8971. https://doi.org/10.1021/jm400856t

Pinar-Sueiro, S., Zorrilla Hurtado, J. Á., Veiga-Crespo, P., Sharma, S. C., & Vecino, E. (2013). Neuroprotective effects of topical CB1 agonist WIN 55212-2 on retinal ganglion cells after acute rise in intraocular pressure induced ischemia in rat. *Experimental Eye Research*, *110*, 55–58. https://doi.org/10.1016/j.exer.2013.02.009

Prenderville, J. A., Kelly, Á. M., & Downer, E. J. (2015). The role of cannabinoids in adult neurogenesis. *British Journal of Pharmacology*, *172*(16), 3950–3963. https://doi.org/10.1111/bph.13186

Proschak, E., Stark, H., & Merk, D. (2019). Polypharmacology by Design: A Medicinal Chemist's Perspective on Multitargeting Compounds. *Journal of Medicinal Chemistry*, *62*(2), 420–444. https://doi.org/10.1021/acs.jmedchem.8b00760

Rabino, M., Mallia, S., Castiglioni, E., Rovina, D., Pompilio, G., & Gowran, A. (2021). The Endocannabinoid System and Cannabidiol: Past, Present, and Prospective for Cardiovascular Diseases. *Pharmaceuticals*, *14*(9), 936. https://doi.org/10.3390/ph14090936

Rampa, A., Bartolini, M., Bisi, A., Belluti, F., Gobbi, S., Andrisano, V., Ligresti, A., & Di Marzo, V. (2012). The First Dual ChE/FAAH Inhibitors: New Perspectives for Alzheimer's Disease? *ACS Medicinal Chemistry Letters*, *3*(3), 182–186. https://doi.org/10.1021/ml200313p

Reyes-Resina, I., Navarro, G., Aguinaga, D., Canela, E. I., Schoeder, C. T., Załuski, M., Kieć-Kononowicz, K., Saura, C. A., Müller, C. E., & Franco, R. (2018). Molecular and functional interaction between GPR18 and cannabinoid CB2 G-protein-coupled receptors. Relevance in neurodegenerative diseases. *Biochemical Pharmacology*, *157*, 169–179. https://doi.org/10.1016/j.bcp.2018.06.001

Rose, T. M., Reilly, C. A., Deering-Rice, C. E., Brewster, C., & Brewster, C. (2014). Inhibition of FAAH, TRPV1, and COX2 by NSAID–serotonin conjugates. *Bioorganic & Medicinal Chemistry Letters*, *24*(24), 5695–5698. https://doi.org/10.1016/j.bmcl.2014.10.064

Rosengren, R., & Cridge, B. (2013). Critical appraisal of the potential use of cannabinoids in cancer management. *Cancer Management and Research*, 301. https://doi.org/10.2147/CMAR.S36105

Rubino, T., Realini, N., Castiglioni, C., Guidali, C., Vigano, D., Marras, E., Petrosino, S., Perletti, G., Maccarrone, M., Di Marzo, V., & Parolaro, D. (2008). Role in Anxiety Behavior of the Endocannabinoid System in the Prefrontal Cortex. *Cerebral Cortex*, *18*(6), 1292–1301. https://doi.org/10.1093/cercor/bhm161

Ryszkiewicz, P., Malinowska, B., & Schlicker, E. (2023). Polypharmacology: Promises and new drugs in 2022. *Pharmacological Reports*, *75*(4), 755–770. https://doi.org/10.1007/s43440-023-00501-4

Sagheddu, C., Muntoni, A. L., Pistis, M., & Melis, M. (2015). Endocannabinoid Signaling in Motivation, Reward, and Addiction. In *International Review of Neurobiology* (Vol. 125, pp. 257–302). Elsevier. https://doi.org/10.1016/bs.irn.2015.10.004

Sasso, O., Migliore, M., Habrant, D., Armirotti, A., Albani, C., Summa, M., Moreno-Sanz, G., Scarpelli, R., & Piomelli, D. (2015). Multitarget fatty acid amide hydrolase/cyclooxygenase blockade suppresses intestinal inflammation and protects against nonsteroidal anti-inflammatory drug-dependent gastrointestinal damage. *The FASEB Journal*, *29*(6), 2616–2627. https://doi.org/10.1096/fj.15-270637

Sasso, O., Wagner, K., Morisseau, C., Inceoglu, B., Hammock, B. D., & Piomelli, D. (2015). Peripheral FAAH and soluble epoxide hydrolase inhibitors are synergistically antinociceptive. *Pharmacological Research*, *97*, 7–15. https://doi.org/10.1016/j.phrs.2015.04.001

Savinainen, J. R., Kansanen, E., Pantsar, T., Navia-Paldanius, D., Parkkari, T., Lehtonen, M., Laitinen, T., Nevalainen, T., Poso, A., Levonen, A.-L., & Laitinen, J. T. (2014). Robust Hydrolysis of Prostaglandin Glycerol Esters by Human Monoacylglycerol Lipase (MAGL). *Molecular Pharmacology*, *86*(5), 522–535. https://doi.org/10.1124/mol.114.094284

Scherma, M., Satta, V., Collu, R., Boi, M. F., Usai, P., Fratta, W., & Fadda, P. (2017). Cannabinoid CB$_1$/CB$_2$ receptor agonists attenuate hyperactivity and body weight loss in a rat model of activity-based anorexia. *British Journal of Pharmacology*, *174*(16), 2682–2695. https://doi.org/10.1111/bph.13892

Scopinho, A. A., Guimarães, F. S., Corrêa, F. M. A., & Resstel, L. B. M. (2011). Cannabidiol inhibits the hyperphagia induced by cannabinoid-1 or serotonin-1A receptor agonists. *Pharmacology Biochemistry and Behavior*, *98*(2), 268–272. https://doi.org/10.1016/j.pbb.2011.01.007

Scotter, E. L., Abood, M. E., & Glass, M. (2010). The endocannabinoid system as a target for the treatment of neurodegenerative disease. *British Journal of Pharmacology*, *160*(3), 480–498. https://doi.org/10.1111/j.1476-5381.2010.00735.x

Seillier, A., Dominguez Aguilar, D., & Giuffrida, A. (2014). The dual FAAH/MAGL inhibitor JZL195 has enhanced effects on endocannabinoid transmission and motor behavior in rats as compared to those of the MAGL inhibitor JZL184. *Pharmacology Biochemistry and Behavior*, *124*, 153–159. https://doi.org/10.1016/j.pbb.2014.05.022

Shah, M. M. (2014). Cortical HCN channels: Function, trafficking and plasticity. *The Journal of Physiology*, *592*(13), 2711–2719. https://doi.org/10.1113/jphysiol.2013.270058

Singh, A., Saluja, S., Kumar, A., Agrawal, S., Thind, M., Nanda, S., & Shirani, J. (2018). Cardiovascular Complications of Marijuana and Related Substances: A Review. *Cardiology and Therapy*, *7*(1), 45–59. https://doi.org/10.1007/s40119-017-0102-x

Sipe, J. C., Arbour, N., Gerber, A., & Beutler, E. (2005). Reduced endocannabinoid immune modulation by a common cannabinoid 2 (CB2) receptor gene polymorphism: Possible risk for autoimmune disorders. *Journal of Leukocyte Biology*, *78*(1), 231–238. https://doi.org/10.1189/jlb.0205111

Sloan, M. E., Gowin, J. L., Yan, J., Schwandt, M. L., Spagnolo, P. A., Sun, H., Hodgkinson, C. A., Goldman, D., & Ramchandani, V. A. (2018). Severity of alcohol dependence is associated with the fatty acid amide hydrolase Pro129Thr missense variant. *Addiction Biology*, *23*(1), 474–484. https://doi.org/10.1111/adb.12491

Slusar, J. E., Cairns, E. A., Szczesniak, A.-M., Bradshaw, H. B., Di Polo, A., & Kelly, M. E. M. (2013). The fatty acid amide hydrolase inhibitor, URB597, promotes retinal ganglion cell neuroprotection in a rat model of optic nerve axotomy. *Neuropharmacology*, *72*, 116–125. https://doi.org/10.1016/j.neuropharm.2013.04.018

Solas, M., Francis, P. T., Franco, R., & Ramirez, M. J. (2013). CB2 receptor and amyloid pathology in frontal cortex of Alzheimer's disease patients. *Neurobiology of Aging*, *34*(3), 805–808. https://doi.org/10.1016/j.neurobiolaging.2012.06.005

Spadoni, G., Bedini, A., Furiassi, L., Mari, M., Mor, M., Scalvini, L., Lodola, A., Ghidini, A., Lucini, V., Dugnani, S., Scaglione, F., Piomelli, D., Jung, K.-M., Supuran, C. T., Lucarini, L., Durante, M., Sgambellone, S., Masini, E., & Rivara, S. (2018). Identification of Bivalent Ligands with Melatonin Receptor Agonist and Fatty Acid Amide Hydrolase (FAAH) Inhibitory Activity That Exhibit Ocular Hypotensive Effect in the Rabbit. *Journal of Medicinal Chemistry*, *61*(17), 7902–7916. https://doi.org/10.1021/acs.jmedchem.8b00893

Staiano, R. I., Loffredo, S., Borriello, F., Iannotti, F. A., Piscitelli, F., Orlando, P., Secondo, A., Granata, F., Lepore, M. T., Fiorelli, A., Varricchi, G., Santini, M., Triggiani, M., Di Marzo, V., & Marone, G. (2016). Human lung-resident macrophages express CB1 and CB2 receptors whose activation inhibits the release of angiogenic and lymphangiogenic factors. *Journal of Leukocyte Biology*, *99*(4), 531–540. https://doi.org/10.1189/jlb.3HI1214-584R

Stampanoni Bassi, M., Gilio, L., Maffei, P., Dolcetti, E., Bruno, A., Buttari, F., Centonze, D., & Iezzi, E. (2018). Exploiting the Multifaceted Effects of Cannabinoids on Mood to Boost Their Therapeutic Use Against Anxiety and Depression. *Frontiers in Molecular Neuroscience*, *11*, 424. https://doi.org/10.3389/fnmol.2018.00424

Staton, P. C., Hatcher, J. P., Walker, D. J., Morrison, A. D., Shapland, E. M., Hughes, J. P., Chong, E., Mander, P. K., Green, P. J., Billinton, A., Fulleylove, M., Lancaster, H. C., Smith, J. C., Bailey, L. T., Wise, A., Brown, A. J., Richardson, J. C., & Chessell, I. P. (2008). The putative cannabinoid receptor GPR55 plays a role in mechanical hyperalgesia associated with inflammatory and neuropathic pain. *Pain*, *139*(1), 225–236. https://doi.org/10.1016/j.pain.2008.04.006

Stella, N. (2010). Cannabinoid and cannabinoid-like receptors in microglia, astrocytes, and astrocytomas. *Glia*, *58*(9), 1017–1030. https://doi.org/10.1002/glia.20983

Storr, M. A., Keenan, C. M., Zhang, H., Patel, K. D., Makriyannis, A., & Sharkey, K. A. (2009). Activation of the cannabinoid 2 receptor (CB2) protects against experimental colitis: *Inflammatory Bowel Diseases*, *15*(11), 1678–1685. https://doi.org/10.1002/ibd.20960

Szafran, B., Lee, J., Borazjani, A., Morrison, P., Zimmerman, G., Andrzejewski, K., Ross, M., & Kaplan, B. (2018). Characterization of Endocannabinoid-Metabolizing Enzymes in Human Peripheral Blood Mononuclear Cells under Inflammatory Conditions. *Molecules*, *23*(12), 3167. https://doi.org/10.3390/molecules23123167

Tan, Z., Chaudhai, R., & Zhang, S. (2016). Polypharmacology in Drug Development: A Minireview of Current Technologies. *ChemMedChem*, *11*(12), 1211–1218. https://doi.org/10.1002/cmdc.201600067

Tripathi, R. K. P. (2020). A perspective review on fatty acid amide hydrolase (FAAH) inhibitors as potential therapeutic agents. *European Journal of Medicinal Chemistry*, *188*, 111953. https://doi.org/10.1016/j.ejmech.2019.111953

Turcotte, C., Blanchet, M.-R., Laviolette, M., & Flamand, N. (2016). Impact of Cannabis, Cannabinoids, and Endocannabinoids in the Lungs. *Frontiers in Pharmacology*, *7*. https://doi.org/10.3389/fphar.2016.00317

Valant, C., Sexton, P. M., & Christopoulos, A. (2009). Orthosteric/Allosteric Bitopic Ligands: Going Hybrid at GPCRs. *Molecular Interventions*, *9*(3), 125–135. https://doi.org/10.1124/mi.9.3.6

Van Der Schueren, B. J., Van Laere, K., Gérard, N., Bormans, G., & De Hoon, J. N. (2012). Interictal Type 1 Cannabinoid Receptor Binding is Increased in Female Migraine Patients. *Headache: The Journal of Head and Face Pain*, *52*(3), 433–440. https://doi.org/10.1111/j.1526-4610.2011.02030.x

Velasco, G., Sánchez, C., & Guzmán, M. (2016). Anticancer Mechanisms of Cannabinoids. *Current Oncology*, *23*(11), 23–32. https://doi.org/10.3747/co.23.3080

Vitale, R. M., Iannotti, F. A., & Amodeo, P. (2021). The (Poly)Pharmacology of Cannabidiol in Neurological and Neuropsychiatric Disorders: Molecular Mechanisms and Targets. *International Journal of Molecular Sciences*, *22*(9), 4876. https://doi.org/10.3390/ijms22094876

Vučković, S., Srebro, D., Vujović, K. S., Vučetić, Č., & Prostran, M. (2018). Cannabinoids and Pain: New Insights From Old Molecules. *Frontiers in Pharmacology*, *9*, 1259. https://doi.org/10.3389/fphar.2018.01259

Walsh, S. K., Hepburn, C. Y., Kane, K. A., & Wainwright, C. L. (2010). Acute administration of cannabidiol *in vivo* suppresses ischaemia-induced cardiac arrhythmias and reduces infarct size when given at reperfusion. *British Journal of Pharmacology*, *160*(5), 1234–1242. https://doi.org/10.1111/j.1476-5381.2010.00755.x

Wang, Z., Kai, L., Day, M., Ronesi, J., Yin, H. H., Ding, J., Tkatch, T., Lovinger, D. M., & Surmeier, D. J. (2006). Dopaminergic Control of Corticostriatal Long-Term Synaptic Depression in Medium Spiny Neurons Is Mediated by Cholinergic Interneurons. *Neuron*, *50*(3), 443–452. https://doi.org/10.1016/j.neuron.2006.04.010

Wawryk-Gawda, E., Chłapek, K., Zarobkiewicz, M. K., Lis-Sochocka, M., Chylińska-Wrzos, P., Boguszewska-Czubara, A., Sławiński, M. A., Franczak, A., Jodłowska-Jędrych, B., & Biała, G. (2018). CB2R agonist prevents nicotine induced lung fibrosis. *Experimental Lung Research*, *44*(7), 344–351. https://doi.org/10.1080/01902148.2018.1543368

Wilkerson, J. L., Ghosh, S., Mustafa, M., Abdullah, R. A., Niphakis, M. J., Cabrera, R., Maldonado, R. L., Cravatt, B. F., & Lichtman, A. H. (2017). The endocannabinoid hydrolysis inhibitor SA-57: Intrinsic antinociceptive effects, augmented morphine-induced antinociception, and attenuated heroin seeking behavior in mice. *Neuropharmacology*, *114*, 156–167. https://doi.org/10.1016/j.neuropharm.2016.11.015

Wilt, S., Kodani, S., Valencia, L., Hudson, P. K., Sanchez, S., Quintana, T., Morisseau, C., Hammock, B. D., Kandasamy, R., & Pecic, S. (2021). Further exploration of the structure-activity relationship of dual soluble epoxide hydrolase/fatty acid amide hydrolase inhibitors. *Bioorganic & Medicinal Chemistry*, *51*, 116507. https://doi.org/10.1016/j.bmc.2021.116507

Wongprayoon, P., & Govitrapong, P. (2020). Melatonin Receptor as a Drug Target for Neuroprotection. *Current Molecular Pharmacology*, *14*(2), 150–164. https://doi.org/10.2174/1874467213666200421160835

Wright, K. L., Duncan, M., & Sharkey, K. A. (2008). Cannabinoid CB $_2$ receptors in the gastrointestinal tract: A regulatory system in states of inflammation. *British Journal of Pharmacology*, *153*(2), 263–270. https://doi.org/10.1038/sj.bjp.0707486

Xiong, Y., Yao, H., Cheng, Y., Gong, D., Liao, X., & Wang, R. (2018). Effects of monoacylglycerol lipase inhibitor URB602 on lung ischemia-reperfusion injury in mice. *Biochemical and Biophysical Research Communications*, *506*(3), 578–584. https://doi.org/10.1016/j.bbrc.2018.10.098

Xu, S., Ma, H., Bo, Y., & Shao, M. (2019). The oncogenic role of CB2 in the progression of non-small-cell lung cancer. *Biomedicine & Pharmacotherapy*, *117*, 109080. https://doi.org/10.1016/j.biopha.2019.109080

Yesilyurt, O., Cayirli, M., Sakin, Y. S., Seyrek, M., Akar, A., & Dogrul, A. (2016). Systemic and spinal administration of FAAH, MAGL inhibitors and dual FAAH/MAGL inhibitors produce antipruritic effect in mice. *Archives of Dermatological Research*, *308*(5), 335–345. https://doi.org/10.1007/s00403-016-1649-4

Yin, H., Li, X., Xia, R., Yi, M., Cheng, Y., Wu, Y., Ke, B., & Wang, R. (2019). Posttreatment With the Fatty Acid Amide Hydrolase Inhibitor URB937 Ameliorates One-Lung Ventilation–Induced Lung Injury in a Rabbit Model. *Journal of Surgical Research*, *239*, 83–91. https://doi.org/10.1016/j.jss.2019.01.009

Zhang, M., Mahadevan, A., Amere, M., Li, H., Ganea, D., & Tuma, R. F. (2012). Unique Effects of Compounds Active at Both Cannabinoid and Serotonin Receptors During Stroke. *Translational Stroke Research*, *3*(3), 348–356. https://doi.org/10.1007/s12975-012-0197-2

Zhu, F., Wang, X., Chen, Y., Yang, N., Lang, S., Zuo, P., Zhang, J., & Li, R. (2015). Changes and overlapping distribution in the expression of CB1/OX1-GPCRs in rat hippocampus by kainic acid-induced status epilepticus. *Brain Research*, *1597*, 14–27. https://doi.org/10.1016/j.brainres.2014.11.002

Zhu, M., Yu, B., Bai, J., Wang, X., Guo, X., Liu, Y., Lin, J., Hu, S., Zhang, W., Tao, Y., Hu, C., Yang, H., Xu, Y., & Geng, D. (2019). Cannabinoid Receptor 2 Agonist Prevents Local and Systemic Inflammatory Bone Destruction in Rheumatoid Arthritis. *Journal of Bone and Mineral Research*, *34*(4), 739–751. https://doi.org/10.1002/jbmr.3637